

QCD splitting functions beyond kinematical limits

John M. Campbell,¹ Stefan Höche,¹ Max Knobbe,¹ Christian T. Preuss,² and Daniel Reichelt³

¹*Fermi National Accelerator Laboratory, Batavia, IL, 60510*

²*Institut für Theoretische Physik, Georg-August-Universität Göttingen, 37077 Göttingen, Germany*

³*Theoretical Physics Department, CERN, CH-1211 Geneva, Switzerland*

We present a systematic decomposition of QCD splitting functions into scalar dipole radiators and pure splitting remainders up to second order in the strong coupling. The individual components contain terms that are formally sub-leading in soft or collinear scaling parameters, but well understood and universal due to their origin in scalar QCD. The multipole radiator functions which we derive share essential features of the known double-soft and one-loop soft gluon currents, and are not based on kinematical approximations.

I. INTRODUCTION

For more than half a century, experiments at particle colliders have shaped our understanding of the building blocks of matter. They continue to be at the forefront of fundamental science [1, 2]. The quantitative description of particle production in these experiments received a strong boost from the development of QCD as a gauge theory of the strong interactions [3]. High-energy collider experiments often make detailed measurements of QCD dynamics in the region where partons are asymptotically free and form jets. The production and evolution of these jets is one of the key features of the strong interactions at high energy and remains of greatest interest, both because of its importance as an often irreducible background to new physics searches, and as a precision test of QCD dynamics.

Being a non-abelian, asymptotically free gauge theory, QCD presents many obstacles to the practitioner. Perturbative calculations are typically hampered both by the number and the complexity of the Feynman diagrams associated with a particular partonic final state [4–7]. In addition, at higher orders in the perturbative expansion, scattering matrix elements exhibit infrared singularities that cancel to all orders between real and virtual corrections [8–11], often leading to enormous complications for the numerical evaluation of observables with the help of Monte-Carlo integration methods. Generic techniques to address this problem at next-to-leading order (NLO) in the perturbative expansion were introduced long ago [12–14], and have been fully automated in various computer codes. A similar automation at the next-to-next-to leading order (NNLO) seems within reach [7].

The two sources of infrared singularities are soft gluon radiation and the collinear decay of massless partons. However, when multiple particles become collinear one or more of them can still be soft, leading to an overlap between the two types of divergence. Removing this overlap is key to identifying all singular regions of scattering matrix elements, and to providing the infrared subtraction counterterms that enable numerical computations. The goal of this work is therefore to construct process-independent NNLO double-real and real-virtual splitting functions that have no remaining overlaps. This is achieved as follows. First, the universal component of all splitting functions involving final-state gluons is extracted by making the *scalar* part of the theory manifest. This part generates the pole structure in the soft limit and is related to the classical limit [15–18]. For the purpose of infrared subtraction, it can be computed in the dipole approximation [19, 20]. Consistently going beyond the leading power soft approximation by using scalar dipoles allows us to capture universal contributions which appear in the splitting functions in a well-understood manner. Second, we identify the factorizable part of the higher-order splitting functions based on diagrammatic considerations, which results in an improved understanding of sub-leading singular terms, especially those involving azimuthal correlations. Third, the scalar radiators are formulated differentially in color space, in order to make them maximally useful for practical calculations. Similarly, the spin-dependent remainders are differential in spin.

Our algorithm makes use of the techniques introduced in [21, 22], in particular the choice of an axial gauge to obtain a physical interpretation of the gluon polarization tensor [23–30]. We provide the scalar extension of the double-soft radiators in both axial and Feynman gauge, allowing for an unambiguous matching to the splitting functions. Using the background field method [31–37], we compute scalar dipole radiator functions at one-loop level, which are matched to the known one-loop splitting amplitudes. The outline of this manuscript is as follows. In Section II we introduce the basic ideas and illustrate the spin decomposition at the vertex level. Section III describes the methodology for the computation of tree-level splitting functions, reviews the results of [21] and presents their spin decomposition. Section IV includes our results for the one-loop scalar radiator functions and one-loop splitting functions and discusses their spin decomposition. Section V contains some concluding remarks and an outlook.

II. SPIN DECOMPOSITION OF QCD AMPLITUDES

In the soft vector-boson limit, QCD matrix elements develop well-understood infrared singularities [38–43]. Their source is gluon interactions in the eikonal limit, which can be derived by making kinematical approximations to fixed-order QCD scattering matrix elements. However, their physical origin is better understood by investigating the minimal coupling of the vector potential to a classical, accelerated charge [44, 45]. In QED, the corresponding current in momentum space reads

$$j_{ik}^\mu(q) = igQ \left(\frac{p_k^\mu}{p_k q} - \frac{p_i^\mu}{p_i q} \right), \quad (1)$$

where g is the coupling constant, Q is the charge of the particle, and p_i and p_k are the momenta of the radiating charge dipole formed by the particle before and after an instantaneous impact. Once the radiation field, A_μ , sourced by the dipole is quantized, radiative effects can be computed in perturbation theory using the interaction Hamiltonian density $j^\mu(x)A_\mu(x)$. It can be shown that singularities in the infrared that are induced by this interaction cancel between real-emission corrections and virtual corrections [8, 10, 11].

Equation (1) does not account for the quantum nature of the charged particle. However, a minimal change to it yields the expression for scalar QED with massless radiators, and thus provides an extension to a full quantum field theory without kinematical constraints:

$$j_{ik}^\mu(q) = igQ \left(S^\mu(p_k, q) - S^\mu(p_i, q) \right), \quad \text{where} \quad S^\mu(p, q) = \frac{(2p + q)^\mu}{(p + q)^2}. \quad (2)$$

For the emission of a single on-shell vector boson, this expression results in the exact same scattering matrix elements as the eikonal current in Eq. (1). It has in fact been shown in the case of scalar QED that both the leading and sub-leading contributions to the squared amplitudes in the soft-photon limit can be obtained from classical calculations [17, 18]. We make this observation the basis for using scalar currents instead of the commonly employed eikonal currents when constructing multipole radiator functions. In the soft or double-soft limit, these radiators yield the known leading soft or double-soft behavior of the theory, but they also contain additional sub-leading contributions which are important for the correct matching to collinear splitting functions away from the soft region.

The QCD equivalent of the QED current in Eq. (2) can be obtained by using the techniques of [13, 43]:

$$\mathbf{J}^\mu(q) = ig_s \sum_i \hat{\mathbf{T}}_i S^\mu(p_i, q). \quad (3)$$

Here, $\hat{\mathbf{T}}$, are the charge operators, which are defined as $(\hat{\mathbf{T}}_i^c)_{ab} = T_{ab}^c$ for quarks, $(\hat{\mathbf{T}}_i^c)_{ab} = -T_{ba}^c$ for anti-quarks, and $(\hat{\mathbf{T}}_i^c)_{ab} = if^{acb}$ for gluons [13, 43]. Charge conservation in the QCD multipole implies $\sum_i \hat{\mathbf{T}}_i = 0$. For the emission of a single on-shell vector boson, Eq. (3) results in exactly the same scattering matrix elements as the QCD eikonal current. Moreover, the numerators in Eq. (3) obey elementary Ward identities, such that the single-gluon current is conserved, as long as the radiating particles remain on their mass shell.

In Sec. III C we will use Eq. (3) and its extension to the two-emission case to derive the scalar component of matrix elements that form the basis of the higher-order tree-level splitting functions. As the complete calculation is quite cumbersome, we highlight the basic correspondence using two simple examples at the amplitude level. The first is the quark-to-quark-gluon splitting process shown in Fig. 1(a) left. The scattering amplitude is proportional to the following combination of the coupling-stripped quark-gluon vertex and the quark propagator:

$$\frac{\not{p} + \not{q}}{(p + q)^2} T_{ij}^a \gamma^\mu = T_{ij}^a \left[S^\mu(p, q) + \frac{i\sigma^{\nu\mu} q_\nu}{(p + q)^2} - \frac{\gamma^\mu \not{p}}{(p + q)^2} \right]. \quad (4)$$

A decomposition of this current has been provided for the first time in [46], and an extension to massless fermions is given in [47]. The first term in the square bracket is the scalar current of Eq. (2). The second term, proportional to $\sigma^{\nu\mu} = \frac{i}{2}[\gamma^\nu, \gamma^\mu]$, describes the magnetic interaction due to the fermion's spin. This contribution is sub-leading in the soft and collinear limits. The contribution proportional to $\gamma^\mu \not{p}$ vanishes in the squared amplitude for one-to-two splittings due to the equations of motion. Using an axial gauge for the final-state gluon, after squaring the amplitude we obtain the standard quark-to-quark splitting function, cf. Sec. III A. We emphasize that this is achieved without any kinematical approximations. Additionally, the squared scalar interaction term can be identified at the amplitude squared level, where it emerges as a nontrivial combination of the square of the scalar contribution in Eq. (4) and the interference of the scalar and the magnetic term. This is a consequence of the fact that a magnetic interaction is needed to make the chiral kinetic theory Lorentz invariant [48, 49]. The vertex decomposition is sketched in Fig. 1(a) right, and discussed in detail in App. A.

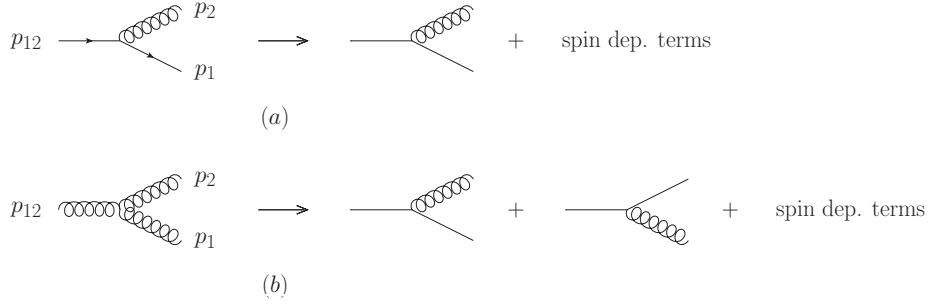


FIG. 1. Examples of one-to-two splitting processes. Figure (a) shows the splitting of a quark into a quark and a gluon, Fig. (b) the branching of a gluon into two gluons. The right-hand side sketches the decomposition of the full vertices into scalar and spin-dependent components.

Our second example will be the gluon-to-gluon-gluon splitting, shown in Fig. 1(b) left. The gluon propagator times the coupling stripped triple gluon vertex can be written as a sum of two components in two different permutations

$$\frac{d^\mu_\sigma(p_{12})}{p_{12}^2} f^{abc} \Gamma^{\sigma\nu\rho}(p_1, p_2) = id^\mu_\sigma(p_{12}) \left\{ \text{Tr}(T^c[T^b, T^a]) \left[S^\nu(p_1, p_2) g^{\rho\sigma} - \frac{(p_1 - p_2)^\rho}{2p_{12}^2} g^{\sigma\nu} \right] + \left(\begin{array}{cc} a \leftrightarrow b \\ \sigma \leftrightarrow \nu \\ 1 \leftrightarrow 2 \end{array} \right) \right\}, \quad (5)$$

where $\Gamma^{\mu\nu\rho}(p, q) = g^{\mu\nu}(p - q)^\rho + g^{\nu\rho}(2q + p)^\mu - g^{\rho\mu}(2p + q)^\nu$. Here, $d^{\mu\sigma}(p_{12})$ is the gluon polarization tensor. The two orderings of the color operators in the commutator appear because either the color charge or the anti-color charge of the incoming gluon can be the source of the gluon field. The first, scalar term in the square brackets is proportional to a metric tensor connecting the polarization vectors of the external particle to the incoming gluon. This agrees with the requirement that the classical interaction described by $S^\mu(p, k)$ must be both spin-independent and helicity preserving. In the limit where the emitted gluon becomes soft, the second term in the square brackets does not scale due to the transversality of the Born amplitude. In the collinear limit, it scales as the inverse of the transverse momentum. We have again achieved a separation into different types of splitting vertices, without having to perform any kinematical approximations. The one-to-two splitting function derived in Sec. III A has a similar structure. The vertex decomposition is sketched in Fig. 1(b) right and discussed in detail in App. A.

Before discussing the tree-level splitting functions in Sec. III, we will comment on the gauge choices for our calculations. The tree-level expressions are simplest to obtain in an axial gauge. Axial gauges benefit from being ghost free [50–54], because they encode only the physical degrees of freedom of the gluon field [23–30, 55], see also the later discussion of Eq. (12) in Section III. The corresponding polarization tensor,

$$d^{\mu\nu}(p, n) = -g^{\mu\nu} + \frac{p^\mu n^\nu + p^\nu n^\mu}{pn} - \frac{n^2 p^\mu p^\nu}{(pn)^2}, \quad (6)$$

satisfies the physical requirements for on-shell gluons, namely $-d^\mu_\mu(p, n) = D - 2$ and $p_\mu d^{\mu\nu}(p, n) = 0$, where $D = 4 - 2\epsilon$ is the number of space-time dimensions. The vector n^μ is an auxiliary gauge vector. When used in the computation of a splitting amplitude, the axial gauge mimicks the effects of coherent gluon emission off particles that are omitted from the explicit computation, but whose physical presence can be inferred from color charge conservation. As a simple example, consider a process with two charged scalars. The leading-order matrix element for the production of these scalars is just an overall constant. The real-emission matrix element is given by the constant times the eikonal in Eq. (1), contracted with the polarization vector of the external vector boson. The key observation is that one can choose the auxiliary vector, n^μ , in the polarization sum such that one term in the current, Eq. (1), is eliminated. In this manner, one moves contributions needed to describe coherent vector boson radiation from one Feynman diagram to another [56, 57]. In the computation of collinear splitting functions to leading power, this technique makes the result independent of the hard process.

At one-loop order, we will use the axial gauge to compute the splitting functions using the methods of [58, 59]. In order to determine their scalar components, we would ideally determine the scalar radiators in the same gauge. As this calculation is very cumbersome we use a different approach. The scalar radiators at one-loop level are an extension of the one-loop soft current [22, 60, 61] to the full scalar theory. They are determined from the same set of diagrams and acquire a physical meaning when computed in the background field method [31–37, 62–64]. We can therefore match the collinear limit of the scalar radiators in the background field method to the one-loop splitting amplitudes computed in axial gauge. By means of this technique, the one-loop integrals needed for the calculation can be limited to a small set which is known to all orders in the dimensional regularization parameter.

III. TREE-LEVEL EXPRESSIONS

In order to capture the singularity structure of a tree-level process in the m -particle collinear limit, one can compute the relevant off-shell current in axial gauge and project the result onto the physical polarization states [21]. We obtain the relevant expressions from a general definition of the tree-level currents using recursive techniques [65–68]

$$\begin{aligned} \Psi_i(p_\alpha) &= \sum_{\substack{\{\beta,\gamma\} \in \\ P(\alpha,2)}} g_s T_{ij}^a M^\mu(p_\beta, p_\gamma) J_\mu^a(p_\gamma, n) \Psi_j(p_\beta) , \\ &+ \sum_{\substack{\{\beta,\gamma\} \in \\ P(\alpha,2)}} \left[g_s T_{ij}^a S^\mu(p_\beta, p_\gamma) J_\mu^a(p_\gamma, n) - \sum_{\substack{\{\delta,\epsilon\} \in \\ OP(\gamma,2)}} \frac{g_s^2}{p_{ij}^2} \{T^a, T^b\}_{ij} J^{\mu,a}(p_\delta, n) J_\mu^b(p_\epsilon, n) \right] \Psi_j(p_\beta) , \end{aligned} \quad (7)$$

$$\begin{aligned} J_\mu^a(p_\alpha, n) &= \sum_{\substack{\{\beta,\gamma\} \in \\ P(\alpha,2)}} \left[g_s \frac{F_{bc}^a}{2} D_\mu(p_\beta, p_\gamma) J^{\rho,b}(p_\beta, n) J_\rho^c(p_\gamma, n) + g_s T_{ij}^a \bar{\Psi}_i(p_\gamma) F_\mu(p_\beta, p_\gamma) \Psi_j(p_\beta) \right] \\ &- \sum_{\substack{\{\beta,\gamma\} \in \\ P(\alpha,2)}} \left[g_s F_{ab}^c S^\sigma(p_\beta, p_\gamma) J_\sigma^c(p_\gamma, n) - \sum_{\substack{\{\delta,\epsilon\} \in \\ OP(\gamma,2)}} \frac{g_s^2}{p_{ij}^2} \{F^c, F^d\}_{ab} J^{\sigma,c}(p_\delta, n) J_\sigma^d(p_\epsilon, n) \right] d_\mu{}^\nu(p_\alpha, n) J_\nu^b(p_\beta, n) . \end{aligned} \quad (8)$$

For details on the above notation, see App. A. The individual building blocks of the recursion are defined as

$$\begin{aligned} S^\mu(p_i, p_j) &= \frac{(2p_i + p_j)^\mu}{p_{ij}^2} , & D^\mu(p_i, p_j, n) &= \frac{d_\nu^\mu(p_{ij}, n)}{p_{ij}^2} (p_i - p_j)^\nu , \\ M^\mu(p_i, p_j) &= \frac{i\sigma^{\mu\nu}}{p_{ij}^2} p_{j,\nu} , & F^\mu(p_i, p_j, n) &= d^{\mu\nu}(p_{ij}, n) \frac{\gamma_\nu}{p_{ij}^2} . \end{aligned} \quad (9)$$

They correspond to the scalar (S) and magnetic (M) interactions introduced in Eq. (A3), as well as the scalar decay vertex (D) and fermionic decay vertex (F) of the gluon introduced in Eq. (A9). The m -particle quark and gluon collinear splitting functions are given as a ratio of the m -particle to 1-particle quark and gluon currents after projection onto an auxiliary wave function conserving color charge and spin:

$$\begin{aligned} P_q^{ss'}(1, \dots, m) &= \delta^{ss'} \left(\frac{s_{1\dots m}}{8\pi\alpha_s \mu^{2\varepsilon}} \right)^{m-1} \frac{\text{Tr}[\not{n}\Psi(\{p_1, \dots, p_m\})\bar{\Psi}(\{p_1, \dots, p_m\})]}{\text{Tr}[\not{n}\Psi(\{\bar{p}_{1\dots m}\})\bar{\Psi}(\{\bar{p}_{1\dots m}\})]} , \\ P_g^{\mu\nu}(1, \dots, m) &= \frac{D-2}{2} \left(\frac{s_{1\dots m}}{8\pi\alpha_s \mu^{2\varepsilon}} \right)^{m-1} \frac{d^{\mu\rho}(p_{1\dots m}, \bar{n}) J_\rho(\{p_1, \dots, p_m\}) J_\sigma^\dagger(\{p_1, \dots, p_m\}) d^{\sigma\nu}(p_{1\dots m}, \bar{n})}{d^{\kappa\lambda}(\bar{p}_{1\dots m}, \bar{n}) J_\lambda(\{\bar{p}_{1\dots m}\}) J_\tau^\dagger(\{\bar{p}_{1\dots m}\}) d^\tau{}_\kappa(\bar{p}_{1\dots m}, \bar{n})} . \end{aligned} \quad (10)$$

For a discussion of the scaling behavior of the splitting functions, it is convenient to parametrize the final-state momenta in terms of a forward, transverse, and backward component as [21, 69]

$$p_i^\mu = z_i \bar{p}_{1\dots m}^\mu + \tilde{k}_i^\mu - \frac{\tilde{k}_i^2}{z_i} \frac{\bar{n}^\mu}{2\bar{p}_{1\dots m} \bar{n}} , \quad \text{where} \quad \bar{p}_{1\dots m}^\mu = p_{1\dots m}^\mu - p_{1\dots m}^2 \frac{\bar{n}^\mu}{2p_{1\dots m} \bar{n}} . \quad (11)$$

This allows us to express all results in terms of the forward light-cone momentum fractions, z_i , and transverse momenta, \tilde{k}_i . Local four-momentum conservation takes the form $z_1 + z_2 + \dots + z_m = 1$ and $\tilde{k}_1 + \tilde{k}_2 + \dots + \tilde{k}_m = 0$. To simplify the computation, we have changed the so far arbitrary vector n^μ defining the axial gauge to a light-like vector, which we denote as \bar{n}^μ . For $p^2 = 0$, the light-like axial gauge allows a simple interpretation of Eq. (6) in terms of polarizations of massless particles in the helicity formalism [57]¹:

$$d^{\mu\nu}(p, \bar{n}) = \frac{1}{4p\bar{n}} \sum_{\lambda=\pm} \text{Tr}[\not{p}\gamma^\mu \not{\bar{n}}\gamma^\nu P_\lambda] = \sum_{\lambda=\pm} \epsilon_\lambda^\mu(p, \bar{n}) \epsilon_\lambda^{\nu*}(p, \bar{n}) , \quad \text{where} \quad \epsilon_\pm^\mu(p, \bar{n}) = \pm \frac{\langle \bar{n}^\mp | \gamma^\mu | p^\mp \rangle}{\sqrt{2} \langle \bar{n}^\mp | p^\pm \rangle} . \quad (12)$$

¹ At higher orders in the perturbative expansion, this identity requires the four-dimensional helicity scheme [70, 71]

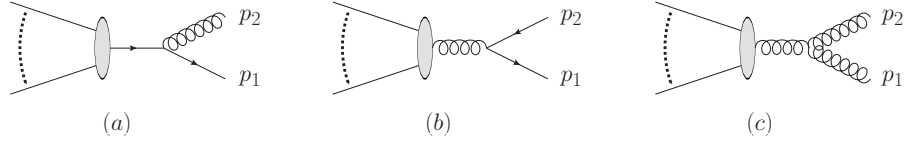


FIG. 2. Feynman diagrams leading to the $1 \rightarrow 2$ parton splitting functions discussed in Sec. III A. The shaded blob and lines to the left represent the hard process with its associated external partons. See the main text for details.

Here $P_{\pm} = (1 \pm \gamma^5)/2$ are the left- and right-chiral projectors. For off-shell vector bosons, one can use the shifted momentum defined in Eq. (11), which leads to the following generalization of Eq. (12):

$$d^{\mu\nu}(p, \bar{n}) = d^{\mu\nu}(\bar{p}, \bar{n}) + p^2 \frac{\bar{n}^\mu \bar{n}^\nu}{(p\bar{n})^2} = -d^{\mu\rho}(p, \bar{n}) d_\rho{}^\nu(p, \bar{n}) + p^2 \frac{\bar{n}^\mu \bar{n}^\nu}{(p\bar{n})^2}. \quad (13)$$

We have implicitly used this relation in Eq. (10) to define the collinear splitting functions. In the m -particle collinear limit, $\tilde{k}_i \rightarrow \lambda \tilde{k}_i$, $\lambda \rightarrow 0$, the second term on the right-hand side of Eq. (13) scales as λ^2 . It can therefore be neglected in the computation of the leading-power gluon splitting functions. The factorized form of the first term allows us to absorb one of the polarization tensors into the splitting amplitude, while the other is associated with the gluon current produced by the hard matrix element. Any \bar{n}^μ -dependent contribution to the gluon splitting function in Eq. (10) will then vanish upon multiplication by this current and can therefore be dropped. We will use this particular feature of the collinear limit in Sec. III D 2.

A. One-to-two splittings

In this subsection we re-derive the well-known two-parton splitting functions and systematically extend them to the off-shell region, which is needed to derive factorized expressions for the three-parton final states.

1. Quark initial state

The $1 \rightarrow 2$ quark splitting function can be computed from Eq. (10) using the 2-particle fermion current [21]. The corresponding Feynman diagram is shown in Fig. 2(a). We find

$$P_{q \rightarrow q}^{ss'}(p_1, p_2) = \frac{\delta^{ss'} s_{12}}{8\pi\alpha_s \mu^{2\varepsilon}} \frac{\text{Tr}[\not{p}_1 \Psi(\{p_1, p_2\}) \bar{\Psi}(\{p_1, p_2\})]}{\text{Tr}[\not{p}_1 \Psi(\{\bar{p}_{12}\}) \bar{\Psi}(\{\bar{p}_{12}\})]} = \delta^{ss'} P_{\bar{q} \rightarrow \bar{q}}(p_1, p_2) + P_{q \rightarrow q}^{ss'(\text{f})}(p_1, p_2). \quad (14)$$

Following Ref. [21], we denote spin-averaged quark splitting functions by $\langle P_{q \rightarrow X}(1, \dots, m) \rangle = \delta_{ss'} P_{q \rightarrow X}^{ss'}(1, \dots, m)/2$. As the quark splitting tensors are diagonal in spin space, we will refrain from listing both their spin-dependent and spin-averaged version. The individual components of the one-to-two quark splitting function are given by the $1 \rightarrow 2$ scalar splitting function and the purely fermionic term

$$P_{\bar{q} \rightarrow \bar{q}}(p_1, p_2) = C_F \frac{2z_1}{z_2} \left(1 - \frac{p_1^2}{p_{12}^2} \frac{z_{12}}{z_1} - \frac{p_2^2}{p_{12}^2} \frac{z_{12}}{z_2} \right), \quad (15)$$

$$\langle P_{q \rightarrow q}^{(\text{f})}(p_1, p_2) \rangle = C_F (1 - \varepsilon) \left(\frac{z_2}{z_{12}} - \frac{z_2}{z_1} \frac{p_1^2}{p_{12}^2} - \frac{p_2^2}{p_{12}^2} \right),$$

where $p_1^2 \rightarrow 0$ and $p_2^2 \rightarrow 0$ in the standard collinear factorization approach. In order to extend the massless result to the off-shell region, we have replaced $d^{\mu\nu}(p_2, \bar{n}) \rightarrow d^{\mu\nu}(\bar{p}_2, \bar{n})$, see the discussion of Eq. (13). In complete analogy, we have replaced the spinors $u(p_1)$ by $u(\bar{p}_1)$. Both these shifts are needed to achieve the expected scaling behavior of the remainder functions computed in Sec. III D. The gluon-spin dependent quark-to-quark splitting tensor is given by

$$\langle P_{q \rightarrow q}^{\mu\nu}(p_1, p_2) \rangle = P_{\bar{q} \rightarrow \bar{q}}^{\mu\nu}(p_1, p_2) + \langle P_{q \rightarrow q}^{(\text{f})\mu\nu}(p_1, p_2) \rangle. \quad (16)$$

Its scalar and purely fermionic components are given by

$$P_{\bar{q} \rightarrow \bar{q}}^{\mu\nu}(p_1, p_2) = \frac{C_F}{2} p_{12}^2 S^\mu(p_1, p_2) S^\nu(p_1, p_2), \quad (17)$$

$$\langle P_{q \rightarrow q}^{(\text{f})\mu\nu}(p_1, p_2) \rangle = -\frac{C_F}{2} \left[g^{\mu\nu} \left(\frac{z_2}{z_{12}} - \frac{z_2}{z_1} \frac{p_1^2}{p_{12}^2} - \frac{p_2^2}{p_{12}^2} \right) + \frac{p_2^\mu p_2^\nu}{p_{12}^2} \right] + \dots,$$

where the dots stand for contributions proportional to the gauge vector, \bar{n}^μ or \bar{n}^ν . Such terms vanish after multiplication by a gluon polarization tensor of the form $d^{\mu\nu}(p_2, \bar{n})$ or $d^{\mu\nu}(\bar{p}_2, \bar{n})$, and can therefore be dropped.

2. Gluon initial state

The Feynman diagrams leading to the tree-level $g \rightarrow q\bar{q}$ and $g \rightarrow gg$ splitting tensors are shown in Figs. 2(b) and (c), respectively. The algebraic expressions are obtained from Eq. (10) as follows [21].

$$\begin{aligned} P_{g \rightarrow q}^{\mu\nu}(p_1, p_2) &= \frac{T_R}{2p_{12}^2} d_\rho^\mu(p_{12}, \bar{n}) \text{Tr}[\not{p}_1 \gamma^\rho \not{p}_2 \gamma^\sigma] d_\sigma^\nu(p_{12}, \bar{n}), \\ P_{g \rightarrow g}^{\mu\nu, \alpha\beta}(p_1, p_2) &= \frac{C_A}{2p_{12}^2} d_\lambda^\mu(p_{12}, \bar{n}) \Gamma^{\kappa\alpha\lambda}(p_1, p_2) \Gamma^{\rho\beta\tau}(p_1, p_2) d_{\kappa\rho}(\bar{p}_1, \bar{n}) d_\tau^\nu(p_{12}, \bar{n}), \end{aligned} \quad (18)$$

where $\Gamma^{\mu\nu\rho}(p, q)$ implements the Lorentz structure of the three-gluon vertex, and where the Lorentz indices α and β refer to the final-state gluon with momentum p_2 , while the indices μ and ν refer to the initial-state gluon. Computing the gluon-to-quark splitting tensor is straightforward, and we obtain

$$P_{g \rightarrow q}^{\mu\nu}(p_1, p_2) = T_R \left[d^{\mu\nu}(\bar{p}_{12}, \bar{n}) \left(1 - \frac{z_{12}}{p_{12}^2} \left(\frac{p_1^2}{z_1} + \frac{p_2^2}{z_2} \right) \right) + p_{12}^2 \frac{\bar{n}^\mu \bar{n}^\nu}{(p_{12} \bar{n})^2} - p_{12}^2 D^\mu(p_1, p_2, \bar{n}) D^\nu(p_1, p_2, \bar{n}) \right], \quad (19)$$

where we have summed over the spins of the final-state quarks. In the final-state on-shell case Eq. (19) reduces to

$$P_{g \rightarrow q}^{\mu\nu(\text{os})}(p_1, p_2) = T_R \left[d^{\mu\nu}(p_{12}, \bar{n}) - \frac{4\tilde{p}_{1,2}^\mu \tilde{p}_{1,2}^\nu}{p_{12}^2} \right], \quad \text{where} \quad \tilde{p}_{i,j}^\mu = \frac{z_i p_j^\mu - z_j p_i^\mu}{z_i + z_j}. \quad (20)$$

The momenta \tilde{p} are generalizations of the transverse momenta \tilde{k} in Eq. (11). In particular, they fulfill momentum conservation in the form $\tilde{p}_{i,j} + \tilde{p}_{j,i} = 0$ for any i and j . Similarly, in the 3-parton case we have $\tilde{p}_{1,23} + \tilde{p}_{2,13} + \tilde{p}_{3,12} = 0$. Using the standard Sudakov parametrization in Eq. (11) [69], taking the collinear limit, and summing over quark spins, we can write Eq. (19) in the familiar form of the spin-dependent DGLAP splitting kernel

$$P_{g \rightarrow q}^{\mu\nu(\text{os})}(p_1, p_2) \rightarrow T_R \left[-g^{\mu\nu} + 4z_1 z_2 \frac{\tilde{k}_1^\mu \tilde{k}_1^\nu}{\tilde{k}_1^2} \right]. \quad (21)$$

Averaging over the polarizations of the initial-state gluon using conventional dimensional regularization (CDR), $\langle P_{g \rightarrow X}(1, \dots, m) \rangle = d_{\mu\nu}(p_{1\dots m}, \bar{n}) P_{g \rightarrow X}^{\mu\nu}(1, \dots, m)/(2 - 2\varepsilon)$, yields the CDR DGLAP splitting kernel

$$\langle P_{g \rightarrow q}(p_1, p_2) \rangle = T_R \left[1 - \frac{2}{1 - \varepsilon} \frac{z_1 z_2}{z_{12}^2} \right]. \quad (22)$$

The computation of the gluon-to-gluon splitting tensor is aided by the observation that any function multiplying this object must be symmetric in the Lorentz indices μ and ν . It is known that, in the on-shell case, this causes all interferences between the three components of $\Gamma^{\mu\nu\rho}$ to vanish [72]. In the following, we derive the corresponding expression, including some of the off-shell effects needed in Sec. IIID. We assume that $p_1^2 = 0$, which is sufficient to compute all factorizable components of the three-parton splitting functions. The relation $d^{\mu\rho}(p_1, \bar{n}) d_\rho^\nu(p_1, \bar{n}) = d^{\mu\nu}(p_1, \bar{n})$ can then be exploited to factorize the triple-gluon vertex functions in Eq. (18). We separate the resulting splitting tensor into a symmetric and an interference part

$$P_{g \rightarrow g}^{\mu\nu, \alpha\beta}(p_1, p_2) = P_{g \rightarrow g, (s)}^{\mu\nu, \alpha\beta}(p_1, p_2) + P_{g \rightarrow g, (i)}^{\mu\nu, \alpha\beta}(p_1, p_2) + P_{g \rightarrow g, (i)}^{\nu\mu, \beta\alpha}(p_1, p_2). \quad (23)$$

The symmetric component is given by the sum of squared scalar emission and decay vertices

$$\begin{aligned} P_{g \rightarrow g, (s)}^{\mu\nu, \alpha\beta}(p_1, p_2) &= \frac{C_A}{2} \left[p_{12}^2 S^\alpha(p_1, p_2) S^\beta(p_1, p_2) d^{\mu\nu}(\bar{p}_{12}, \bar{n}) \right. \\ &\quad \left. + 2d^{\mu\alpha}(p_{12}, \bar{n}) d^{\nu\beta}(p_{12}, \bar{n}) \frac{2z_2}{z_1} \left(1 - \frac{p_2^2}{p_{12}^2} \frac{z_{12}}{z_2} \right) + p_{12}^2 d^{\alpha\beta}(p_1, \bar{n}) D^\mu(p_1, p_2, \bar{n}) D^\nu(p_1, p_2, \bar{n}) \right]. \end{aligned} \quad (24)$$

The interference component is better understood by contracting $P_{g \rightarrow g, (i)}^{\mu\nu, \gamma\delta}(p_1, p_2)$ with the polarization tensors for the decay of gluon 2. The definitions in Eqs. (9) lead to

$$S_\nu(p_1, p_2) d^{\mu\nu}(p_2, \bar{n}) = \frac{2}{p_{12}^2} \frac{\tilde{p}_{1,2}^\mu}{z_2/z_{12}} + \dots, \quad D^\mu(p_1, p_2, \bar{n}) = \frac{2}{p_{12}^2} \tilde{p}_{1,2}^\mu + \dots, \quad (25)$$

where the ellipses represent terms proportional to \bar{n}^μ that vanish upon multiplication with $d_\mu^\rho(p, \bar{n})$ for any momentum, p . We can use these identities to simplify the interference contribution as follows

$$\begin{aligned} P_{g \rightarrow g, (i)}^{\mu\nu, \gamma\delta}(p_1, p_2) d_\gamma^\alpha(p_2, \bar{n}) d_\delta^\beta(p_2, \bar{n}) &= \frac{4C_A}{z_1 z_2} \left(z_{12} \tilde{p}_{1,2}^\alpha - \frac{p_2^2 \bar{n}^\alpha}{2p_{12} \bar{n}} \right) z_{12} \tilde{p}_{1,2}^\rho d^{\nu\sigma}(p_{12}, \bar{n}) d_\rho^\mu(p_{12}, \bar{n}) d_\sigma^\beta(p_2, \bar{n}) \\ &- \frac{4C_A}{z_1 z_2} \left(z_{12} \tilde{p}_{1,2}^\nu - \frac{p_2^2 \bar{n}^\nu}{2p_{12} \bar{n}} \right) \left[z_2 z_{12} \tilde{p}_{1,2}^\sigma d^{\rho\alpha}(p_2, \bar{n}) + z_1 \left(z_{12} \tilde{p}_{1,2}^\alpha - \frac{p_2^2 \bar{n}^\alpha}{2p_{12} \bar{n}} \right) d^{\rho\sigma}(p_1, \bar{n}) \right] d_\rho^\mu(p_{12}, \bar{n}) d_\sigma^\beta(p_2, \bar{n}). \end{aligned} \quad (26)$$

In the strongly ordered soft and collinear limits, $\tilde{p}_{i,j}^\nu d_\nu^\mu(p, \bar{n})$ reduces to $\tilde{p}_{i,j}^\mu$, and we find that the sum of asymmetric terms in Eq. (23) vanishes when combined with a tensor that is symmetric in μ and ν . The complete gluon splitting tensor is then effectively given by the sum of squared diagrams that led to Eq. (24). In the final-state on-shell case the symmetric component is given by

$$\begin{aligned} P_{g \rightarrow g}^{\mu\nu, \alpha\beta \text{ (os)}}(p_1, p_2) &= \frac{C_A}{2} \left[p_{12}^2 S^\alpha(p_1, p_2) S^\beta(p_1, p_2) d^{\mu\nu}(\bar{p}_{12}, \bar{n}) \right. \\ &\quad \left. + 2d^{\mu\alpha}(p_{12}, \bar{n}) d^{\nu\beta}(p_{12}, \bar{n}) \frac{2z_2}{z_1} + p_{12}^2 d^{\alpha\beta}(p_1, \bar{n}) D^\mu(p_1, p_2, \bar{n}) D^\nu(p_1, p_2, \bar{n}) \right]. \end{aligned} \quad (27)$$

Contracting Eq. (24) with the external polarization sum for gluon 2, we find

$$P_{g \rightarrow g}^{\mu\nu}(p_1, p_2) = 2C_A \left[d^{\mu\nu}(\bar{p}_{12}, \bar{n}) \left(\frac{z_1}{z_2} + \frac{z_2}{z_1} - \frac{z_{12}}{z_1} \frac{p_2^2}{p_{12}^2} \right) + 2(1 - \varepsilon) \frac{\tilde{p}_{1,2}^\mu \tilde{p}_{1,2}^\nu}{p_{12}^2} \right]. \quad (28)$$

Using the standard Sudakov parametrization in Eq. (11) [69], Eq. (27) yields the spin-dependent DGLAP kernel [72]

$$P_{g \rightarrow g}^{\mu\nu, \alpha\beta \text{ (os)}}(p_1, p_2) \rightarrow 2C_A \left[\frac{z_1}{z_2} \frac{\tilde{k}_1^\alpha \tilde{k}_1^\beta}{\tilde{k}_1^2} g^{\mu\nu} + \frac{z_2}{z_1} g^{\mu\alpha} g^{\nu\beta} - d^{\alpha\beta}(p_{12}, \bar{n}) \frac{z_1 z_2}{z_{12}^2} \frac{\tilde{k}_1^\mu \tilde{k}_1^\nu}{\tilde{k}_1^2} \right]. \quad (29)$$

Contracting this with the polarization tensor for gluon 2, we find the familiar expression

$$d_{\alpha\beta}(p_2, \bar{n}) P_{g \rightarrow g}^{\mu\nu, \alpha\beta \text{ (os)}}(p_1, p_2) \rightarrow 2C_A \left[-g^{\mu\nu} \left(\frac{z_1}{z_2} + \frac{z_2}{z_1} \right) - 2(1 - \varepsilon) \frac{z_1 z_2}{z_{12}^2} \frac{\tilde{k}_1^\mu \tilde{k}_1^\nu}{\tilde{k}_1^2} \right]. \quad (30)$$

Averaging over the polarizations of the initial-state gluon yields the DGLAP splitting kernel

$$\langle P_{g \rightarrow g}(p_1, p_2) \rangle = 2C_A \left[\frac{z_1}{z_2} + \frac{z_2}{z_1} + \frac{z_1 z_2}{z_{12}^2} \right]. \quad (31)$$

Based on the above derivation, this function can be decomposed as

$$\langle P_{g \rightarrow g}(p_1, p_2) \rangle = P_{g \rightarrow g}^{(\text{sc})}(p_1, p_2) + P_{g \rightarrow g}^{(\text{sc})}(p_2, p_1) + \langle P_{g \rightarrow g}^{(\text{v})}(p_1, p_2) \rangle, \quad (32)$$

where the scalar and purely vectorial part are defined as

$$\begin{aligned} P_{g \rightarrow g}^{(\text{sc})}(p_1, p_2) &= C_A \frac{2z_1}{z_2} = \frac{C_A}{C_F} P_{\bar{q} \rightarrow \bar{q}}(p_1, p_2) \Big|_{p_1^2 \rightarrow 0, p_2^2 \rightarrow 0}, \\ \langle P_{g \rightarrow g}^{(\text{v})}(p_1, p_2) \rangle &= 2C_A \frac{z_1 z_2}{z_{12}^2}. \end{aligned} \quad (33)$$

Note that Eqs. (19) and (24) are independent of the kinematics parametrization, as the invariants have not yet been expressed in terms of transverse momenta, and the light-cone momentum fractions are defined unambiguously.

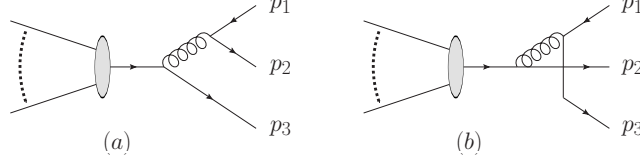


FIG. 3. Feynman diagrams leading to the $1 \rightarrow 3$ quark only splitting functions discussed in Sec. III B 1. The shaded blob and lines to the left represent the hard process with its associated external partons. See the main text for details.

B. One-to-three splittings

The leading terms of the three-parton splitting functions have been computed in [21, 73]. We will re-derive them here, together with their scalar QCD counterparts. We begin with the simpler quark initial states, which do not have a spin dependence, before discussing the gluon initial states that have a non-trivial Lorentz structure.

1. Quark initial state

The sole Feynman diagram leading to the flavor-changing quark-to-quark three-parton splitting function is shown in Fig. 3(a). It can be obtained from the product of the off-shell quark splitting function in Eq. (16) and the spin-dependent gluon-to-quark splitting function, Eq. (19). The result is [21]

$$\langle P_{q \rightarrow \bar{q}' q' q}(p_1, p_2, p_3) \rangle = \frac{C_F T_R}{2} \frac{s_{123}}{s_{12}} \left[-\frac{t_{12,3}^2}{s_{12} s_{123}} + \frac{4z_3 + (z_1 - z_2)^2}{z_1 + z_2} + (1 - 2\varepsilon) \left(1 - z_3 - \frac{s_{12}}{s_{123}} \right) \right], \quad (34)$$

where $s_{ij} = (p_i + p_j)^2$, and where we have defined

$$t_{12,3} = s_{123} S^\mu(p_3, p_{12}) s_{12} D_\mu(p_1, p_2, \bar{n}) = 2 \frac{z_1 2p_2 p_3 - z_2 2p_1 p_3}{z_1 + z_2} + \frac{z_1 - z_2}{z_1 + z_2} 2p_1 p_2. \quad (35)$$

The corresponding scalar-to-quark splitting function is given by the product of the scalar part of Eq. (17) and Eq. (19).

$$P_{\bar{q} \rightarrow \bar{q}' q' \bar{q}}(p_1, p_2, p_3) = \frac{s_{123}}{s_{12}} P_{\bar{q} \rightarrow \bar{q}}^{\mu\nu}(p_3, p_{12}) P_{g \rightarrow q, \mu\nu}(p_1, p_2) = \frac{C_F T_R}{2} \frac{s_{123}}{s_{12}} \left[\frac{4z_3}{z_1 + z_2} + \frac{s_{12}}{s_{123}} \left(1 - \frac{t_{12,3}^2}{s_{12}^2} \right) \right]. \quad (36)$$

As a consequence of the fact that only a single diagram contributes to Eq. (34), the splitting function factorizes. A simple, yet non-trivial observation is that, in the double-soft limit, both Eq. (34) and Eq. (36) yield

$$\langle P_{q \rightarrow \bar{q}' q' q}^{(\text{ds})}(p_1, p_2, p_3) \rangle = C_F T_R \frac{2(s_{13} + s_{23})}{s_{12}(z_1 + z_2)} \left[1 - \frac{(z_1 s_{23} - z_2 s_{13})^2}{(z_1 + z_2)(s_{13} + s_{23})s_{12}} \right]. \quad (37)$$

Compared to the complete scalar expression, this result lacks sub-leading power contributions. In particular, the azimuthal angle dependence differs between Eqs. (34), (36) and (37), because Eq. (35) is reduced to the first term alone. This exemplifies how higher-order splitting functions based on kinematic limits can obscure the origin of soft-collinear overlaps at sub-leading power in the soft scaling parameter.

The three-parton quark-to-quark splitting function is obtained as the coherent sum of the two Feynman diagrams in Figs. 3(a) and (b). It can be written as the sum of splitting functions for identical quarks, and an interference part [21].

$$\langle P_{q \rightarrow \bar{q} q q}(p_1, p_2, p_3) \rangle = \left(\langle P_{q \rightarrow \bar{q}' q' q}(p_1, p_2, p_3) \rangle + \langle P_{q \rightarrow \bar{q} q q}^{(\text{id})}(p_1, p_2, p_3) \rangle \right) + (2 \leftrightarrow 3), \quad (38)$$

where

$$\begin{aligned} \langle P_{q \rightarrow \bar{q} q q}^{(\text{id})}(p_1, p_2, p_3) \rangle = & C_F \left(C_F - \frac{C_A}{2} \right) \left\{ (1 - \varepsilon) \left(\frac{2s_{23}}{s_{12}} - \varepsilon \right) \right. \\ & + \frac{s_{123}}{s_{12}} \left[\frac{1 + z_1^2}{1 - z_2} - \frac{2z_2}{1 - z_3} - \varepsilon \left(\frac{(1 - z_3)^2}{1 - z_2} + 1 + z_1 - \frac{2z_2}{1 - z_3} \right) - \varepsilon^2 (1 - z_3) \right] \\ & \left. - \frac{s_{123}^2}{s_{12} s_{13}} \frac{z_1}{2} \left[\frac{1 + z_1^2}{(1 - z_2)(1 - z_3)} - \varepsilon \left(1 + 2 \frac{1 - z_2}{1 - z_3} \right) - \varepsilon^2 \right] \right\}. \end{aligned} \quad (39)$$

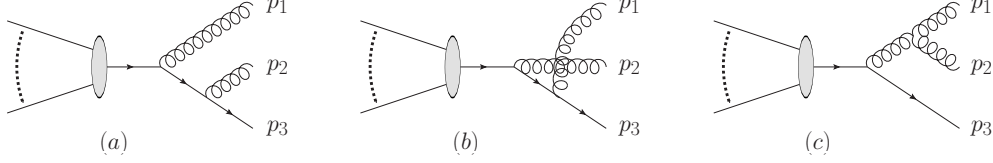


FIG. 4. Feynman diagrams leading to the $1 \rightarrow 3$ quark-to-quark-gluon splitting functions discussed in Sec. III B 1. The shaded blob and lines to the left represent the hard process with its associated external partons. See the main text for details.

The scalar-to-quark splitting function corresponding to this interference term does not exist.

Next we investigate double gluon radiation. The splitting function can be separated into abelian and purely non-abelian components [21], which are derived from the diagrams in Figs. 4(a) and (b), and from Figs. 4(a)-(c), respectively. The result for the abelian component is

$$\begin{aligned} \langle P_{q \rightarrow g g q}^{(\text{ab})}(p_1, p_2, p_3) \rangle &= C_F^2 \left\{ \frac{s_{123}^2}{2s_{13}s_{23}} z_3 \left[\frac{1+z_3^2}{z_1 z_2} - \varepsilon \frac{z_1^2 + z_2^2}{z_1 z_2} - \varepsilon(1+\varepsilon) \right] + \varepsilon(1-\varepsilon) - \frac{s_{23}}{s_{13}} (1-\varepsilon)^2 \right. \\ &\quad \left. + \frac{s_{123}}{s_{13}} \left[\frac{z_3(1-z_1) + (1-z_2)^3}{z_1 z_2} + \varepsilon^2(1+z_3) - \varepsilon(z_1^2 + z_1 z_2 + z_2^2) \frac{1-z_2}{z_1 z_2} \right] \right\} + (1 \leftrightarrow 2). \end{aligned} \quad (40)$$

In the scalar case, we obtain

$$P_{\tilde{q} \rightarrow g g \tilde{q}}^{(\text{ab})}(p_1, p_2, p_3) = C_F^2 \left\{ \frac{s_{123}^2}{s_{13}s_{23}} \frac{z_3^2}{z_1 z_2} + \frac{s_{123}}{s_{13}} \frac{2z_3(1-z_2)}{z_1 z_2} + (1-\varepsilon) \right\} + (1 \leftrightarrow 2). \quad (41)$$

This is the first splitting function involving the seagull vertices in Eq. (7).

The non-abelian part of the splitting function can be written as (see [21])

$$\begin{aligned} \langle P_{q \rightarrow g g q}^{(\text{nab})}(p_1, p_2, p_3) \rangle &= -\frac{C_A}{2C_F} P_{q \rightarrow g g q}^{(\text{ab})}(p_1, p_2, p_3) + C_F C_A \left\{ \frac{1-\varepsilon}{4} \left(\frac{t_{12,3}^2}{s_{12}^2} + 1 \right) - (1-\varepsilon)^2 \frac{s_{23}}{2s_{13}} \right. \\ &\quad + \frac{s_{123}}{2s_{12}} \left[(1-\varepsilon) \frac{z_1(2-2z_1+z_1^2) - z_2(6-6z_2+z_2^2)}{z_2(1-z_3)} + 2\varepsilon \frac{z_3(z_1-2z_2)-z_2}{z_2(1-z_3)} \right] \\ &\quad + \frac{s_{123}}{2s_{13}} \left[(1-\varepsilon) \frac{(1-z_2)^3 + z_3^2 - z_2}{z_2(1-z_3)} - \varepsilon \frac{2(1-z_2)(z_2-z_3)}{z_2(1-z_3)} - \varepsilon(1-\varepsilon)(1-z_1) \right] \\ &\quad \left. + \frac{s_{123}^2}{2s_{12}s_{13}} \left[\frac{(1-z_3)^2(1-\varepsilon) + 2z_3}{z_2} + \frac{z_2^2(1-\varepsilon) + 2(1-z_2)}{1-z_3} \right] + (1 \leftrightarrow 2) \right\}. \end{aligned} \quad (42)$$

In the scalar case, we obtain instead

$$\begin{aligned} P_{\tilde{q} \rightarrow g g \tilde{q}}^{(\text{nab})}(p_1, p_2, p_3) &= -\frac{C_A}{2C_F} P_{\tilde{q} \rightarrow g g \tilde{q}}^{(\text{ab})}(p_1, p_2, p_3) + C_F C_A \left\{ \left(\frac{s_{23}}{s_{13}} - \frac{t_{13,2}}{2s_{13}} \right) \frac{(1-z_2)^2}{2z_1 z_2} \right. \\ &\quad + \frac{s_{123}}{s_{12}} \left[\frac{z_3}{z_2} - \frac{1+3z_3}{1-z_3} + \frac{s_{123}}{s_{13}} \left(\frac{z_3}{z_2} + \frac{1-z_2}{1-z_3} \right) + \frac{1-\varepsilon}{4} \frac{t_{12,3}^2}{s_{123}s_{12}} \right] \\ &\quad \left. + \frac{s_{123}}{s_{13}} \left[\frac{z_3(1-z_2)}{2z_1 z_2} - \frac{(1-z_2)^2}{z_1(1-z_3)} \right] + \frac{z_3+z_1^2}{4z_1 z_2} + \frac{1-\varepsilon}{4} + (1 \leftrightarrow 2) \right\}. \end{aligned} \quad (43)$$

In the strongly ordered soft-collinear limit, $p_1 \parallel p_2$, one obtains the product of a soft-emission term, times a spin-correlated decay to two gluons. This factorized form is obtained from Eqs. (17) and (28). The result is

$$\begin{aligned} P_{\tilde{q} \rightarrow g g \tilde{q}}^{(\text{nab})}(p_1, p_2, p_3) &\rightarrow \frac{s_{123}}{s_{12}} P_{\tilde{q} \rightarrow \tilde{q}}^{\mu\nu}(p_3, p_{12}) P_{g \rightarrow g, \mu\nu}(p_1, p_2) \\ &= C_F C_A \frac{s_{123}}{s_{12}} \left[\frac{4z_3}{z_1 + z_2} \left(1 - \frac{s_{12}}{s_{123}} \frac{1}{z_1 + z_2} \right) \left(\frac{z_1}{z_2} + \frac{z_2}{z_1} \right) + \frac{1-\varepsilon}{2} \frac{t_{12,3}^2}{s_{123}s_{12}} \right]. \end{aligned} \quad (44)$$

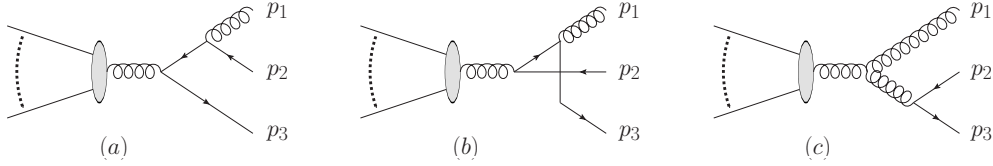


FIG. 5. Feynman diagrams leading to the $1 \rightarrow 3$ gluon-to-quark-gluon splitting functions discussed in Sec. III B 2. The shaded blob and lines to the left represent the hard process with its associated external partons. See the main text for details.

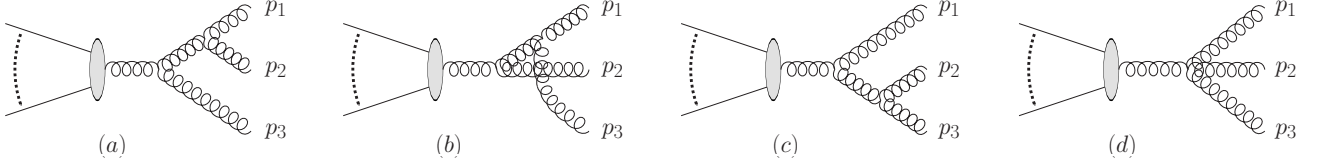


FIG. 6. Feynman diagrams leading to the $1 \rightarrow 3$ gluon-to-gluon splitting function discussed in Sec. III B 2. The shaded blob and lines to the left represent the hard process with its associated external partons. See the main text for details.

2. Gluon initial state

The Feynman diagrams needed to compute the three-parton gluon-to-quark splitting function are shown in Fig. 5. The abelian component is determined from Figs. 5(a) and (b). We find

$$P_{g \rightarrow gq\bar{q}}^{\mu\nu(\text{ab})}(p_1, p_2, p_3) = C_F T_R \left\{ d^{\mu\nu}(p_{123}, \bar{n}) \left[\frac{2s_{123}s_{23}}{s_{12}s_{13}} + (1 - \varepsilon) \left(\frac{s_{12}}{s_{13}} + \frac{s_{13}}{s_{12}} \right) - 2\varepsilon \right] + \frac{4s_{123}}{s_{12}s_{13}} \left(\tilde{p}_{2,13}^\mu \tilde{p}_{3,12}^\nu + \tilde{p}_{3,12}^\mu \tilde{p}_{2,13}^\nu - (1 - \varepsilon) \tilde{p}_{1,23}^\mu \tilde{p}_{1,23}^\nu \right) \right\}. \quad (45)$$

With the help of the Sudakov decomposition in Eq. (11), the expression can be written in terms of transverse momenta and reduced to the leading-power result given in [21]. Similarly, the on-shell non-abelian part of the splitting tensor of a gluon into a gluon and a $q\bar{q}$ -pair is determined from the diagrams in Figs. 5(a)-(c).

$$P_{g \rightarrow gq\bar{q}}^{\mu\nu(\text{nab})}(p_1, p_2, p_3) = -\frac{C_A}{2C_F} P_{g \rightarrow gq\bar{q}}^{\mu\nu(\text{ab})}(p_1, p_2, p_3) + \frac{C_A T_R}{4} \left\{ \frac{s_{123}}{s_{23}^2} \left[-d^{\mu\nu}(p_{123}, \bar{n}) \frac{t_{23,1}^2}{s_{123}} - 16 \frac{1 - z_1}{z_1} \tilde{p}_{2,3}^\mu \tilde{p}_{2,3}^\nu \right] + d^{\mu\nu}(p_{123}, \bar{n}) \left[\frac{2s_{13}}{s_{12}} (1 - \varepsilon) + \frac{2s_{123}}{s_{12}} \left(\frac{1 - z_3}{z_1(1 - z_1)} - 2 \right) + \frac{2s_{123}}{s_{23}} \frac{1 - z_1 + 2z_1^2}{z_1(1 - z_1)} - 1 \right] + \frac{s_{123}}{s_{12}s_{23}} \left[2s_{123} d^{\mu\nu}(p_{123}, \bar{n}) \frac{z_2(1 - 2z_1)}{z_1(1 - z_1)} - 16 \tilde{p}_{3,12}^\mu \tilde{p}_{3,12}^\nu \frac{z_2^2}{z_1(1 - z_1)} + 8(1 - \varepsilon) \tilde{p}_{2,13}^\mu \tilde{p}_{2,13}^\nu + 4(\tilde{p}_{2,13}^\mu \tilde{p}_{3,12}^\nu + \tilde{p}_{3,12}^\mu \tilde{p}_{2,13}^\nu) \left(\frac{2z_2(z_3 - z_1)}{z_1(1 - z_1)} + 1 - \varepsilon \right) \right] + (2 \leftrightarrow 3) \right\} + P_{g \rightarrow gq\bar{q}}^{\mu\nu(\text{nab}, \bar{n})}(p_1, p_2, p_3). \quad (46)$$

This splitting tensor contains an explicitly \bar{n} -dependent contribution, listed in App. C, which does not contribute in the triple-collinear limit, cf. the discussion of Eq. (13). The spin-averaged splitting functions can be obtained by contracting Eqs. (45) and (46) with $d_{\mu\nu}(p_{123}, \bar{n})$. They are given in Eqs. (68) and (69) of [21].

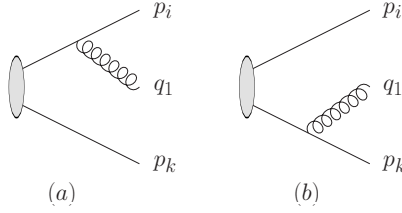


FIG. 7. Diagrams contributing to the radiation of a single gluon from scalar dipoles.

The one-to-three gluon splitting tensor is obtained from the diagrams in Fig. 6. It was computed in [21] and reads

$$\begin{aligned}
 P_{g \rightarrow ggg}^{\mu\nu}(p_1, p_2, p_3) = & C_A^2 \left\{ \frac{1-\varepsilon}{4s_{12}^2} \left[d^{\mu\nu}(p_{123}, \bar{n}) \left(t_{12,3}^2 + 3s_{12}^2 \right) + 16s_{123} \frac{1-z_3}{z_3} \tilde{p}_{1,2}^\mu \tilde{p}_{1,2}^\nu \right] \right. \\
 & - \frac{s_{123}}{s_{12}} \frac{d^{\mu\nu}(p_{123}, \bar{n})}{z_3} \left[\frac{2(1-z_3) + 4z_3^2}{1-z_3} - \frac{1-2z_3(1-z_3)}{z_1(1-z_1)} \right] \\
 & + \frac{s_{123}(1-\varepsilon)}{s_{12}s_{13}} \left[2z_1 \left(\tilde{p}_{2,13}^\mu \tilde{p}_{2,13}^\nu \frac{1-2z_3}{z_3(1-z_3)} + \tilde{p}_{3,12}^\mu \tilde{p}_{3,12}^\nu \frac{1-2z_2}{z_2(1-z_2)} \right) \right. \\
 & - \frac{s_{123}}{2(1-\varepsilon)} d^{\mu\nu}(p_{123}, \bar{n}) \left(\frac{4z_2z_3 + 2z_1(1-z_1) - 1}{(1-z_2)(1-z_3)} - \frac{1-2z_1(1-z_1)}{z_2z_3} \right) \\
 & \left. \left. + (\tilde{p}_{2,13}^\mu \tilde{p}_{3,12}^\nu + \tilde{p}_{3,12}^\mu \tilde{p}_{2,13}^\nu) \left(\frac{2z_2(1-z_2)}{z_3(1-z_3)} - 3 \right) \right] + (5 \text{ permutations}) \right\} + P_{g \rightarrow ggg}^{\mu\nu}(\bar{n})(p_1, p_2, p_3) .
 \end{aligned} \tag{47}$$

This splitting tensor contains an explicitly \bar{n} -dependent contribution, listed in App. C, which does not contribute in the triple-collinear limit, cf. the discussion of Eq. (13). The spin-averaged splitting function, obtained by contracting Eq. (47) with $d_{\mu\nu}(p_{123}, \bar{n})$, is given in Eq. (70) of [21].

C. Scalar multipoles

In this section we focus on the radiation pattern of the scalar emitters in Eq. (9), which is given by the current in Eq. (3), applied to QCD. The emission of a single gluon from a pair of charged scalar particles in the fundamental representation is described by the coherent sum of the two diagrams in Fig. 7:

$$\mathcal{S}_g^\mp(p_i, p_k; q_1; n) = (T_{ij}^a S^\mu(p_i, q_1) \mp T_{lk}^a S^\mu(p_k, q_1)) (T_{ij}^a S^\nu(p_i, q_1) \mp T_{lk}^a S^\nu(p_k, q_1)) d_{\mu\nu}(q_1, n) , \tag{48}$$

where \mathcal{S}^- applies to opposite sign charges and \mathcal{S}^+ to same sign charges. Note that we have dropped the coupling factors still present in Eq. (3), to be consistent with the definition of the splitting functions in Secs. III A and III B. We can use the notation of [13, 43] to generalize Eq. (48) to arbitrary radiators

$$\mathcal{S}_g(\{p\}; q_1; \bar{n}) = \sum_{i,k} \hat{\mathbf{T}}_i \hat{\mathbf{T}}_k \mathcal{S}_{i,k}(q_1; \bar{n}) . \tag{49}$$

The space-time dependent part of individual radiators for on-shell gluons is given by

$$\mathcal{S}_{i,k}(q_1; \bar{n}) = \frac{1}{p_{i1}^2} \frac{2z_i}{z_1} \left(1 - \frac{p_k^2}{p_{k1}^2} \right) + \frac{1}{p_{k1}^2} \frac{2z_k}{z_1} \left(1 - \frac{p_i^2}{p_{i1}^2} \right) - \frac{4p_i p_k}{p_{i1}^2 p_{k1}^2} . \tag{50}$$

To simplify the notation in Sec. III D, we introduce an analogous notation for the gluon-spin dependent radiator.

$$\mathcal{S}_g^{\mu\nu}(\{p\}; q_1) = \sum_{i,k} \hat{\mathbf{T}}_i \hat{\mathbf{T}}_k \mathcal{S}_{i,k}^{\mu\nu}(q_1) , \quad \text{where} \quad \mathcal{S}_{i,k}^{\mu\nu}(q_1) = S^\mu(p_i, q_1) S^\nu(p_k, q_1) . \tag{51}$$

Neglecting the momentum dependence of the hard matrix element, and assuming on-shell radiators, we can use color conservation in the form $\hat{\mathbf{T}}_i^2 = -\sum_{k \neq i} \hat{\mathbf{T}}_i \hat{\mathbf{T}}_k$ to eliminate the terms where $i = k$ from Eq. (49).

$$\mathcal{S}_g(\{p\}; q_1; \bar{n}) = - \sum_{i,k \neq i} \frac{\hat{\mathbf{T}}_i \hat{\mathbf{T}}_k}{p_i q_1} \left(\frac{p_i p_k}{p_k q_1} - \frac{p_i^2}{p_i q_1} + \frac{z_i}{z_1} - \frac{z_k}{z_1} \frac{p_i q_1}{p_k q_1} \right) . \tag{52}$$

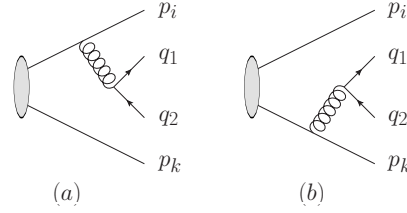


FIG. 8. Double-branching diagrams contributing to the emission of a quark-antiquark pair from scalar dipoles.

If the gauge vector n^μ is chosen such as to define the frame of the color multipole, this expression is simply the additively matched radiator function in the angular ordered parton shower approach to QCD resummation [74, 75]. However, the more common way to write Eq. (52) is to use its symmetry properties and remove the ratios of z factors, making positivity and gauge invariance manifest.

$$\mathcal{S}_g(\{p\}; q_1) = - \sum_{i,k \neq i} \hat{\mathbf{T}}_i \hat{\mathbf{T}}_k \left(\frac{p_i p_k}{(p_i q_1)(p_k q_1)} - \frac{p_i^2/2}{(p_i q_1)^2} - \frac{p_k^2/2}{(p_k q_1)^2} \right). \quad (53)$$

In any collinear limit, $p_i \parallel q_1$, the $i = k$ term in Eq. (49) approaches $p_{i1}^{-2} 4z_i/z_j$, which, up to a color prefactor and the collinear propagator agrees with the $2z_i/z_j$ contribution of the DGLAP splitting functions in Eqs. (15) and (31). In this case the color correlations become trivial, and the sole remaining term is proportional to the quadratic Casimir operator. In general, we can identify the $i = k$ term in Eq. (49) with the contributions proportional to the scalar radiators squared in Eqs. (17) and (24).

1. Quark-antiquark emission

The emission of a quark-antiquark pair from a pair of scalar radiators in the fundamental representation is given by the coherent sum of the two diagrams in Fig. 8. Making use of color charge operators, this can be generalized to the emission off a scalar current in the form of Eq. (3). Charge conservation and the transversality of the decay vertex F^μ in Eq. (9) can be used to simplify the computation [21], leading to the following result for massless final-state partons:

$$\mathcal{S}_{q\bar{q}}(\{p\}; q_1, q_2) = \sum_{i,k} \hat{\mathbf{T}}_i \hat{\mathbf{T}}_k 4T_R \frac{s_{i1}s_{k2} + s_{i2}s_{k1} - s_{ik}s_{12}}{s_{12}^2 s_{i12} s_{k12}}. \quad (54)$$

Note that in contrast to Eq. (96) in Ref. [21], Eq. (54) contains the physical propagators rather than their eikonal counterparts. The matching to the squared amplitudes in Sec. IIIB is better understood when retaining the gauge dependence term by term. This leads to the following result

$$\mathcal{S}_{q\bar{q}}(\{p\}; q_1, q_2; \bar{n}) = \sum_{i,k} \hat{\mathbf{T}}_i \hat{\mathbf{T}}_k T_R \mathcal{S}_{i,k}^{(q\bar{q})}(q_1, q_2; \bar{n}), \quad (55)$$

where the space-time dependent part of the individual radiators is given by

$$\mathcal{S}_{i,k}^{(q\bar{q})}(q_1, q_2; \bar{n}) = \frac{2}{s_{i12} s_{k12}} \left[\frac{2}{s_{12}} \left(\frac{z_i s_{k12} + z_k s_{i12}}{z_1 + z_2} - s_{ik} \right) + 1 - \frac{t_{12,i} t_{12,k}}{s_{12}^2} \right]. \quad (56)$$

For $i = k$, this expression corresponds to twice the squared scalar splitting amplitude in Eq. (36).

2. Two-gluon emission

The emission of a gluon pair can be described in a fashion similar to the double-gluon soft current in [21]. The diagrams contributing to this current are shown in Fig. 9. The main difference to the computation of the soft current lies in the form of the one-gluon current, which is given by Eq. (3) rather than its eikonal counterpart. However, this current is not conserved if the scalar particle is off mass-shell, a problem that is solved in the abelian case by

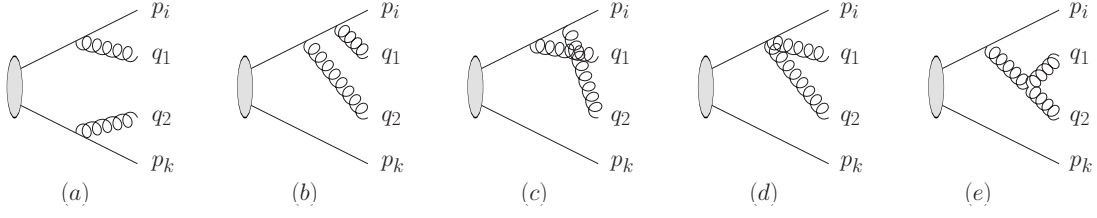


FIG. 9. Types of diagrams contributing to the two-gluon current for emission of the charged parton pair $\{i, k\}$. The same diagrams exist with i and k interchanged.

the seagull diagrams in Fig. 9(d), and in the non-abelian case by the use of a physical gauge or external ghosts. For massless partons, we obtain the following simple result

$$J_{ab}^{\mu\nu}(q_1, q_2) = \sum_{i,k} \{ \hat{\mathbf{T}}_i^a, \hat{\mathbf{T}}_k^b \} \mathcal{J}_{ik}^{(ab),\mu\nu}(q_1, q_2) + \sum_i i f^{abc} \hat{\mathbf{T}}_i^c \mathcal{J}_i^{(nab),\mu\nu}(q_1, q_2). \quad (57)$$

The color-stripped abelian and non-abelian two-gluon currents $\mathcal{J}_{ik}^{\mu\nu}$ are defined as

$$\begin{aligned} \mathcal{J}_{ik}^{(ab),\mu\nu}(q_1, q_2) &= \frac{1}{2} S^\mu(p_i, q_1) S^\nu(p_k, q_2) \\ &+ \frac{\delta_{ik}}{(p_i + q_{12})^2} \left[q_1^\nu S^\mu(p_i, q_1) + q_2^\mu S^\nu(p_i, q_2) - q_1 q_2 S^\mu(p_i, q_1) S^\nu(p_i, q_2) - g^{\mu\nu} \right], \\ \mathcal{J}_i^{(nab),\mu\nu}(q_1, q_2) &= S_\rho(p_i, q_{12}) \left(d^{\rho\nu}(q_{12}) S^\mu(q_2, q_1) - d^{\rho\mu}(q_{12}) S^\nu(q_1, q_2) \right) \\ &+ \frac{1}{(p_i + q_{12})^2} \left[q_1^\nu S^\mu(p_i, q_1) - q_2^\mu S^\nu(p_i, q_2) + p_i(q_2 - q_1) S^\mu(p_i, q_1) S^\nu(p_i, q_2) + \frac{t_{12,i}}{q_{12}^2} g^{\mu\nu} \right]. \end{aligned} \quad (58)$$

In the double-soft limit, $q_{1/2} \rightarrow \lambda q_{1/2}$, these functions reduce to the double-soft current in Eq. (101) of Ref. [21]. Making use of the color-space identity²

$$\begin{aligned} \{ \hat{\mathbf{T}}_i^a, \hat{\mathbf{T}}_k^b \} \{ \hat{\mathbf{T}}_l^a, \hat{\mathbf{T}}_m^b \} &= \{ \hat{\mathbf{T}}_i^a \hat{\mathbf{T}}_l^a, \hat{\mathbf{T}}_k^b \hat{\mathbf{T}}_m^b \} + i(2\delta_{kl} - \delta_{lm})(1 - \delta_{ik})(1 - \delta_{km})(1 - \delta_{im}) f^{abc} \hat{\mathbf{T}}_i^a \hat{\mathbf{T}}_k^b \hat{\mathbf{T}}_m^c \\ &- C_A \left(\delta_{kl} - \frac{\delta_{lm}}{2} \right) \left(\delta_{ik} \hat{\mathbf{T}}_i^a \hat{\mathbf{T}}_m^a + (1 - \delta_{ik})(\delta_{km} - \delta_{im}) \hat{\mathbf{T}}_i^a \hat{\mathbf{T}}_k^a \right) + \left(\begin{matrix} i \leftrightarrow k \\ l \leftrightarrow m \end{matrix} \right), \end{aligned} \quad (59)$$

we obtain a relatively compact form of the two-gluon squared current. In particular, due to its symmetries, the result is free of terms of the form $i f^{abc} \hat{\mathbf{T}}_i^a \hat{\mathbf{T}}_k^b \hat{\mathbf{T}}_m^c$.

$$\begin{aligned} [J_{\mu\nu}^{ab}(q_1, q_2)]^\dagger d^{\mu\rho}(q_1, \bar{n}) d^{\nu\sigma}(q_2, \bar{n}) J_{\rho\sigma}^{ab}(q_1, q_2) &= 2 \sum_{i,k} \sum_{l,m} \{ \hat{\mathbf{T}}_i^a \hat{\mathbf{T}}_l^a, \hat{\mathbf{T}}_k^b \hat{\mathbf{T}}_m^b \} \mathcal{S}_{i,k;l,m}^{(ab)}(q_1, q_2; \bar{n}) \\ &+ 2 \sum_{i,k} \sum_l \left(\{ \hat{\mathbf{T}}_i^a \hat{\mathbf{T}}_l^a, \hat{\mathbf{T}}_k^b \hat{\mathbf{T}}_l^b \} + \{ \hat{\mathbf{T}}_l^a \hat{\mathbf{T}}_i^a, \hat{\mathbf{T}}_k^b \hat{\mathbf{T}}_l^b \} \right) \mathcal{S}_{i,k;l}^{(ab)}(q_1, q_2; \bar{n}) + 2 \sum_{i,l} \{ \hat{\mathbf{T}}_i^a \hat{\mathbf{T}}_l^a, \hat{\mathbf{T}}_i^b \hat{\mathbf{T}}_l^b \} \mathcal{S}_{i;l}^{(ab)}(q_1, q_2) \\ &- \sum_{i,l} C_A \hat{\mathbf{T}}_i^c \hat{\mathbf{T}}_l^c \left[\mathcal{S}_{i;l}^{(nab)}(q_1, q_2; \bar{n}) - (1 - 2\delta_{il}) \mathcal{S}_{i;l}^{(ab)}(q_1, q_2) - \mathcal{S}_{i,i;l}^{(ab)}(q_1, q_2; \bar{n}) - \mathcal{S}_{l,l;i}^{(ab)}(q_1, q_2; \bar{n}) \right. \\ &\quad \left. + \mathcal{S}_{i,l;i}^{(ab)}(q_1, q_2; \bar{n}) + \mathcal{S}_{l,i;i}^{(ab)}(q_1, q_2; \bar{n}) + \mathcal{S}_{i,l;l}^{(ab)}(q_1, q_2; \bar{n}) + \mathcal{S}_{l,i;l}^{(ab)}(q_1, q_2; \bar{n}) \right]. \end{aligned} \quad (60)$$

² See also App. B of Ref. [76], which contains the symmetric part of this equation.

We have defined the abelian and non-abelian radiator functions, $\mathcal{S}(q_1, q_2; \bar{n})$, which are natural extensions of the soft functions in Ref. [21]. For on-shell radiators they are given by

$$\begin{aligned}\mathcal{S}_{i,k;l,m}^{(\text{ab})}(q_1, q_2; \bar{n}) &= \frac{1}{4} \mathcal{S}_{i;l}(q_1; \bar{n}) \mathcal{S}_{k;m}(q_2; \bar{n}) = \frac{z_1 s_{il} - z_i s_{l1} - z_l s_{i1}}{z_1 s_{i1} s_{l1}} \frac{z_2 s_{km} - z_k s_{m2} - z_m s_{k2}}{z_2 s_{k2} s_{m2}}, \\ \mathcal{S}_{i,k;l}^{(\text{ab})}(q_1, q_2; \bar{n}) &= \frac{1}{s_{l12}} \frac{s_{il} s_{kl}}{s_{i1} s_{k2}} \left(\frac{s_{k1}}{s_{kl} s_{l1}} + \frac{s_{i2}}{s_{il} s_{l2}} - \frac{s_{12}}{s_{l1} s_{l2}} \right) \\ &\quad + \frac{1}{s_{l12}} \left[\frac{z_l}{z_2} \left(\frac{s_{il} s_{12} - s_{i2} s_{l1}}{s_{i1} s_{l1} s_{l2}} - \frac{z_l s_{12}}{2 z_1 s_{l1} s_{l2}} \right) + \frac{z_i s_{l1} + z_l s_{i1} - z_1 s_{il}}{z_2 s_{i1} s_{l1}} - \frac{s_{ik}}{2 s_{i1} s_{k2}} + \left(\frac{i \leftrightarrow k}{1 \leftrightarrow 2} \right) \right], \\ \mathcal{S}_{i,k}^{(\text{ab})}(q_1, q_2) &= \frac{(s_{i1} s_{k2} - s_{i2} s_{k1})^2 - 2 s_{12} s_{ik} (s_{i1} s_{k2} + s_{i2} s_{k1}) + s_{12}^2 s_{ik}^2}{s_{i12} s_{k12} s_{i1} s_{k1} s_{i2} s_{k2}} + \frac{2(1 - \varepsilon)}{s_{i12} s_{k12}},\end{aligned}\tag{61}$$

and

$$\begin{aligned}\mathcal{S}_{i,k}^{(\text{nab})}(q_1, q_2; \bar{n}) &= \left[\frac{3}{4} + \frac{(s_{i1} - s_{i2})(s_{k1} - s_{k2})}{4 s_{i12} s_{k12}} \right] \left[\frac{s_{ik}}{s_{i1} s_{12} s_{k2}} + \frac{s_{ik}}{s_{i2} s_{12} s_{k1}} - \mathcal{S}_{i,i;k,k}^{(\text{ab})}(q_1, q_2; \bar{n}) \right] \\ &\quad + \frac{1}{s_{i12} s_{k12}} \left\{ \left(1 + \frac{s_{i2} s_{k1}}{s_{i1} s_{k2}} \right) \left(\frac{1}{2} - \frac{z_i z_k}{z_1 z_2} \right) - \frac{z_1 s_{i2}}{z_2 s_{i1}} + \frac{z_i s_{k2}}{z_2 s_{i1}} \left(\frac{4 z_i}{z_1} - 1 \right) - \frac{z_i}{z_2} \left(\frac{3(s_{i2} + s_{k1})}{s_{i1}} + 1 \right) \right. \\ &\quad - \frac{s_{ik}}{s_{i1}} \left(\frac{2 z_i}{z_1} + \frac{2 z_i}{z_2} \frac{s_{k2}}{s_{k1}} + \frac{s_{12}}{z_2} \left(\frac{z_k}{s_{k1}} + \frac{z_k}{s_{k2}} + \frac{z_i}{s_{i2}} \left(1 + \frac{z_2 s_{k1}}{z_1 s_{k2}} \right) \right) + \frac{s_{12}}{2 s_{k2}} + 2 \right) - \frac{2 s_{ik}}{s_{12}} \\ &\quad + \frac{z_i s_{12}}{z_2 s_{i1}} \left(\frac{2 z_i}{z_1} \left(1 + \frac{s_{k1}}{s_{i2}} \right) - \frac{z_k}{z_1} \left(1 + \frac{s_{i2}}{s_{k2}} \right) - 2 \right) + \frac{s_{12}^2 z_i}{2 s_{i1} z_2} \left(\frac{1}{z_1} \left(\frac{2 z_i}{s_{i2}} - \frac{z_k}{s_{k2}} \right) - \frac{2 s_{ik}}{s_{i2} s_{k1}} \right) \\ &\quad - \frac{4 z_2 s_{i1}}{s_{12}^2} \left(\frac{s_{k1}}{z_1} - \frac{s_{k2}}{z_2} \right) - \frac{2 s_{k2}}{s_{12}} \left(\frac{s_{i2}}{s_{i1}} \frac{2 z_i + z_1}{z_2} + \frac{s_{i1}}{s_{i2}} \left(\frac{z_i}{z_1} - 1 \right) + \frac{2 z_i}{z_1} - \frac{z_i - z_1}{z_2} - 1 \right) \\ &\quad - \frac{t_{12,k}}{2 s_{12}} \left[\frac{s_{i1}}{s_{i2}} \left(1 + \frac{z_i}{z_2} \right) \left(\frac{z_2}{z_1} - \frac{z_i s_{12}}{z_1 s_{i1}} \right) + \frac{2 s_{i1}}{s_{12}} \left(1 + \frac{z_2}{z_1} \right) + \frac{3 z_i}{z_2} - (1 \leftrightarrow 2) \right] - \frac{1 - \varepsilon}{2} \frac{t_{12,i} t_{12,k}}{s_{12}^2} \Big\} \\ &\quad + \frac{z_i}{s_{i1} z_1} \left(\frac{2 z_k}{s_{k2} z_2} + \frac{z_i}{s_{i2} z_2} - \frac{2 s_{ik} z_1}{s_{i2} s_{k1} z_2} \right) + (i \leftrightarrow k) + (1 \leftrightarrow 2) + \left(\frac{i \leftrightarrow k}{1 \leftrightarrow 2} \right).\end{aligned}\tag{62}$$

These radiators are related to the splitting functions in Eqs. (41) and (43) as follows³:

$$\begin{aligned}\langle P_{\hat{q} \rightarrow g g \bar{q}}^{(\text{ab})}(p_1, p_2, p_i) \rangle &= s_{i12}^2 C_F^2 \left(\mathcal{S}_{i,i;i,i}^{(\text{ab})}(p_1, p_2; \bar{n}) + 2 \mathcal{S}_{i,i,i}^{(\text{ab})}(p_1, p_2; \bar{n}) + \mathcal{S}_{i,i}^{(\text{ab})}(p_1, p_2) \right), \\ \langle P_{\hat{q} \rightarrow g g \bar{q}}^{(\text{nab})}(p_1, p_2, p_i) \rangle &= -s_{i12}^2 \frac{C_F C_A}{4} \mathcal{S}_{i,i}^{(\text{nab})}(p_1, p_2; \bar{n}) - \frac{C_A}{4 C_F} P_{\hat{q} \rightarrow g g \bar{q}}^{(\text{ab})}(p_1, p_2, p_i).\end{aligned}\tag{63}$$

Next we derive the radiator functions in covariant gauge. Their abelian components are given by

$$\begin{aligned}\mathcal{S}_{i,k;l,m}^{(\text{ab})}(q_1, q_2) &= \frac{s_{il} + s_{il1}}{2 s_{i1} s_{l1}} \frac{s_{km} + s_{km2}}{2 s_{k2} s_{m2}}, \\ \mathcal{S}_{i,k;l}^{(\text{ab})}(q_1, q_2) &= \frac{1}{s_{l12}} \left[\frac{s_{il}}{s_{i1} s_{l1}} \frac{s_{k1}}{s_{k2}} - \frac{s_{ik}}{2 s_{i1} s_{k2}} + \frac{s_{i2}}{2 s_{i1} s_{l2}} - \frac{s_{12}}{8 s_{l1} s_{l2}} \left(1 + \frac{2 s_{il}}{s_{i1}} \right) \left(1 + \frac{2 s_{kl}}{s_{k2}} \right) \right] + \left(\frac{i \leftrightarrow k}{1 \leftrightarrow 2} \right).\end{aligned}\tag{64}$$

The computation of the non-abelian components requires the introduction of external ghosts [77–80], because the currents corresponding to gluon 1 and 2 are not conserved independently. We find

$$\begin{aligned}\mathcal{S}_{i,k}^{(\text{nab})}(q_1, q_2) &= \left[\frac{3}{4} + \frac{(s_{i1} - s_{i2})(s_{k1} - s_{k2})}{4 s_{i12} s_{k12}} \right] \left[\frac{s_{ik}}{s_{i1} s_{12} s_{k2}} + \frac{s_{ik}}{s_{i2} s_{12} s_{k1}} - \frac{s_{ik}^2}{s_{i1} s_{k1} s_{i2} s_{k2}} \right] \\ &\quad + \frac{1}{s_{i1}} \left(\frac{s_{ik}}{s_{i2} s_{k1}} + \frac{1}{4 s_{i2}} + \frac{1}{2 s_{k2}} \right) + \frac{1}{s_{i12}} \left\{ \frac{2 s_{i1}}{s_{12}^2} - \frac{5}{4 s_{12}} - \frac{s_{ik} + s_{12}}{s_{i1} s_{k2}} - \frac{s_{12}}{8 s_{i1} s_{i2}} - \frac{s_{ik}}{s_{i1} s_{k1}} \left(1 + \frac{s_{12}}{s_{i2}} \right) \right\} \\ &\quad + \frac{1}{s_{i12} s_{k12}} \left\{ \frac{s_{i1}}{s_{12}} \left(\frac{3 s_{k2} + s_{k1}}{s_{i2}} - \frac{1}{2} \right) - \frac{2 s_{ik}}{s_{i1}} \left(1 + \frac{s_{i1}}{s_{12}} \right) - \frac{s_{12}(s_{ik} - s_{12})}{2 s_{i1} s_{k2}} - \frac{1}{4} \right. \\ &\quad \left. - \frac{1 - \varepsilon}{2} \frac{(s_{i1} - s_{i2})(s_{k1} - s_{k2})}{s_{12}^2} \right\} + (i \leftrightarrow k) + (1 \leftrightarrow 2) + \left(\frac{i \leftrightarrow k}{1 \leftrightarrow 2} \right).\end{aligned}\tag{65}$$

³ Note that the factor 1/4 relating the abelian and non-abelian scalar splitting function in Eq. (63) is a consequence of the color algebra leading to the definition of the non-abelian radiator function in Eq. (60). It therefore differs from the factor 1/2 obtained by direct diagrammatic calculation and resulting in the relation between the abelian and non-abelian splitting functions in Eqs. (42) and (43).

In the double-soft limit, Eq. (65) reduces to the double-soft function in Eq. (110) of Ref. [21].

D. Composition of one-to-three splitting functions

In this section, we present a decomposition of the splitting functions in Eqs. (34), (38), (40) and (42), and of the splitting tensors in Eqs. (45), (46) and (47). In most existing approaches, their singular components are identified by analyzing the strongly ordered soft and collinear limits, as well as the double soft limit. Knowing that the splitting functions are in fact just off-shell squared matrix elements in a particular gauge, we find it more useful to investigate their diagrammatic structure. This allows us to achieve a clean separation into the off-shell splitting tensors derived in Eqs. (16), (19) and (24), and the two-gluon scalar radiators in Eqs. (41) and (43), which are related via Eq. (63) to the general scalar radiators derived in Sec. III C 2.

1. Quark initial state

Equation (34) describes the splitting of a quark to a quark and a distinct flavor quark pair. The result is due to the sole Feynman diagram in Fig. 3 (a), hence the splitting function trivially factorizes and can be written as the product of Eqs. (16) and (19)

$$\langle P_{q \rightarrow \bar{q}' q' q}(p_1, p_2, p_3) \rangle = \frac{s_{123}}{s_{12}} \langle P_{q \rightarrow q}^{\mu\nu}(p_3, p_{12}) \rangle P_{g \rightarrow q, \mu\nu}(p_1, p_2). \quad (66)$$

By means of Eq. (16), the result can be assembled from the scalar radiator in Eq. (51), the magnetic remainder in Eq. (17), and the splitting function in Eq. (19)

$$\langle P_{q \rightarrow \bar{q}' q' q}(p_1, p_2, p_3) \rangle = \frac{s_{123}}{s_{12}} \left[\frac{C_F}{2} s_{123} \mathcal{S}_{3,3}^{\mu\nu}(p_{12}) + \langle P_{q \rightarrow q}^{(f)\mu\nu}(p_3, p_{12}) \rangle \right] P_{g \rightarrow q, \mu\nu}(p_1, p_2). \quad (67)$$

Equation (38) describes the splitting of a quark to a quark and a same flavor quark pair. The result involves both Feynman diagrams in Fig. 3, and hence it is expected that it cannot be fully factorized. The leading singularities do, however, originate in the two possible double-collinear limits. One can therefore express the splitting function in terms of its leading components and the interference term [21]

$$\begin{aligned} \langle P_{q \rightarrow \bar{q} q q}(p_1, p_2, p_3) \rangle &= \frac{s_{123}}{s_{12}} \langle P_{q \rightarrow q}^{\mu\nu}(p_3, p_{12}) \rangle P_{g \rightarrow q, \mu\nu}(p_1, p_2) + \frac{s_{123}}{s_{13}} \langle P_{q \rightarrow q}^{\mu\nu}(p_2, p_{13}) \rangle P_{g \rightarrow q, \mu\nu}(p_1, p_3) \\ &\quad + \langle P_{q \rightarrow \bar{q} q q}^{(p)}(p_1, p_2, p_3) \rangle, \end{aligned} \quad (68)$$

where

$$\langle P_{q \rightarrow \bar{q} q q}^{(p)}(p_1, p_2, p_3) \rangle = \langle P_{q \rightarrow \bar{q} q q}^{(\text{id})}(p_1, p_2, p_3) \rangle + (2 \leftrightarrow 3). \quad (69)$$

We will call $\langle P_{q \rightarrow \bar{q} q q}^{(p)} \rangle$ the (spin-averaged) pure $q \rightarrow q q \bar{q}$ splitting function, as it cannot be reconstructed from lower-order results. By means of Eq. (16), the splitting function can be assembled systematically from the scalar radiator in Eq. (51), the magnetic remainder in Eq. (17), the splitting function in Eq. (19), and the pure interference contribution

$$\begin{aligned} \langle P_{q \rightarrow \bar{q} q q}(p_1, p_2, p_3) \rangle &= \left\{ \frac{s_{123}}{s_{12}} \left[\frac{C_F}{2} s_{123} \mathcal{S}_{3,3}^{\mu\nu}(p_{12}) + \langle P_{q \rightarrow q}^{(f)\mu\nu}(p_3, p_{12}) \rangle \right] P_{g \rightarrow q, \mu\nu}(p_1, p_2) + (2 \leftrightarrow 3) \right\} \\ &\quad + \langle P_{q \rightarrow \bar{q} q q}^{(p)}(p_1, p_2, p_3) \rangle. \end{aligned} \quad (70)$$

Equation (40) describes the abelian component of a splitting of a quark to a quark and a pair of gluons. The result involves factorized contributions corresponding to the Feynman diagrams in Fig. 4(a) and (b), plus a non-factorizable component. It takes the simple form

$$\begin{aligned} \langle P_{q \rightarrow g g q}^{(\text{ab})}(p_1, p_2, p_3) \rangle &= \frac{s_{123}}{s_{13}} \langle P_{q \rightarrow q}(p_{13}, p_2) \rangle \langle P_{q \rightarrow q}(p_3, p_1) \rangle + \frac{s_{123}}{s_{23}} \langle P_{q \rightarrow q}(p_{23}, p_1) \rangle \langle P_{q \rightarrow q}(p_3, p_2) \rangle \\ &\quad + P_{q \rightarrow g g q}^{(\text{ab}, p)}(p_1, p_2, p_3) + \langle P_{q \rightarrow g g q}^{(\text{ab}, p, f)}(p_1, p_2, p_3) \rangle, \end{aligned} \quad (71)$$

which can be written in terms of the scalar radiator, Eq. (51), and the magnetic remainder, Eq. (17), as follows:

$$\begin{aligned} \langle P_{q \rightarrow g g q}^{(\text{ab})}(p_1, p_2, p_3) \rangle = & \left[\frac{C_F^2}{4} s_{123}^2 \mathcal{S}_{13;13}(p_2; \bar{n}) \mathcal{S}_{3;3}(p_1; \bar{n}) + \frac{C_F}{2} \frac{s_{123}^2}{s_{13}} \mathcal{S}_{13;13}(p_2; \bar{n}) \langle P_{q \rightarrow q}^{(\text{f})}(p_3, p_1) \rangle \right. \\ & + \frac{C_F}{2} s_{123} \langle P_{q \rightarrow q}^{(\text{f})}(p_{13}, p_2) \rangle \mathcal{S}_{3;3}(p_1; \bar{n}) + \frac{s_{123}}{s_{13}} \langle P_{q \rightarrow q}^{(\text{f})}(p_{13}, p_2) \rangle \langle P_{q \rightarrow q}^{(\text{f})}(p_3, p_1) \rangle + (1 \leftrightarrow 2) \Big] \\ & + P_{\bar{q} \rightarrow g g \bar{q}}^{(\text{ab}, p)}(p_1, p_2, p_3) + \langle P_{q \rightarrow g g q}^{(\text{ab}, p, \text{f})}(p_1, p_2, p_3) \rangle. \end{aligned} \quad (72)$$

The scalar remainder function, $P_{\bar{q} \rightarrow g g \bar{q}}^{(\text{ab}, p)}$, is defined as the difference between Eq. (63) and the factorized scalar contributions in the two different permutations induced by the diagrams in Fig. 4(a) and (b), with the fermion replaced by a scalar:

$$\begin{aligned} P_{\bar{q} \rightarrow g g \bar{q}}^{(\text{ab}, p)}(p_1, p_2, p_3) = & C_F^2 s_{123}^2 \left[\mathcal{S}_{3;3;3;3}^{(\text{ab})}(p_1, p_2; \bar{n}) + 2 \mathcal{S}_{3;3;3}^{(\text{ab})}(p_1, p_2; \bar{n}) + \mathcal{S}_{3;3}^{(\text{ab})}(p_1, p_2) \right. \\ & \left. - \frac{1}{4} \mathcal{S}_{13;13}(p_2; \bar{n}) \mathcal{S}_{3;3}(p_1; \bar{n}) - \frac{1}{4} \mathcal{S}_{23;23}(p_1; \bar{n}) \mathcal{S}_{3;3}(p_2; \bar{n}) \right] \\ = & C_F^2 \left\{ \frac{s_{123}^2}{s_{13} s_{23}} \frac{z_3^2}{z_1 z_2} - \frac{s_{123}}{s_{13}} \frac{2 z_3 (1 - z_2)}{z_1 z_2} + \frac{4 z_3}{z_1 z_2} + 1 - \varepsilon \right\} + (1 \leftrightarrow 2). \end{aligned} \quad (73)$$

The pure fermionic splitting contribution is defined as the overall remainder and is given by

$$\begin{aligned} \langle P_{q \rightarrow g g q}^{(\text{ab}, p, \text{f})}(p_1, p_2, p_3) \rangle = & C_F^2 (1 - \varepsilon) \left\{ \frac{s_{123}^2}{2 s_{13} s_{23}} z_3 \left(\frac{(z_1 + z_2)^2}{z_1 z_2} + \varepsilon \right) + \left(\frac{s_{12}}{s_{13}} + \frac{z_1 z_2}{(1 - z_2)^2} \right) (1 - \varepsilon) \right. \\ & \left. - \frac{s_{123}}{s_{13}} \left[(1 - z_2) \left(\frac{(z_1 + z_2)^2}{z_1 z_2} + 1 \right) + (1 - \varepsilon) \left(\frac{z_1 z_2}{1 - z_2} - z_3 \right) \right] + \frac{2 z_1}{z_2} \left(\frac{1}{1 - z_2} + \frac{z_3}{1 - z_1} \right) \right\} + (1 \leftrightarrow 2). \end{aligned} \quad (74)$$

To reconstruct the non-abelian part of the $q \rightarrow g g q$ splitting function, we first note that there is an additional factorization channel, corresponding to the diagram in Fig. 4(c), which is singular in the $1 \parallel 2$ collinear limit. In this configuration, Eq. (42) can be written as a gluon emission term, times a spin-correlated decay to two gluons. Due to color coherence, the non-abelian splitting function has no leading or sub-leading singularities associated with the $1 \parallel 3$ and $2 \parallel 3$ collinear limits. However, it does have single-soft singularities associated with the interferences between the diagrams in Fig. 4(c) and (a), and between the diagrams in Fig. 4(c) and (b). We therefore obtain the following result for its decomposition into lower-order components

$$\begin{aligned} \langle P_{q \rightarrow g g q}^{(\text{nab})}(p_1, p_2, p_3) \rangle = & \frac{C_F C_A}{4} s_{123}^2 \left[\bar{\mathcal{S}}_{3;3}(p_{12}; \bar{n}) \left(\mathcal{S}_{1;1}(p_2; \bar{n}) + \mathcal{S}_{2;2}(p_1; \bar{n}) - \mathcal{S}_{1;3}(p_2; \bar{n}) - \mathcal{S}_{2;3}(p_1; \bar{n}) \right) \right. \\ & \left. + 2(1 - \varepsilon) \mathcal{S}_{3;3}^{\mu\nu}(p_{12}; \bar{n}) D_\mu(p_1, p_2, \bar{n}) D_\nu(p_1, p_2, \bar{n}) \right] \\ & + \frac{C_A}{2} s_{123} \left[\langle P_{q \rightarrow q}^{(\text{f})}(p_3, p_{12}) \rangle \left(\mathcal{S}_{1;1}(p_2; \bar{n}) + \mathcal{S}_{2;2}(p_1; \bar{n}) - \mathcal{S}_{1;3}(p_2; \bar{n}) - \mathcal{S}_{2;3}(p_1; \bar{n}) \right) \right. \\ & \left. + 2(1 - \varepsilon) \langle P_{q \rightarrow q}^{(\text{f})\mu\nu}(p_3, p_{12}) \rangle D_\mu(p_1, p_2, \bar{n}) D_\nu(p_1, p_2, \bar{n}) \right] \\ & - \frac{C_A}{2 C_F} \left[P_{\bar{q} \rightarrow g g \bar{q}}^{(\text{ab}, p)}(p_1, p_2, p_3) + \langle P_{q \rightarrow g g q}^{(\text{ab}, p, \text{f})}(p_1, p_2, p_3) \rangle \right] \\ & + P_{\bar{q} \rightarrow g g \bar{q}}^{(\text{pnab}, p)}(p_1, p_2, p_3) + \langle P_{q \rightarrow g g q}^{(\text{pnab}, p, \text{f})}(p_1, p_2, p_3) \rangle. \end{aligned} \quad (75)$$

The shifted scalar radiator function, $\bar{\mathcal{S}}$, is defined as an extension of Eq. (50) to off-shell gluons

$$\bar{\mathcal{S}}_{i;k}(q_1; \bar{n}) = \mathcal{S}_{i;k}^{\mu\nu}(q_1; \bar{n}) d_{\mu\nu}(\bar{q}_1, \bar{n}) = \frac{1}{p_{i1}^2} \frac{2 z_i}{z_1} \left(1 - \frac{p_k^2}{p_{k1}^2} - \frac{q_1^2}{p_{k1}^2} \frac{z_{k1}}{z_1} \right) - \frac{2 p_i p_k}{p_{i1}^2 p_{k1}^2} + (i \leftrightarrow k). \quad (76)$$

The shifted momentum, \bar{q}_1 , is given by Eq. (11). It is not related to an actual alteration of the kinematics, but simply accounts for the fact that gluon propagators are evaluated in axial gauge. By means of Eq. (13) we can relate this to the fact that only transverse gluon polarizations appear in the factorizable components of Eq. (75). Equation (15) is a special case of this radiator, $P_{\bar{q} \rightarrow \bar{q}}(p_1, p_2) = C_F/2 s_{12} \bar{\mathcal{S}}_{1;1}(p_2, \bar{n})$.

The purely non-abelian component of the scalar splitting function is defined as the difference between the double-gluon emission result for scalar radiators, Eq. (43), and the corresponding factorized contributions. Using Eq. (63) to

make the origin of this splitting function in a dipole radiator manifest, we can write

$$\begin{aligned}
P_{\bar{q} \rightarrow gg\bar{q}}^{(\text{pnab},p)}(p_1, p_2, p_3) = & -\frac{C_F C_A}{4} s_{123}^2 \left[\mathcal{S}_{3;3}^{(\text{nab})}(p_1, p_2; \bar{n}) + \mathcal{S}_{3;3}^{(\text{ab})}(p_1, p_2) + 2\mathcal{S}_{3,3,3}^{(\text{ab})}(p_1, p_2; \bar{n}) \right. \\
& + \mathcal{S}_{3,3,3,3}^{(\text{ab})}(p_1, p_2; \bar{n}) + \bar{\mathcal{S}}_{3;3}(p_{12}; \bar{n}) \left(\mathcal{S}_{2;2}(p_1; \bar{n}) + \mathcal{S}_{1;1}(p_2; \bar{n}) - \mathcal{S}_{2;3}(p_1; \bar{n}) - \mathcal{S}_{1;3}(p_2; \bar{n}) \right) \\
& \left. + 2(1 - \varepsilon) \mathcal{S}_{3;3}^{\mu\nu}(p_{12}; \bar{n}) D_\mu(p_1, p_2, \bar{n}) D_\nu(p_1, p_2, \bar{n}) \right] + \frac{C_A}{2C_F} P_{\bar{q} \rightarrow gg\bar{q}}^{(\text{ab},p)}(p_1, p_2, p_3) .
\end{aligned} \tag{77}$$

The explicit form of this function is given by

$$\begin{aligned}
P_{\bar{q} \rightarrow gg\bar{q}}^{(\text{pnab},p)}(p_1, p_2, p_3) = & C_F C_A \left\{ \left(\frac{s_{23}}{s_{13}} - \frac{t_{13,2}}{2s_{13}} \right) \frac{(1 - z_2)^2}{2z_1 z_2} + \frac{s_{123}}{s_{12}} \left[\frac{s_{123}}{s_{13}} \left(\frac{z_3}{z_2} + \frac{z_1 - z_3}{1 - z_3} \right) - \frac{1 - z_1}{z_2} \right] \right. \\
& - \frac{s_{123}}{s_{13}} \left[\frac{3z_3(1 - z_2)}{2z_1 z_2} + \frac{1 - z_2}{1 - z_3} \left(1 - \frac{z_3}{z_1} \right) - \frac{2z_3}{(1 - z_3)^2} \right] - \frac{s_{12}}{s_{13}} \frac{2z_3(1 - z_2)}{z_1(1 - z_3)^2} \\
& \left. + \frac{2z_3(z_1 - z_2)}{z_2(1 - z_3)^2} + \frac{9z_3 + z_1^2}{4z_1 z_2} + \frac{1 - \varepsilon}{4} \right\} + (1 \leftrightarrow 2) .
\end{aligned} \tag{78}$$

In analogy to the purely non-abelian component of the scalar splitting function, we have defined a purely non-abelian component of the fermionic part of the splitting function. It is given by

$$\begin{aligned}
\langle P_{q \rightarrow ggq}^{(\text{pnab},p,f)}(p_1, p_2, p_3) \rangle = & C_F C_A \left\{ \frac{s_{123}}{2s_{13}} \left[\left(\frac{s_{123}}{s_{12}} - \frac{1 - z_2}{z_1} \right) \left(\frac{(1 - z_3)^2}{z_2} + \frac{z_2^2}{1 - z_3} \right) (1 - \varepsilon) - \frac{1 - z_2}{z_2} \right] \right. \\
& + \left[\frac{z_2}{z_1} \left(\frac{1}{1 - z_1} + \frac{z_3}{1 - z_2} \right) + \left(\frac{2z_2}{z_1} + 1 \right) \left(1 - \frac{3}{4} \frac{s_{123}}{s_{12}} (1 - z_3) \right) - \frac{3}{4} \right] (1 - \varepsilon) \\
& + \left(\frac{s_{12}}{s_{13}} + \frac{t_{13,2}}{2s_{13}} + \frac{1}{2} \right) \frac{(1 - z_2)^2}{2z_1 z_2} + \frac{(1 - \varepsilon)^2}{2} \left[1 + \frac{s_{12}}{s_{13}} + \frac{z_1}{1 - z_2} \left(\frac{z_2}{1 - z_2} - \frac{s_{123}}{s_{13}} \right) \right] \\
& \left. + \left(\frac{s_{123}}{s_{12}} \frac{1 - z_3}{z_1} + \frac{s_{123}}{s_{13}} \frac{1 - z_2}{z_1} - \frac{s_{123}^2}{s_{12}s_{13}} \right) \left(1 - z_3 - \frac{s_{12}}{s_{123}} \right) (1 - \varepsilon) \right\} + (1 \leftrightarrow 2) .
\end{aligned} \tag{79}$$

2. Gluon initial state

Equations (45) and (46) describe the splitting of a gluon to a gluon and a quark-antiquark pair. The results involve factorized contributions corresponding to each individual Feynman diagram in Fig. 5, plus a non-factorizable component. For the abelian part we find

$$\begin{aligned}
P_{g \rightarrow gq\bar{q}}^{\mu\nu(\text{ab})}(p_1, p_2, p_3) = & \left[\frac{C_F}{2} s_{123} P_{g \rightarrow q}^{\mu\nu}(p_{12}, p_3) \left(\mathcal{S}_{2;2}(p_1; \bar{n}) - \mathcal{S}_{2;3}(p_1; \bar{n}) \right) \right. \\
& \left. + \frac{s_{123}}{s_{12}} P_{g \rightarrow q}^{\mu\nu}(p_{12}, p_3) \langle P_{q \rightarrow q}^{(f)}(p_2, p_1) \rangle + (2 \leftrightarrow 3) \right] + P_{g \rightarrow gq\bar{q}}^{\mu\nu(\text{ab},p)}(p_1, p_2, p_3) + \dots .
\end{aligned} \tag{80}$$

Here and in the remainder of this section, the dots stand for terms proportional to \bar{n}^μ or \bar{n}^ν . These terms vanish after the splitting function is combined with a gluon current in the triple-collinear limit and can therefore be dropped, see the discussion following Eq. (13). Because a new scalar color dipole is created by the $g \rightarrow q\bar{q}$ splitting, Eq. (81) contains a soft singular contribution proportional to $P_{g \rightarrow q}^{\mu\nu}(p_2, p_3) \mathcal{S}_{2;3}(p_1; \bar{n})$. The abelian pure $g \rightarrow gq\bar{q}$ splitting function must in fact be interpreted as a subtracted single-gluon radiator function, similar to $P_{\bar{q} \rightarrow gg\bar{q}}^{(\text{ab},p)}$, but with a non-trivial helicity dependence. We find

$$\begin{aligned}
P_{g \rightarrow gq\bar{q}}^{\mu\nu(\text{ab},p)}(p_1, p_2, p_3) = & C_F T_R \left\{ \frac{2\varepsilon s_{123}}{s_{12}s_{13}} \tilde{p}_{1,23}^\mu \tilde{p}_{1,23}^\nu - d^{\mu\nu}(p_{123}, \bar{n}) \left[\frac{(s_{123} - s_{23})^2}{2s_{12}s_{13}} (1 + \varepsilon) - \frac{z_1(1 - \varepsilon)}{(1 - z_3)^2} \right] \right. \\
& - d^{\mu\nu}(p_{123}, \bar{n}) \left[\frac{s_{123}}{s_{12}} \frac{z_2}{z_1(1 - z_2)} + \frac{s_{23}}{s_{12}} \left(1 - \frac{z_2}{z_1} \frac{1 + z_1}{1 - z_2} \right) - \frac{1 - z_1}{z_1(1 - z_3)} + 1 \right] \\
& \left. + \left(d^{\mu\nu}(p_{123}, \bar{n}) - \frac{4\tilde{p}_{12,3}^\mu \tilde{p}_{12,3}^\nu}{s_{123}} \right) \left[\frac{s_{123}}{s_{12}} \left(\frac{z_1 - z_2}{z_1} - (1 - \varepsilon) \frac{z_1}{1 - z_3} \right) + \frac{s_{123}}{s_{13}} \frac{1 - z_2}{z_1} \right] \right\} + (2 \leftrightarrow 3) .
\end{aligned} \tag{81}$$

To reconstruct the components of the non-abelian splitting function, we first note that the non-abelian splitting function itself has no leading or sub-leading singularities associated with the $1 \parallel 2$ or $1 \parallel 3$ collinear limits. This is a consequence of color coherence. The $2 \parallel 3$ collinear limit projects Eq. (46) onto the product of a gluon emission term, times a spin-correlated decay to a quark-antiquark pair. Schematically,

$$P_{g \rightarrow gq\bar{q}}^{\mu\nu(\text{nab})}(p_1, p_2, p_3) = \frac{s_{123}}{s_{23}} P_{g \rightarrow g, (s)}^{\mu\nu, \alpha\beta}(p_1, p_{23}) P_{g \rightarrow q, \alpha\beta}(p_2, p_3) + \text{remainder} , \quad (82)$$

where $P_{g \rightarrow g, (s)}^{\mu\nu, \alpha\beta}(p_1, p_{23})$ is the symmetric part of the off-shell gluon splitting function, defined in Eq. (24). This gives the final expression for the assembly of the $g \rightarrow gq\bar{q}$ splitting function

$$\begin{aligned} P_{g \rightarrow gq\bar{q}}^{\mu\nu(\text{nab})}(p_1, p_2, p_3) = & \frac{C_A}{2} \frac{s_{123}^2}{s_{23}} \left[\mathcal{S}_{1;1}^{\alpha\beta}(p_{23}) P_{g \rightarrow q, \alpha\beta}(p_2, p_3) d^{\mu\nu}(p_{123}, \bar{n}) + \mathcal{S}_{23;23}(p_1; \bar{n}) P_{g \rightarrow q}^{\mu\nu}(p_2, p_3) \right] \\ & + \frac{C_A}{2} \frac{s_{123}^2}{s_{23}} 2(1 - \varepsilon) D^\mu(p_1, p_{23}, \bar{n}) D^\nu(p_1, p_{23}, \bar{n}) \langle P_{g \rightarrow q}(p_2, p_3) \rangle \\ & + \frac{C_A}{4} s_{123} \left[P_{g \rightarrow q}^{\mu\nu}(p_{12}, p_3) + P_{g \rightarrow q}^{\mu\nu}(p_2, p_{13}) \right] \mathcal{S}_{2;3}(p_1; \bar{n}) \\ & - \frac{C_A}{2C_F} P_{g \rightarrow gq\bar{q}}^{\mu\nu(\text{ab}, p)}(p_1, p_2, p_3) + P_{g \rightarrow gq\bar{q}}^{\mu\nu(\text{pnab}, p)}(p_1, p_2, p_3) + \dots \end{aligned} \quad (83)$$

The purely non-abelian component is given by

$$\begin{aligned} P_{g \rightarrow gq\bar{q}}^{\mu\nu(\text{pnab}, p)}(p_1, p_2, p_3) = & \frac{C_A T_R}{2} \left\{ -d^{\mu\nu}(p_{123}, \bar{n}) (1 - \varepsilon) \left(\frac{s_{123}}{s_{12}} \frac{z_1}{1 - z_3} - \frac{s_{13}}{s_{12}} - \frac{z_1}{(1 - z_3)^2} \right) \right. \\ & - d^{\mu\nu}(p_{123}, \bar{n}) \left[\frac{1 - 2z_1}{z_1} \left(\frac{s_{123}}{s_{12}} \frac{1 - z_3}{1 - z_1} + \frac{s_{123}}{s_{23}} - \frac{s_{123}^2}{s_{12}s_{23}} \frac{z_2}{1 - z_1} \right) - \frac{2}{z_1} - \frac{2z_2}{z_1(1 - z_3)} + 1 \right] \\ & + \frac{2(\tilde{p}_{2,13}^\mu \tilde{p}_{3,12}^\nu + \tilde{p}_{3,12}^\mu \tilde{p}_{2,13}^\nu)}{s_{23}} \frac{s_{123}}{s_{12}} \left[\frac{2z_2}{z_1} \frac{z_3 - z_1}{1 - z_1} + 1 - \varepsilon \right] + \frac{4\tilde{p}_{1,23}^\mu \tilde{p}_{1,23}^\nu}{s_{23}} \left[\frac{2z_2 z_3}{(1 - z_1)^2} - (1 - \varepsilon) \right] \\ & \left. - \frac{4\tilde{p}_{3,12}^\mu \tilde{p}_{3,12}^\nu}{s_{23}} \left[\frac{2z_2}{z_1} \left(\frac{s_{123}}{s_{12}} \frac{z_2}{1 - z_1} - \frac{s_{23}}{s_{12}} \right) - (1 - \varepsilon) \left(\frac{s_{123}}{s_{13}} + \frac{s_{23}}{s_{12}} \frac{z_1}{1 - z_3} \right) \right] - \frac{2}{z_1} \frac{4\tilde{p}_{2,3}^\mu \tilde{p}_{2,3}^\nu}{s_{23}} \right\} + (2 \leftrightarrow 3) . \end{aligned} \quad (84)$$

This expression is regular in the single-soft gluon limit, as well as in all double-collinear limits, see Sec. IIID 3.

Equation (47) describes the splitting of a gluon to three gluons. The result involves factorized contributions corresponding to each Feynman diagram containing a propagator, plus a non-factorizable component. To reconstruct the splitting function, we first note that only one transverse projector is needed, while all remaining terms can be inferred from the symmetry. We obtain

$$\begin{aligned} P_{g \rightarrow ggg}^{\mu\nu}(p_1, p_2, p_3) = & \left[\frac{1}{2} \frac{s_{123}}{s_{12}} P_{g \rightarrow g}^{\mu\nu, \alpha\beta}(p_3, p_{12}) P_{g \rightarrow g, \alpha\beta}(p_1, p_2) + \frac{C_A^2}{4C_F^2} P_{\bar{q} \rightarrow gq\bar{q}}^{\mu\nu(\text{ab}, p)}(p_1, p_2, p_3) d^{\mu\nu}(p_{123}, \bar{n}) \right. \\ & \left. + \frac{C_A}{2C_F} P_{\bar{q} \rightarrow gq\bar{q}}^{\mu\nu(\text{pnab}, p)}(p_1, p_2, p_3) d^{\mu\nu}(p_{123}, \bar{n}) + (5 \text{ permutations}) \right] + \text{remainder} . \end{aligned} \quad (85)$$

As in the case of the abelian and non-abelian $q \rightarrow gq\bar{q}$ splitting functions, we need to account for the fact that the full single-gluon dipole radiation pattern includes interference terms which appear explicitly in the three-parton splitting functions. Color coherence dictates that this overlap must factorize into the gluon splitting tensor and a single-gluon dipole radiator, while Bose symmetry requires that it appears in all permutations. The $g \rightarrow ggg$ splitting function can therefore be assembled as

$$\begin{aligned} P_{g \rightarrow ggg}^{\mu\nu}(p_1, p_2, p_3) = & \left\{ \frac{C_A}{4} s_{123} \left[\frac{s_{123}}{s_{12}} \mathcal{S}_{12;12}(p_3; \bar{n}) P_{g \rightarrow g}^{\mu\nu}(p_1, p_2) \right. \right. \\ & + \left(\frac{s_{123}}{s_{12}} \mathcal{S}_{3;3}^{\alpha\beta}(p_{12}) P_{g \rightarrow g, \alpha\beta}(p_1, p_2) - C_A s_{123} \bar{\mathcal{S}}_{3;3}(p_{12}; \bar{n}) \mathcal{S}_{2;3}(p_1; \bar{n}) \right) d^{\mu\nu}(p_{123}, \bar{n}) \\ & + 2(1 - \varepsilon) D^\mu(p_{12}, p_3, \bar{n}) D^\nu(p_{12}, p_3, \bar{n}) \left(\frac{s_{123}}{s_{12}} \langle P_{g \rightarrow g}(p_1, p_2) \rangle - \frac{C_A}{2} s_{123} \mathcal{S}_{2;3}(p_1; \bar{n}) \right) \Big] \\ & + \frac{C_A^2}{4C_F^2} P_{\bar{q} \rightarrow gq\bar{q}}^{\mu\nu(\text{ab}, p)}(p_1, p_2, p_3) d^{\mu\nu}(p_{123}, \bar{n}) + \frac{C_A}{2C_F} P_{\bar{q} \rightarrow gq\bar{q}}^{\mu\nu(\text{pnab}, p)}(p_1, p_2, p_3) d^{\mu\nu}(p_{123}, \bar{n}) \\ & \left. + (5 \text{ permutations}) \right\} + P_{g \rightarrow ggg}^{\mu\nu(p)}(p_1, p_2, p_3) + \dots \end{aligned}$$

Function $\times s_{123}^{-2}$	Definition	Scaling behavior for $\lambda \rightarrow 0$			
		$p_1 \rightarrow \lambda p_1, p_2 \rightarrow \lambda p_2$	$p_1 \rightarrow \lambda p_1$	$\tilde{p}_{1,2} \rightarrow \lambda \tilde{p}_{1,2}$	$\tilde{p}_{2,3} \rightarrow \lambda \tilde{p}_{2,3}$
$P_{\tilde{q} \rightarrow q' \tilde{q}' \tilde{q}}$	Eq. (36)	$\propto \lambda^{-4}$	–	$\propto \lambda^{-2}$	–
$\langle P_{q \rightarrow q \tilde{q} \tilde{q}}^{(p)} \rangle$	Eq. (69)	$\propto \lambda^{-3}$	–	$\propto \lambda^{-2}$	$\propto \lambda^{-2}$
$P_{\tilde{q} \rightarrow g g \tilde{q}}^{(\text{ab})}$	Eq. (41)	$\propto \lambda^{-4}$	$\propto \lambda^{-2}$	–	$\propto \lambda^{-2}$
$P_{\tilde{q} \rightarrow g g \tilde{q}}^{(\text{ab}, p)}$	Eq. (73)	$\propto \lambda^{-4}$	$\propto \lambda^{-1}$	–	$\propto \lambda^0$
$\langle P_{q \rightarrow g g q}^{(\text{ab})} \rangle$	Eq. (40)	$\propto \lambda^{-4}$	$\propto \lambda^{-2}$	–	$\propto \lambda^{-2}$
$\langle P_{q \rightarrow g g q}^{(\text{ab}, p, f)} \rangle$	Eq. (74)	$\propto \lambda^{-2}$	$\propto \lambda^{-1}$	–	$\propto \lambda^0$
$P_{\tilde{q} \rightarrow g g \tilde{q}}^{(\text{nab})}$	Eq. (43)	$\propto \lambda^{-4}$	$\propto \lambda^{-2}$	$\propto \lambda^{-2}$	–
$P_{\tilde{q} \rightarrow g g \tilde{q}}^{(\text{pnab}, p)}$	Eq. (78)	$\propto \lambda^{-4}$	$\propto \lambda^{-1}$	$\propto \lambda^0$	–
$\langle P_{q \rightarrow g g q}^{(\text{nab})} \rangle$	Eq. (42)	$\propto \lambda^{-4}$	$\propto \lambda^{-2}$	$\propto \lambda^{-2}$	–
$\langle P_{q \rightarrow g g q}^{(\text{pnab}, p, f)} \rangle$	Eq. (79)	$\propto \lambda^{-2}$	$\propto \lambda^{-1}$	$\propto \lambda^0$	–
$P_{g \rightarrow g q \tilde{q}}^{\mu\nu (\text{ab})}$	Eq. (45)	–	$\propto \lambda^{-2}$	–	$\propto \lambda^{-2}$
$P_{g \rightarrow g q \tilde{q}}^{\mu\nu (\text{ab}, p)}$	Eq. (81)	–	$\propto \lambda^{-1}$	–	$\propto \lambda^0$
$P_{g \rightarrow g q \tilde{q}}^{\mu\nu (\text{nab})}$	Eq. (46)	$\propto \lambda^{-4}$	$\propto \lambda^{-2}$	–	$\propto \lambda^{-2}$
$P_{g \rightarrow g q \tilde{q}}^{\mu\nu (\text{pnab}, p)}$	Eq. (84)	$\propto \lambda^{-3}$	$\propto \lambda^{-1}$	–	$\propto \lambda^0$
$P_{g \rightarrow g g g}^{\mu\nu}$	Eq. (47)	$\propto \lambda^{-4}$	$\propto \lambda^{-2}$	$\propto \lambda^{-2}$	
$P_{g \rightarrow g g g}^{\mu\nu (p)}$	Eq. (87)	$\propto \lambda^{-3}$	$\propto \lambda^{-1}$	$\propto \lambda^0$	

TABLE I. Scaling behavior of the tree-level splitting functions and their pure components. See the main text for details.

(86)

The relative prefactors of the abelian and pure non-abelian pure splitting functions, $P_{\tilde{q} \rightarrow g g \tilde{q}}^{(\text{ab}, p)}$ and $P_{\tilde{q} \rightarrow g g \tilde{q}}^{(\text{pnab}, p)}$, are due to the color structure of the scalar multipole radiator in the octet case, cf. Sec. IIIC, and the remainder function is defined as

$$\begin{aligned}
P_{g \rightarrow g g g}^{\mu\nu (p)}(p_1, p_2, p_3) = & C_A^2 \left\{ -d^{\mu\nu}(p_{123}, \bar{n}) \left[\frac{s_{123}}{s_{12}} \frac{z_2}{1-z_1} + \frac{s_{123}^2}{s_{12}s_{13}} \left(\frac{1-z_2^2-z_3^2}{2(1-z_2)(1-z_3)} - 1 \right) + \frac{4z_3}{z_1 z_2} \right] \right. \\
& + (1-\varepsilon) \frac{4\tilde{p}_{12,3}^\mu \tilde{p}_{12,3}^\nu}{s_{123}} \left[\frac{s_{123}^2}{s_{12}s_{13}} \left(\frac{z_1}{z_2} - \frac{z_1}{1-z_2} - \frac{1}{2} \right) + \frac{s_{123}}{2s_{13}} \frac{1-z_2}{z_1} \right. \\
& \quad \left. \left. - \frac{s_{123}}{s_{12}} \left(\frac{3(1-z_3)^2}{4z_1 z_2} + \frac{z_1 z_2}{(1-z_3)^2} - 2 \right) \right] \right. \\
& + (1-\varepsilon) \frac{\tilde{p}_{12,3}^\mu \tilde{p}_{2,13}^\nu + \tilde{p}_{2,13}^\mu \tilde{p}_{12,3}^\nu}{s_{123}} \frac{s_{123}^2}{s_{12}s_{13}} \left(3 - \frac{2z_2(1-z_2)}{z_3(1-z_3)} \right) \Big\} \\
& + \frac{C_A}{z_3} P_{g \rightarrow g}^{\mu\nu}(p_1, p_2) + (5 \text{ permutations}) .
\end{aligned} \tag{87}$$

3. Singularity structure of the remainder functions

Here we summarize the singularity structure of the various three-parton splitting functions introduced in Secs. IIIB and IIID. The kinematical limits are taken according to Ref. [21] and are parametrized in terms of a scaling parameter λ . In the limit where particle i becomes soft, λ enters the computation as $p_i \rightarrow \lambda p_i$. In the limit where particles i and j both become soft, λ enters the computation as $p_i \rightarrow \lambda p_i$ and $p_j \rightarrow \lambda p_j$. In the limit where particles i and j become collinear, λ enters the computation as $\tilde{p}_{i,j} \rightarrow \lambda \tilde{p}_{i,j}$. The results are given in Tab. I. A few comments are in order

- The function $\langle P_{q \rightarrow q \tilde{q} \tilde{q}}^{(p)} \rangle$ has a leading pole in the double-collinear limits because it constitutes a new type of interference term for which no unique Born splitting function exists at the next lower order.

- All other pure splitting functions are sub-leading in the single soft limits, and sub-sub-leading in the double-collinear limits. This is achieved by consistently subtracting the single-soft and double-collinear enhanced components, including spin correlations. We emphasize that the subtraction must be performed in the same axial gauge that has been used to determine the splitting functions, in order to avoid remainders which would create spurious singularities that cannot be removed systematically.
- The functions $P_{\tilde{q} \rightarrow gg\tilde{q}}^{(\text{ab},p)}$ and $P_{\tilde{q} \rightarrow gg\tilde{q}}^{(\text{pnab},p)}$ have leading poles in the double-soft limit. By means of Eqs. (73) and (77), these two splitting functions are identified as scalar radiators rather than genuine splitting functions. The double-soft singularities arise from interferences in the two-gluon emission pattern, which occur for the first time in the computation of the three-parton final state.
- All other pure splitting functions are sub-leading in the double-soft limit. As in the single-gluon radiator case, it is important that the scalar components are subtracted using the same gauge that was used to compute the full splitting function. In particular, using Eqs. (63) with radiator functions in covariant gauge would lead to an inconsistent result that contains spurious sub-leading poles.

IV. ONE-LOOP EXPRESSIONS

The one-to-two parton splitting functions at one loop have been discussed and computed in multiple ways [58, 60, 61, 81–84], and their soft limits have been analyzed in great detail [58, 61, 85]. In this section we derive a composition of the corresponding splitting amplitudes in terms of scalar and spin-dependent components, as needed for a correspondence with the treatment of the tree-level splitting functions in Sec. IIIB. We will also derive a generalization of the one-loop soft current in [22] and discuss its relation to the one-loop splitting amplitudes.

A. One-to-two splittings

The calculation is performed using the techniques of Ref. [58, 59]. As in the tree-level case, we make use of the conventional dimensional regularization scheme in $D = 4 - 2\varepsilon$ dimensions. Taking gauge invariance of on-shell amplitudes as a guiding principle, we evaluate t -channel gluon propagators in Feynman gauge, while s -channel gluon propagators are in light-like axial gauge. The calculation of one-loop splitting amplitudes was performed in FORM [86–88], with all standard and light-cone integrals cross-checked against the literature with the help of MATHEMATICA [89]. The reduction of tensor integrals was carried out using a dedicated implementation of the Passarino-Veltman scheme [90] using the FEYN CALC [91–93] package. All scalar and tensor integrals needed for the computation are listed in App. B. Following the notation of [58], we express the one-loop splitting amplitudes in terms of the basis functions

$$f_1(z) = \frac{2c_\Gamma}{\varepsilon^2} \left[-\Gamma(1-\varepsilon)\Gamma(1+\varepsilon)\frac{1}{z} \left(\frac{1-z}{z} \right)^\varepsilon - \frac{1}{z} + \frac{(1-z)^\varepsilon}{z} {}_2F_1(\varepsilon, \varepsilon, 1+\varepsilon, z) \right], \quad (88)$$

$$f_2 = -\frac{c_\Gamma}{\varepsilon^2}, \quad (89)$$

where

$$c_\Gamma = (4\pi)^\varepsilon \frac{\Gamma(1+\varepsilon)\Gamma^2(1-\varepsilon)}{\Gamma(1-2\varepsilon)}. \quad (90)$$

Note that, in contrast to [58], we have chosen to pull out a factor of $1/(4\pi)^2$ from the definition of c_Γ .

Unlike the tree-level $1 \rightarrow 2$ splittings considered earlier, where it was important to track the momentum fractions z_1 and z_2 in order to use them as building blocks for $1 \rightarrow 3$ splitting functions, in this section we simply identify $z_1 \equiv z$ and $z_2 \equiv 1 - z$.

1. Quark initial state

The $q \rightarrow qg$ splitting amplitude at one-loop order is determined from the diagrams shown in Fig. 10. It has been shown that due to the gauge invariance of the sum of cut diagrams, any t -channel gluon propagators can be evaluated

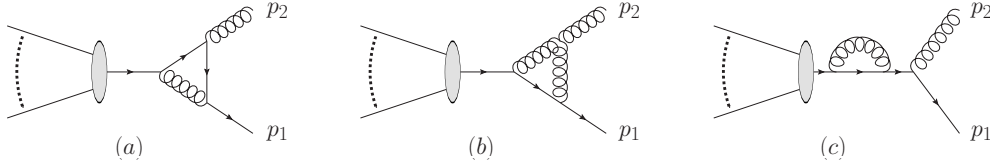


FIG. 10. Feynman diagrams leading to the $1 \rightarrow 2$ quark splitting function at one loop discussed in Sec. IV A 1.

in Feynman gauge [58, 59], which substantially simplifies the calculation. For future reference, we introduce the tree-level quark-splitting amplitude,

$$\mathcal{P}_{q \rightarrow qg}^{(0)}(p_1, p_2) = g_s T_{ij}^a \bar{u}(p_1) \not{\epsilon}^*(p_2) \not{p}_{12} u(n). \quad (91)$$

Using the results of App. B, the integration of the abelian contribution in Fig. 10(a) yields

$$\begin{aligned} \mathcal{P}_{q \rightarrow qg}^{(1),a}(p_1, p_2) &= \frac{g_s^2}{16\pi^2} \left(C_F - \frac{C_A}{2} \right) \left(-\frac{\mu^2}{s_{12}} \right)^\epsilon \left[z f_1(z) + \left(\frac{2}{1-2\epsilon} - \epsilon \right) f_2 \right] \mathcal{P}_{q \rightarrow qg}^{(0)}(p_1, p_2) \\ &\quad - \frac{g_s^3}{16\pi^2} T_{ij}^a \left(C_F - \frac{C_A}{2} \right) \left(-\frac{\mu^2}{s_{12}} \right)^\epsilon \frac{2}{s_{12}} \frac{\epsilon^2}{1-2\epsilon} f_2 \bar{u}(p_1) \not{p}_2 \not{p}_{12} u(n) (p_1 \epsilon^*(p_2)). \end{aligned} \quad (92)$$

The non-abelian contribution in Fig. 10(b) is given by

$$\begin{aligned} \mathcal{P}_{q \rightarrow qg}^{(1),b}(p_1, p_2) &= \frac{g_s^2}{16\pi^2} \frac{C_A}{2} \left(-\frac{\mu^2}{s_{12}} \right)^\epsilon \left[(1-z) f_1(1-z) + \frac{4-5\epsilon}{1-2\epsilon} f_2 \right] \mathcal{P}_{q \rightarrow qg}^{(0)}(p_1, p_2) \\ &\quad + \frac{g_s^3}{16\pi^2} T_{ij}^a \frac{C_A}{2} \left(-\frac{\mu^2}{s_{12}} \right)^\epsilon \frac{2}{s_{12}} \frac{\epsilon^2}{1-2\epsilon} f_2 \bar{u}(p_1) \not{p}_2 \not{p}_{12} u(n) (p_1 \epsilon^*(p_2)). \end{aligned} \quad (93)$$

The self-energy in Fig. 10(c) yields

$$\mathcal{P}_{q \rightarrow qg}^{(1),c}(p_1, p_2) = -\frac{g_s^2}{16\pi^2} C_F \left(-\frac{\mu^2}{s_{12}} \right)^\epsilon \frac{(4-\epsilon)(1-\epsilon)}{1-2\epsilon} f_2 \mathcal{P}_{q \rightarrow qg}^{(0)}(p_1, p_2). \quad (94)$$

The complete splitting amplitude is given by the sum of the above terms and reads [58, 61]

$$\begin{aligned} \mathcal{P}_{q \rightarrow qg}^{(1)}(p_1, p_2) &= \frac{g_s^2}{16\pi^2} \frac{C_A}{2} \left(-\frac{\mu^2}{s_{12}} \right)^\epsilon \left[(1-z) f_1(1-z) - \frac{1}{N_C^2} (z f_1(z) - 2 f_2) \right] \mathcal{P}_{q \rightarrow qg}^{(0)}(p_1, p_2) \\ &\quad - \frac{g_s^3}{16\pi^2} T_{ij}^a \left(\frac{N_C}{2} + \frac{1}{2N_C} \right) \left(-\frac{\mu^2}{s_{12}} \right)^\epsilon \left[\bar{u}(p_1) \not{\epsilon}^*(p_2) \not{p}_{12} u(n) - \frac{2}{s_{12}} \bar{u}(p_1) \not{p}_2 \not{p}_{12} u(n) (p_1 \epsilon^*(p_2)) \right] \frac{\epsilon^2}{1-2\epsilon} f_2. \end{aligned} \quad (95)$$

The scalar one-loop splitting amplitude corresponding to the $q \rightarrow qg$ case is determined from the three diagrams in Fig. 10 and the bubble-type diagrams involving seagull vertices. However, the latter vanish in light-like axial gauge. Upon integration of the loop momentum, the abelian contribution corresponding to the scalar analogue of Fig. 10(a) is given by

$$\mathcal{P}_{\bar{q} \rightarrow \bar{q}g}^{(1),a}(p_1, p_2) = \frac{g_s^2}{16\pi^2} \left(C_F - \frac{C_A}{2} \right) \left(-\frac{\mu^2}{s_{12}} \right)^\epsilon \left[z f_1(z) + \frac{2}{1-2\epsilon} f_2 \right] \mathcal{P}_{\bar{q} \rightarrow \bar{q}g}^{(0)}(p_1, p_2), \quad (96)$$

where we have introduced the tree-level (anti-)triplet scalar amplitude

$$\mathcal{P}_{\bar{q} \rightarrow \bar{q}g}^{(0)}(p_1, p_2) = g_s T_{ij}^a (2p_1^\mu \epsilon_\mu^*(p_2)). \quad (97)$$

The non-abelian contribution, corresponding to the scalar version of Fig. 10(b), reads

$$\mathcal{P}_{\bar{q} \rightarrow \bar{q}g}^{(1),b}(p_1, p_2) = \frac{g_s^2}{16\pi^2} \frac{C_A}{2} \left(-\frac{\mu^2}{s_{12}} \right)^\epsilon \left[(1-z) f_1(1-z) + \frac{4(1-\epsilon)}{1-2\epsilon} f_2 \right] \mathcal{P}_{\bar{q} \rightarrow \bar{q}g}^{(0)}(p_1, p_2), \quad (98)$$

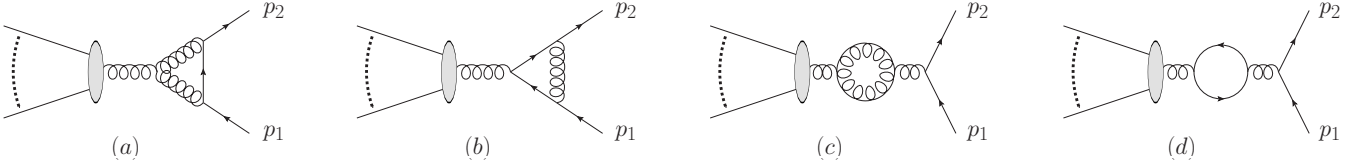


FIG. 11. Feynman diagrams leading to the $1 \rightarrow 2$ gluon-to-quark splitting function at one loop discussed in Sec. IV A 2.

while the scalar counterpart of the self-energy in Fig. 10(c) yields

$$\mathcal{P}_{\bar{q} \rightarrow \bar{q}g}^{(1),c}(p_1, p_2) = -\frac{g_s^2}{16\pi^2} C_F \left(-\frac{\mu^2}{s_{12}} \right)^\varepsilon \frac{4(1-\varepsilon)}{1-2\varepsilon} f_2 \mathcal{P}_{\bar{q} \rightarrow \bar{q}g}^{(0)}(p_1, p_2). \quad (99)$$

Combining the three contributions gives the (anti-)triplet scalar one-loop splitting amplitude

$$\mathcal{P}_{\bar{q} \rightarrow \bar{q}g}^{(1)}(p_1, p_2) = \frac{g_s^2}{16\pi^2} \frac{C_A}{2} \left(-\frac{\mu^2}{s_{12}} \right)^\varepsilon \left[(1-z)f_1(1-z) - \frac{1}{N_C^2} (zf_1(z) - 2f_2) \right] \mathcal{P}_{\bar{q} \rightarrow \bar{q}g}^{(0)}(p_1, p_2). \quad (100)$$

We note that this result has the same singularity structure as $\mathcal{P}_{q \rightarrow qg}^{(1)}$, given by the first line of Eq. (95).

2. Gluon initial state

There are two one-to-two splittings initiated by a gluon, $g \rightarrow q\bar{q}$ and $g \rightarrow gg$. The calculation of the corresponding splitting functions is again performed in light-like axial gauge, as this gauge choice reflects the physical degrees of freedom in the gluon propagators. As before, due to the gauge invariance of the on-shell amplitude arising from the sum of cut diagrams, any t -channel gluon propagator can be evaluated in Feynman gauge [58, 59].

The one-loop $g \rightarrow q\bar{q}$ splitting function is determined by the four diagrams in Fig. 11. In diagrams (a) and (c), the s -channel gluon loop momenta are labeled by k and $p_1 + p_2 - k$, in diagrams (b) and (d) the same denote the quark and anti-quark loop momenta. Integrands involving two light-cone denominators are rewritten using the partial fractioning,

$$\frac{1}{(kn)((p_1 + p_2 - k)n)} = \frac{1}{n(p_1 + p_2)} \left(\frac{1}{kn} + \frac{1}{(p_1 + p_2 - k)n} \right), \quad (101)$$

and a subsequent shift of the loop momentum $k \rightarrow -k + p_1 + p_2$ in the second term. This allows us to express all amplitudes in terms of the loop integrals in App. B.

For the triangle contributions in Figs. 11(a) and 11(b), integration of the loop momentum leads to

$$\mathcal{P}_{g \rightarrow q\bar{q}}^{(1),a}(p_1, p_2) = \frac{g_s^2}{16\pi^2} C_A \left(-\frac{\mu^2}{s_{12}} \right)^\varepsilon \left[zf_1(z) + (1-z)f_1(1-z) + \frac{4-5\varepsilon}{1-2\varepsilon} f_2 \right] \mathcal{P}_{g \rightarrow q\bar{q}}^{(0)}(p_1, p_2), \quad (102)$$

$$\mathcal{P}_{g \rightarrow q\bar{q}}^{(1),b}(p_1, p_2) = -\frac{g_s^2}{16\pi^2} (C_A - 2C_F) \left(-\frac{\mu^2}{s_{12}} \right)^\varepsilon \left(\frac{2}{1-2\varepsilon} - \varepsilon \right) f_2 \mathcal{P}_{g \rightarrow q\bar{q}}^{(0)}(p_1, p_2), \quad (103)$$

with the tree-level gluon-to-quark splitting amplitude

$$\mathcal{P}_{g \rightarrow q\bar{q}}^{(0)}(p_1, p_2) = g_s T_{ij}^a \bar{u}(p_2) \not{\epsilon}(p_{12}) v(p_1). \quad (104)$$

The vacuum polarization diagrams in Fig. 11(c) and 11(d) are given by

$$\mathcal{P}_{g \rightarrow q\bar{q}}^{(1),c}(p_1, p_2) = -\frac{g_s^2}{16\pi^2} C_A \left(-\frac{\mu^2}{s_{12}} \right)^\varepsilon \frac{6(1-\varepsilon)(4-3\varepsilon)}{(1-2\varepsilon)(3-2\varepsilon)} f_2 \mathcal{P}_{g \rightarrow q\bar{q}}^{(0)}(p_1, p_2), \quad (105)$$

$$\mathcal{P}_{g \rightarrow q\bar{q}}^{(1),d}(p_1, p_2) = \frac{g_s^2}{16\pi^2} T_R n_f \left(-\frac{\mu^2}{s_{12}} \right)^\varepsilon \frac{4(1-\varepsilon)\varepsilon}{(1-2\varepsilon)(3-2\varepsilon)} f_2 \mathcal{P}_{g \rightarrow q\bar{q}}^{(0)}(p_1, p_2). \quad (106)$$

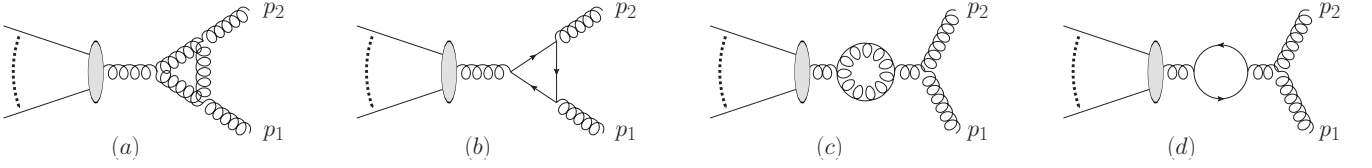


FIG. 12. Feynman diagrams leading to the $1 \rightarrow 2$ gluon-to-gluon splitting function at one loop discussed in Sec. IV A 2.

The full splitting function is given by the sum of the terms above [58, 61],

$$\begin{aligned} \mathcal{P}_{g \rightarrow q\bar{q}}^{(1)}(p_1, p_2; n) = & \frac{g_s^2}{16\pi^2} \left(-\frac{\mu^2}{s_{12}} \right)^\varepsilon \left[C_A \left(z f_1(z) + (1-z) f_1(1-z) - \left(2 + \frac{3(2-\varepsilon)}{(1-2\varepsilon)(3-2\varepsilon)} \right) f_2 \right) \right. \\ & \left. - \frac{1}{N_C} \left(\frac{2}{1-2\varepsilon} - \varepsilon \right) f_2 + T_R n_f \frac{4(1-\varepsilon)\varepsilon}{(1-2\varepsilon)(3-2\varepsilon)} f_2 \right] \mathcal{P}_{g \rightarrow q\bar{q}}^{(0)}(p_1, p_2). \end{aligned} \quad (107)$$

The diagrams leading to the one-loop $g \rightarrow gg$ splitting amplitude are shown in Fig. 12. The additional bubble-like amplitude involving the four-gluon vertex vanishes in light-like axial gauge and is not shown. In diagrams (a) and (c), the s -channel gluon loop momenta are again denoted by k and $p_1 + p_2 - k$, whereas these label the s -channel quark-loop momenta in diagram (b) and (d). The tree-level splitting amplitude is given by

$$\mathcal{P}_{g \rightarrow gg}^{(0)}(p_1, p_2) = 2g_s f^{abc} [\varepsilon^*(p_1) \cdot \varepsilon^*(p_2) \varepsilon(p_{12}) \cdot p_2 + \varepsilon(p_{12}) \cdot \varepsilon^*(p_1) \varepsilon^*(p_2) \cdot p_1 - \varepsilon(p_{12}) \cdot \varepsilon^*(p_2) \varepsilon^*(p_1) \cdot p_2]. \quad (108)$$

After integrating over the loop momentum, the triangle diagrams Fig. 12(a) and Fig. 12(b) yield

$$\begin{aligned} \mathcal{P}_{g \rightarrow gg}^{(1,a)}(p_1, p_2; n) = & \frac{g_s^2}{16\pi^2} \frac{C_A}{2} \left(-\frac{\mu^2}{s_{12}} \right)^\varepsilon \left[\left(z f_1(z) + (1-z) f_1(1-z) \right. \right. \\ & \left. \left. + \left(\frac{6(1-\varepsilon)(4-3\varepsilon)}{(1-2\varepsilon)(3-2\varepsilon)} - 2 \right) f_2 \right) \mathcal{P}_{g \rightarrow gg}^{(0)}(p_1, p_2) \right. \\ & \left. + g_s f^{abc} \frac{2\varepsilon^2}{(1-2\varepsilon)(3-2\varepsilon)} f_2 \left(\varepsilon^*(p_1) \cdot \varepsilon^*(p_2) - \frac{2\varepsilon^*(p_2) \cdot p_1 \varepsilon^*(p_1) \cdot p_2}{s_{12}} \right) \varepsilon(p_{12}) \cdot (p_1 - p_2) \right], \end{aligned} \quad (109)$$

$$\begin{aligned} \mathcal{P}_{g \rightarrow gg}^{(1,b)}(p_1, p_2; n) = & \frac{g_s^2}{16\pi^2} T_R n_f \left(-\frac{\mu^2}{s_{12}} \right)^\varepsilon \left[-\frac{2(1-\varepsilon)\varepsilon}{(1-2\varepsilon)(3-2\varepsilon)} f_2 \mathcal{P}_{g \rightarrow gg}^{(0)}(p_1, p_2) \right. \\ & \left. - g_s f^{abc} \frac{\varepsilon^2}{(1-\varepsilon)(1-2\varepsilon)(3-2\varepsilon)} f_2 \left(\varepsilon^*(p_1) \cdot \varepsilon^*(p_2) - \frac{2\varepsilon^*(p_2) \cdot p_1 \varepsilon^*(p_1) \cdot p_2}{s_{12}} \right) \varepsilon(p_{12}) \cdot (p_1 - p_2) \right]. \end{aligned} \quad (110)$$

The two vacuum-polarization diagrams Fig. 12(c) and 12(d) read

$$\mathcal{P}_{g \rightarrow gg}^{(1,c)}(p_1, p_2; n) = -\frac{g_s^2}{16\pi^2} \frac{C_A}{2} \left(-\frac{\mu^2}{s_{12}} \right)^\varepsilon \frac{6(1-\varepsilon)(4-3\varepsilon)}{(1-2\varepsilon)(3-2\varepsilon)} f_2 \mathcal{P}_{g \rightarrow gg}^{(0)}(p_1, p_2), \quad (111)$$

$$\mathcal{P}_{g \rightarrow gg}^{(1,d)}(p_1, p_2; n) = \frac{g_s^2}{16\pi^2} T_R n_f \left(-\frac{\mu^2}{s_{12}} \right)^\varepsilon \frac{2(1-\varepsilon)\varepsilon}{(1-2\varepsilon)(3-2\varepsilon)} f_2 \frac{1}{2} \mathcal{P}_{g \rightarrow gg}^{(0)}(p_1, p_2). \quad (112)$$

The complete splitting amplitude is given by the sum of the above terms and reads [58, 61]

$$\begin{aligned} \mathcal{P}_{g \rightarrow gg}^{(1)}(p_1, p_2) = & \frac{g_s^2}{16\pi^2} \frac{C_A}{2} \left(-\frac{\mu^2}{s_{12}} \right)^\varepsilon \left[\left(z f_1(z) + (1-z) f_1(1-z) - 2f_2 \right) \mathcal{P}_{g \rightarrow gg}^{(0)}(p_1, p_2) \right. \\ & + g_s f^{abc} \left(1 - \frac{T_R n_f}{N_C} \frac{1}{1-\varepsilon} \right) \frac{2\varepsilon^2}{(1-2\varepsilon)(3-2\varepsilon)} f_2 \\ & \left. \times \left(\varepsilon^*(p_1) \cdot \varepsilon^*(p_2) - \frac{2\varepsilon^*(p_2) \cdot p_1 \varepsilon^*(p_1) \cdot p_2}{s_{12}} \right) \varepsilon(p_{12}) \cdot (p_1 - p_2) \right]. \end{aligned} \quad (113)$$

In order to extract the scalar component of the $g \rightarrow gg$ splitting amplitude, we decompose the triple-gluon vertex according to Eq. (5). For diagram 12(a), the scalar can be routed in two ways, which correspond to the fermion flow of

Fig. 10(a) and (b). Their contributions agree with Eqs. (96) and (98) up to color factors. Diagram 12(c) also gives two contributions, corresponding to routing the scalar piece on each propagator of the loop. These are trivially identical and the sum agrees with Eq. (99) up to color factors. Diagrams 12(b) and 12(d) do not contribute, as they do not contain triple-gluon vertices linking the initial- and final-state gluons. The scalar decomposition of the amplitudes corresponding to Fig.12 can therefore be identified as

$$\mathcal{P}_{g \rightarrow gg}^{(1, \text{sc})}(p_1, p_2; n) = \frac{g_s^3}{16\pi^2} f^{abc} C_A \left(-\frac{\mu^2}{s_{12}} \right)^\varepsilon \left[z f_1(z) + (1-z) f_1(1-z) - 2 f_2 \right] \times (\varepsilon(p_{12}) \cdot \varepsilon^*(p_1) \varepsilon^*(p_2) \cdot p_1 - \varepsilon(p_{12}) \cdot \varepsilon^*(p_2) \varepsilon^*(p_1) \cdot p_2) . \quad (114)$$

As expected this reproduces the pole structure of the full splitting function, $\mathcal{P}_{g \rightarrow gg}^{(1)}$, i.e., the first line of Equation (113). Accounting for the symmetry of the two-gluon final state (see Eq. (5) and Fig. 1(b)), we can read off the one-loop splitting function for a color adjoint scalar,

$$\mathcal{P}_{g \rightarrow g}^{(1, \text{sc})}(p_1, p_2; n) = \frac{g_s^3}{16\pi^2} f^{abc} \frac{C_A}{2} \left(-\frac{\mu^2}{s_{12}} \right)^\varepsilon \left[z f_1(z) + (1-z) f_1(1-z) - 2 f_2 \right] 2 p_1^\mu \varepsilon_\mu^*(p_2) . \quad (115)$$

B. Scalar multipoles

The starting point for the computation of the one-loop scalar radiation pattern is an extension of the decomposition of the soft one-loop amplitude in Eq. (38) of Ref. [22]. It states that, in the soft gluon limit, one can write the matrix element as

$$|\mathcal{M}_{\text{soft}}^{(1)}(q, \{p\})\rangle = \mu^{2\varepsilon} \varepsilon^\mu(q) \mathbf{J}_\mu(q) |\mathcal{M}^{(1)}\rangle + \left(|\mathcal{M}_{\text{soft}}^{(1)}(q, \{p\})\rangle - \mu^{2\varepsilon} \varepsilon^\mu(q) \mathbf{J}_\mu(q) |\mathcal{M}^{(1)}(\{p\})\rangle \right) . \quad (116)$$

The non-factorizable one-loop soft corrections are contained in $|\mathcal{M}_{\text{soft}}^{(1)}(q, \{p\})\rangle$. They can be computed using eikonal Feynman rules. Their explicit poles follow a dipole radiation pattern described by Catani's infrared singularity operators [19, 20]. The natural extension of Eq. (116) to the case of scalar radiators is therefore given by a dipole approximation to the hard process producing the scalar particles. As the matrix elements in this approximation may not include all Feynman diagrams, a systematic and manifestly gauge-invariant approach to the one-loop computation is indispensable. This problem is solved by the background field method [31–36]. The technique allows to obtain individually renormalizable n -point Greens functions that obey the naive Ward identities and are thus physically meaningful quantities. The extension of Eq. (116) reads

$$|\mathcal{M}_{\text{approx}}^{(1)}(q, \{p\})\rangle = \mu^{2\varepsilon} \varepsilon^\mu(q) \mathbf{J}_\mu(q) |\mathcal{M}^{(1)}\rangle + \left(|\mathcal{M}_{\text{BGF, dip}}^{(1)}(q, \{p\})\rangle - \mu^{2\varepsilon} \varepsilon^\mu(q) \mathbf{J}_\mu(q) |\mathcal{M}^{(1)}(\{p\})\rangle \right) , \quad (117)$$

where, $|\mathcal{M}_{\text{BGF, dip}}^{(1)}(q, \{p\})\rangle$ consists of a sum over all dipole contributions and one-particle reducible contributions in the background field technique. We will compute them in the following subsections, using a number of standard methods [90, 94] and tools [86–88, 91–93, 95–98]. Due to the spin-independence of the soft-gluon limit of the one-loop matrix element, Eq. (117) reproduces Eq. (116), but it includes additional terms at sub-leading power in the soft scaling parameter.

We begin with a single term in the dipole approximation, where the antenna is formed by massless scalars with momenta p_i and p_k and color indices i and k . They radiate a gluon of momentum q_1 and color index a . All momenta are considered outgoing. To simplify the notation, we define the invariants

$$s = (p_i + p_k)^2 , \quad t = (p_i + q_1)^2 , \quad u = (p_k + q_1)^2 , \quad \text{and} \quad Q^2 = (p_i + p_k + q_1)^2 . \quad (118)$$

The leading-order diagrams are shown in Fig. 7, and the leading-order dipole component of the current is defined in Eq. (3).

1. Factorizable contributions

We first derive the factorizable one-loop corrections to the production of the scalars. The relevant diagrams are shown in Fig. 13. The one-loop scalar integrals are listed in App. B. Diagrams of type (a) and (b) are given by the leading-order current, times the scalar self energy, which, for a scalar of virtuality p^2 , is given by

$$\hat{\Sigma}_{ij}(p) = -\frac{g_s^2}{16\pi^2} C_F \delta_{ij} 2p^2 \hat{I}_2(p^2) . \quad (119)$$

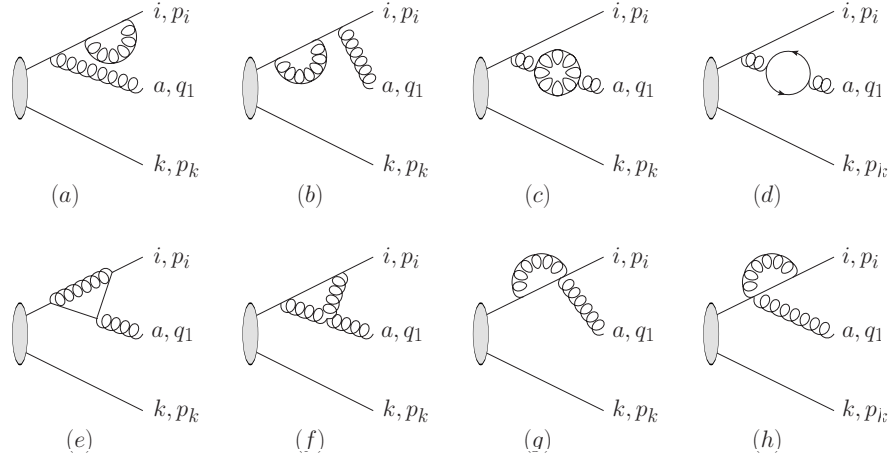


FIG. 13. Factorizable one-loop corrections to the scalar-scalar interference.

Diagrams of type (c) are given by the leading-order current times the C_A part of the vacuum polarization, which, for a gluon of virtuality q^2 is given by

$$\hat{\Pi}_{\mu\nu}^{ab}(q) = -\frac{g_s^2}{16\pi^2} C_A \delta^{ab} P_{\mu\nu}(q) q^2 \hat{I}_2(q^2) \frac{11 - 7\varepsilon}{3 - 2\varepsilon}, \quad \text{where} \quad P^{\mu\nu}(q) = -g^{\mu\nu} + \frac{q^\mu q^\nu}{q^2}. \quad (120)$$

Diagrams of type (d) are given by the leading-order current times the fermionic (n_f part) of the vacuum polarization, which, for a gluon of virtuality q^2 , is given by

$$\hat{\Pi}_{\mu\nu}^{ab(f)}(q) = -\frac{g_s^2}{16\pi^2} T_R n_f \delta^{ab} P_{\mu\nu}(q) q^2 \hat{I}_2(q^2) \frac{4 - 4\varepsilon}{3 - 2\varepsilon}. \quad (121)$$

This contribution is needed as the virtual correction corresponding to Eq. (56), which is schematically shown in Fig. 8. Diagrams of type (e), (f), (g) and (h) are given in terms of the leading-order current, times the vertex correction to the scalar-scalar-gluon vertex, which is given by

$$\hat{\Gamma}_{S,ij}^{\mu,a}(q,p,k) = \frac{g_s^3}{16\pi^2} 2C_F T_{ij}^a \frac{p^\mu}{pk} \left(q^2 \hat{I}_2(q^2) - p^2 \hat{I}_2(p^2) \right), \quad \text{where} \quad q^\mu = p^\mu + k^\mu. \quad (122)$$

As the vertex corrections in the background field method satisfy the naive Ward identities, their abelian contribution cancels the self energies from diagrams of type (a) and (b), while the non-abelian component vanishes identically. This provides the generalization of the soft-gluon result for diagrams of class A in Sec. 4.2 of Ref. [22].

In addition to the self energy, vacuum polarization and vertex correction, we obtain the factorizable one-loop corrections in diagrams of type (c) and (e) of Fig. 14. They are quantum corrections to the production of the charged scalars, times a leading-order current. The result for diagrams of type (c) is given by

$$I_{h,f}(Q^2, t) = -\frac{g_s^2}{16\pi^2} \hat{\mathbf{T}}_i^b \hat{\mathbf{T}}_k^b \left((2Q^2 - t) \hat{I}_3^{2m}(Q^2, t) + \hat{I}_2(Q^2) - \hat{I}_2(t) \right). \quad (123)$$

In the limit $t \rightarrow 0$, the term in parentheses reduces to $2Q^2 \hat{I}_3^{1m}(Q^2) + \hat{I}_2(Q^2)$, which yields the result for diagrams of type (e).

2. Box-type contributions

To obtain a gauge invariant set of box-type diagrams, we combine the box and seagull diagrams in Fig. 14(a), (b) and (d) and add the factorizable contributions in diagrams (c) and (e). In diagrams of type (e), the final-state gluon is emitted off a color charged particle other than i or j , hence the result only depends on s and a leading-order current.

$$I_f(s, \{\vec{p}\}) = \frac{g_s^3}{16\pi^2} \hat{\mathbf{T}}_i^b \hat{\mathbf{T}}_k^b \left[2s \hat{I}_3^{1m}(s) + \hat{I}_2(s) \right] \sum_{l \neq i,k} \hat{\mathbf{T}}_l^a \frac{p_l^\mu}{2p_l q_1} \epsilon_\mu^*(q_1). \quad (124)$$

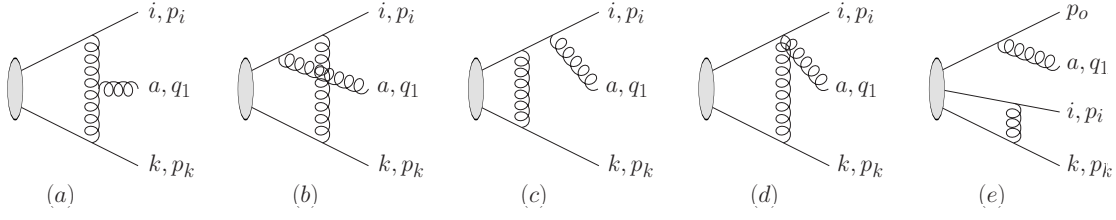


FIG. 14. Box-type diagrams contributing to the scalar-scalar interference at one loop.

We combine these terms with the factorized contribution $-\mu^{2\varepsilon}\varepsilon^\mu(q)\mathbf{J}_\mu(q)|\mathcal{M}^{(1)}(\{p\})\rangle$ in Eq. (117), which can be derived from the hard vertex correction, Eq. (123), and the leading-order current in Eq. (3) [22]. Using the identity $2\hat{\mathbf{T}}_i^a\hat{\mathbf{T}}_i^b = if^{abc}\hat{\mathbf{T}}_i^c + \{\hat{\mathbf{T}}^a, \hat{\mathbf{T}}^b\}_i$, we separate the remainder into an abelian and a purely non-abelian part. The results are

$$C^{(\text{nab})}(s, t, u) = \frac{ig_s^3}{16\pi^2} f^{abc} \hat{\mathbf{T}}_i^b \hat{\mathbf{T}}_k^c \left[2s \hat{I}_3^{1m}(s) + \hat{I}_2(s) \right] \left(\frac{p_i^\mu}{t} - \frac{p_k^\mu}{u} \right) \epsilon_\mu^*(p_2),$$

$$C^{(\text{ab})}(s, t, u) = \frac{g_s^3}{16\pi^2} \{ \hat{\mathbf{T}}^a, \hat{\mathbf{T}}^b \}_i \hat{\mathbf{T}}_k^b \left[2s \hat{I}_3^{1m}(s) + \hat{I}_2(s) \right] \frac{p_i^\mu}{t} \epsilon_\mu^*(q_1) + \left(\begin{array}{c} p_i \leftrightarrow p_k \\ i \leftrightarrow k \\ t \leftrightarrow u \end{array} \right).$$
(125)

The sum of diagrams in Fig. 14 can be split into abelian and non-abelian corrections. The non-abelian part has a dipole structure and factorizes onto the leading-order dipole matrix element. After subtracting off the non-abelian counterterm in Eq. (125), it is given by the expression

$$I_4^{(\text{nab})}(s, t, u) = -\frac{ig_s^3}{16\pi^2} f^{abc} \hat{\mathbf{T}}_i^b \hat{\mathbf{T}}_k^c \left[\hat{I}_2(Q^2) - \hat{I}_2(s) + 2t \hat{I}_3^{1m}(t) + 2u \hat{I}_3^{1m}(u) \right. \\ \left. - st \hat{I}_4^{1m}(s, t, u) - us \hat{I}_4^{1m}(u, s, t) + 2tu \hat{I}_4^{1m}(t, u, s) \right] \left(\frac{p_i^\mu}{t} - \frac{p_k^\mu}{u} \right) \epsilon_\mu^*(q_1).$$
(126)

In the soft limit, Eq. (126) reduces to a dipole contribution to the 1-loop soft current [22, 60, 61]

$$I_4^{(\text{nab})}(s, t, u) \xrightarrow{q_1 \rightarrow 0} \frac{g_s^3}{16\pi^2} f^{abc} \hat{\mathbf{T}}_i^b \hat{\mathbf{T}}_k^c \frac{c_\Gamma}{\varepsilon^2} \frac{4\pi\varepsilon}{\sin(\pi\varepsilon)} \left(-\frac{\mu^2 s}{tu} \right)^\varepsilon \left(\frac{p_i^\mu}{t} - \frac{p_k^\mu}{u} \right) \epsilon_\mu^*(q_1).$$
(127)

For a single dipole, the color factor simplifies to $-i\hat{\mathbf{T}}_{ik}^a C_A/2$, and the result remains otherwise unchanged. In the collinear limit, $t \rightarrow 0$, $s \rightarrow zQ^2$ and $u \rightarrow (1-z)Q^2$, we obtain

$$I_4^{(\text{nab})}(s, t, u) \xrightarrow{t \rightarrow 0} \frac{g_s^3}{16\pi^2} f^{abc} \hat{\mathbf{T}}_i^b \hat{\mathbf{T}}_k^c \frac{c_\Gamma}{\varepsilon^2} \left[(1-z^{-\varepsilon}) \frac{2-3\varepsilon}{1-2\varepsilon} \left(-\frac{\mu^2}{Q^2} \right)^\varepsilon \right. \\ \left. + 2 \left(-\frac{\mu^2}{t} \right)^\varepsilon \left(2(1-z) {}_2F_1(1, 1; 1-\varepsilon; z) - z {}_2F_1(1, 1; 1-\varepsilon; 1-z) + 1 \right) \right] \frac{p_i^\mu}{t} \epsilon_\mu^*(q_1),$$
(128)

where the first term in the square bracket contributes a sub-leading pole due to the scale difference between the 1-loop hard function in Eq. (123) and the counterterm in Eq. (125). A conversion to the functions defined in [58] is obtained by using the following relation between hypergeometric functions

$${}_2F_1(1, 1; 1-\varepsilon; 1-z) = \Gamma(1-\varepsilon)\Gamma(1+\varepsilon) z^{-1-\varepsilon} (1-z)^\varepsilon + \frac{1}{z} - \frac{(1-z)^\varepsilon}{z} {}_2F_1(\varepsilon, \varepsilon; 1+\varepsilon; z),$$
(129)

which gives $f_1(z) = -2c_\Gamma/\varepsilon^2 {}_2F_1(1, 1; 1-\varepsilon; 1-z)$. In the soft-collinear limit, $z \rightarrow 1$, Eq. (128) simplifies to Eq. (127). The entire non-factorizable contribution then comes from the term proportional to $-2(1-z) {}_2F_1(1, 1; 1-\varepsilon; z)$, which can be written as $(1-z)f_1(1-z)\varepsilon^2/c_\Gamma$. This agrees with the soft limit of Eqs. (4.2) and (4.18) in [58], up to color factors. The collinear limit $u \rightarrow 0$ of Eq. (126) is obtained from Eq. (128) by interchanging t and u .

The abelian contribution is symmetric in the particle momenta and color indices, and it factorizes on the leading-order current. After subtracting off the abelian counterterm in Eq. (125), we obtain

$$\begin{aligned}
I_4^{(\text{ab})}(s, t, u) = & \frac{g_s^3}{16\pi^2} \frac{\{\hat{\mathbf{T}}^b, \hat{\mathbf{T}}^a\}_i \hat{\mathbf{T}}_k^b u - \hat{\mathbf{T}}_i^b \{\hat{\mathbf{T}}^b, \hat{\mathbf{T}}^a\}_k t}{u+t} \left[\hat{I}_2(Q^2) - \hat{I}_2(s) \right] \left(\frac{p_i^\mu}{t} - \frac{p_k^\mu}{u} \right) \epsilon_\mu^*(q_1) \\
& + \frac{g_s^3}{16\pi^2} \{\hat{\mathbf{T}}^a, \hat{\mathbf{T}}^b\}_i \hat{\mathbf{T}}_k^b \left[2Q^2 \hat{I}_3^{1m}(Q^2) - 2s \hat{I}_3^{1m}(s) - 2t \hat{I}_3^{1m}(t) + s t \hat{I}_4^{1m}(s, t, u) \right] \left(\frac{p_i^\mu}{t} - \frac{p_k^\mu}{u} \right) \epsilon_\mu^*(q_1) \\
& - \frac{g_s^3}{16\pi^2} \hat{\mathbf{T}}_i^b \{\hat{\mathbf{T}}^a, \hat{\mathbf{T}}^b\}_k \left[2Q^2 \hat{I}_3^{2m}(Q^2) - 2s \hat{I}_3^{1m}(s) - 2u \hat{I}_3^{1m}(u) + u s \hat{I}_4^{1m}(u, s, t) \right] \left(\frac{p_i^\mu}{t} - \frac{p_k^\mu}{u} \right) \epsilon_\mu^*(q_1).
\end{aligned} \tag{130}$$

In the soft limit, Eq. (130) vanishes, in agreement with the non-abelian structure of the soft-gluon current at 1-loop order [22]. In the $t \rightarrow 0$, $s \rightarrow z Q^2$, $u \rightarrow (1-z) Q^2$ limit, Eq. (130) gives

$$\begin{aligned}
I_4^{(\text{ab})}(s, t, u) \xrightarrow{t \rightarrow 0} & \frac{i g_s^3}{16\pi^2} \frac{C_\Gamma}{\varepsilon^2} \{\hat{\mathbf{T}}^a, \hat{\mathbf{T}}^b\}_i \hat{\mathbf{T}}_k^b \\
& \times \left[2 \left(-\frac{\mu^2}{t} \right)^\varepsilon \left({}_2F_1(1, 1; 1 - \varepsilon; 1 - z) - 1 \right) + (1 - z^{-\varepsilon}) \frac{2 - 3\varepsilon}{1 - 2\varepsilon} \left(-\frac{\mu^2}{Q^2} \right)^\varepsilon \right] \frac{p_i^\mu}{t} \epsilon_\mu^*(q_1).
\end{aligned} \tag{131}$$

Again, this can be converted to the conventions used in [58] by means of Eq. (129).

3. Other contributions

In scalar QCD, there are also corrections to the scalar-scalar interference, which involve an s -channel gluon decaying into the two final-state scalars. These corrections factorize on the two-gluon production process and are individually gauge invariant. They do not appear in a spin decomposition of the one-loop splitting amplitudes. The bubble-type corrections to a color conserving hard function are individually gauge invariant as well and vanish identically. We therefore find that Eqs. (120), (121), (126) and (130) are the only relevant corrections to the dipole radiators at one-loop level.

C. Composition of one-loop splitting functions

In order to match the splitting functions derived in Sec. IV A onto the scalar radiators in Sec. IV B, we can use the expressions for a dipole and assume color conservation. The abelian and non-abelian one-loop scalar currents in the collinear limit are given by Eq. (128) and (131). After subtracting the contributions due to the hard vertex correction, and the counterterms in Eq. (125), we find

$$I_{4,f}(s, t, u) \xrightarrow{t \rightarrow 0} \frac{g_s^3}{16\pi^2} C_A T_{ik}^a \left[(1-z) f_1(1-z) - \frac{1}{N_C^2} (z f_1(z) - 2f_2) \right] \left(-\frac{\mu^2}{t} \right)^\varepsilon \frac{p_i^\mu}{t} \epsilon_\mu^*(q_1), \tag{132}$$

for color triplet scalars, and

$$I_{4,a}(s, t, u) \xrightarrow{t \rightarrow 0} \frac{g_s^3}{16\pi^2} C_A F_{ik}^a \left[(1-z) f_1(1-z) + z f_1(z) - 2f_2 \right] \left(-\frac{\mu^2}{t} \right)^\varepsilon \frac{p_i^\mu}{t} \epsilon_\mu^*(q_1), \tag{133}$$

for color octet scalars. These correspond to the scalar components of Eqs. (95) and (113), which are given in Eqs. (100) and (115) respectively. In particular, we find the following relation which makes the correspondence between the collinear limit of the multipole radiator and the splitting amplitude in the axial gauge manifest [59].

$$\begin{aligned}
\lim_{t \rightarrow 0} I_{4,f}(zQ^2, t, (1-z)Q^2) &= \frac{1}{t} \mathcal{P}_{\bar{q} \rightarrow \bar{q}g}^{(1)}(p_i, q_1), \\
\lim_{t \rightarrow 0} I_{4,a}(zQ^2, t, (1-z)Q^2) &= \frac{1}{t} \mathcal{P}_{g \rightarrow gg}^{(1), \text{sc}}(p_i, q_1).
\end{aligned} \tag{134}$$

1. Quark initial state

The full one-loop quark splitting function is determined by the product of Eq. (95) and the tree-level quark splitting amplitude in Eq. (91), in analogy to Eq. (14),

$$P_{q \rightarrow q}^{(1)ss'} = 2\text{Re} \left\{ \delta^{ss'} \sum_{\text{pol}} \mathcal{P}_{q \rightarrow qg}^{(1)}(p_1, p_2) \mathcal{P}_{q \rightarrow qg}^{(0)*}(p_1, p_2) \right\} \left(\frac{16\pi^2}{g_s^4} \right). \quad (135)$$

The spin-averaged unrenormalized one-loop quark splitting function therefore reads

$$\langle P_{q \rightarrow q}^{(1)}(p_1, p_2) \rangle = P_{\bar{q} \rightarrow \bar{q}}^{(1)}(p_1, p_2) + \langle P_{q \rightarrow q}^{(1,p)}(p_1, p_2) \rangle, \quad (136)$$

where the scalar one-loop splitting function is given by the product of Eq. (100) and a tree-level splitting amplitude, c.f. Eq. (15) (note that $p_1^2 = p_2^2 = 0$):

$$P_{\bar{q} \rightarrow \bar{q}}^{(1)}(p_1, p_2) = C_A \left(-\frac{\mu^2}{s_{12}} \right)^\varepsilon \left[(1-z)f_1(1-z) - \frac{1}{N_C^2} (zf_1(z) - 2f_2) \right] P_{\bar{q} \rightarrow \bar{q}}(p_1, p_2). \quad (137)$$

The spin-dependent remainder is given by

$$\begin{aligned} \langle P_{q \rightarrow q}^{(1,p)}(p_1, p_2) \rangle = & + C_A \left(-\frac{\mu^2}{s_{12}} \right)^\varepsilon \left[(1-z)f_1(1-z) - \frac{1}{N_C^2} (zf_1(z) - 2f_2) \right] \langle P_{q \rightarrow q}^{(f)}(p_1, p_2) \rangle \\ & - C_A \left(1 + \frac{1}{N_C^2} \right) \left(-\frac{\mu^2}{s_{12}} \right)^\varepsilon \frac{\varepsilon^2}{1-2\varepsilon} f_2 \langle P_{q \rightarrow q}^{(f,1)}(p_1, p_2) \rangle, \end{aligned} \quad (138)$$

which consists of two terms, one proportional to the purely fermionic tree-level contribution of the tree-level splitting function given in Eq. (15) and a second, new spin structure first appearing at one loop,

$$\langle P_{q \rightarrow q}^{(f,1)}(p_1, p_2) \rangle = \langle P_{q \rightarrow q}(p_1, p_2) \rangle - C_F \frac{(1+z)z}{1-z} = C_F(1 - \varepsilon(1-z)). \quad (139)$$

Hence, only the first term in the one-loop quark splitting function accounts for the semi-classical radiation pattern. As expected, this includes the leading contribution in terms of combined explicit $1/\varepsilon$, and implicit $1/(1-z)$ singularities. All other terms constitute the purely fermionic contribution.

2. Gluon initial state

The full one-loop gluon splitting tensors are determined from the polarization sum over the product of a one-loop splitting amplitude with the respective tree-level amplitude, in analogy to the tree-level case discussed in Eq. (18),

$$P_{g \rightarrow X}^{(1)\mu\nu}(p_1, p_2) = 2\text{Re} \left\{ \sum_{\text{pol}} (\varepsilon^{*\mu}(p_{12}) \mathcal{P}_{g \rightarrow X}^{(1)}(p_1, p_2)) (\mathcal{P}_{g \rightarrow X}^{(0)*}(p_1, p_2) \varepsilon^\nu(p_{12})) \right\} \left(\frac{16\pi^2}{g_s^4} \right). \quad (140)$$

Averaging over the polarizations of the initial-state gluon in the polarization sum over the product of Eq. (113) with the tree-level splitting amplitude in Eq. (108) then yields the complete unrenormalized spin-averaged gluon-to-gluon splitting function,

$$\langle P_{g \rightarrow g}^{(1)}(p_1, p_2) \rangle = P_{g \rightarrow g}^{(1,\text{sc})}(p_1, p_2) + P_{g \rightarrow g}^{(1,\text{sc})}(p_2, p_1) + \langle P_{g \rightarrow g}^{(1,p)}(p_1, p_2) \rangle, \quad (141)$$

where the adjoint scalar and vector tree-level splitting functions are defined in Eq. (33). The adjoint scalar one-loop splitting function is given by the product of Eq. (115) and the tree-level adjoint scalar splitting amplitude as,

$$P_{g \rightarrow g}^{(1,\text{sc})}(p_1, p_2) = C_A \left(-\frac{\mu^2}{s_{12}} \right)^\varepsilon \left[(1-z)f_1(1-z) + zf_1(z) - 2f_2 \right] P_{g \rightarrow g}^{(\text{sc})}(p_1, p_2). \quad (142)$$

The remainder function is given by

$$\begin{aligned} \langle P_{g \rightarrow g}^{(1,p)}(p_1, p_2) \rangle = & C_A \left(-\frac{\mu^2}{s_{12}} \right)^\varepsilon \left[(1-z)f_1(1-z) + zf_1(z) - 2f_2 \right] \langle P_{g \rightarrow g}^{(\text{v})}(p_1, p_2) \rangle \\ & + \left(C_A - \frac{TRn_f}{1-\varepsilon} \right) \left(-\frac{\mu^2}{s_{12}} \right)^\varepsilon \frac{2\varepsilon^2}{(1-2\varepsilon)(3-2\varepsilon)} f_2 \langle P_{g \rightarrow g}^{(\text{v},1)}(p_1, p_2) \rangle, \end{aligned} \quad (143)$$

Function $\times s_{12}^{-1}$	Definition	Scaling behavior for $\lambda \rightarrow 0$	
		$\tilde{p}_2 \rightarrow \lambda \tilde{p}_2$	$\tilde{p}_1 \rightarrow \lambda \tilde{p}_1$
$P_{\tilde{q} \rightarrow \tilde{q}}^{(1)}$	Eq. (137)	$\propto \lambda^{-2-2\varepsilon}/\varepsilon^2$	$\propto \lambda^{-\varepsilon}/\varepsilon^2$
$P_{g \rightarrow g}^{(1,sc)}$	Eq. (142)	$\propto \lambda^{-2-2\varepsilon}/\varepsilon^2$	$\propto \lambda^{-2\varepsilon}/\varepsilon^2$
$\langle P_{q \rightarrow q}^{(1)} \rangle$	Eq. (136)	$\propto \lambda^{-2-2\varepsilon}/\varepsilon^2$	$\propto \lambda^{-1-\varepsilon}/\varepsilon^2$
$\langle P_{q \rightarrow q}^{(1,p)} \rangle$	Eq. (138)	$\propto \lambda^{-2\varepsilon}/\varepsilon^2$	$\propto \lambda^{-1-\varepsilon}/\varepsilon^2$
$\langle P_{g \rightarrow g}^{(1)} \rangle$	Eq. (141)	$\propto \lambda^{-2-2\varepsilon}/\varepsilon^2$	
$\langle P_{g \rightarrow g}^{(1,p)} \rangle$	Eq. (143)	$\propto \lambda^{-2\varepsilon}/\varepsilon^2$	
$\langle P_{g \rightarrow q}^{(1)} \rangle$	Eq. (145)	$\propto \lambda^{-1-\varepsilon}/\varepsilon^2$	

TABLE II. Limits of the various one-loop splitting functions and their pure components. See the main text for details.

where we have introduced the purely spin-dependent component first appearing at one loop,

$$\langle P_{g \rightarrow g}^{(v,1)}(p_1, p_2) \rangle = -C_A \frac{1 - 2\varepsilon z(1 - z)}{1 - \varepsilon}. \quad (144)$$

The complete spin-averaged one-loop gluon-to-quark splitting tensor is determined from averaging over the polarizations of the initial-state gluon in the polarization sum of the product of Eq. (107) with the tree-level splitting amplitude of Eq. (104). It fully factorizes onto the tree-level splitting function in Eq. (22) and does not contain a scalar contribution. It reads

$$\begin{aligned} \langle P_{g \rightarrow q}^{(1)}(p_1, p_2) \rangle = C_A \left(-\frac{\mu^2}{s_{12}} \right)^\varepsilon \left[\left(z f_1(z) + (1 - z) f_1(1 - z) - \left(2 + \frac{3(2 - \varepsilon)}{(1 - 2\varepsilon)(3 - 2\varepsilon)} \right) f_2 \right) \right. \\ \left. - \frac{1}{N_C^2} \left(\frac{2}{1 - 2\varepsilon} - \varepsilon \right) f_2 + \frac{T_R n_f}{N_C} \frac{4(1 - \varepsilon)\varepsilon}{(1 - 2\varepsilon)(3 - 2\varepsilon)} f_2 \right] \langle P_{g \rightarrow q}(p_1, p_2) \rangle. \end{aligned} \quad (145)$$

3. Singularity structure of the remainder functions

Here we summarize the singularity structure of the various one-loop splitting functions introduced in Secs. IV A and IV C. The kinematical limit where particle i becomes soft is parametrized as $p_i \rightarrow \lambda p_i$. We can use the relation

$${}_2F_1(1, 1; 1 - \varepsilon; z) = (1 - z)^{-1-\varepsilon} {}_2F_1(-\varepsilon, -\varepsilon; 1 - \varepsilon; z) = (1 - z)^{-1-\varepsilon} \left(1 + \varepsilon^2 \text{Li}_2(z) + \mathcal{O}(\varepsilon^3) \right) \quad (146)$$

to convert the hypergeometric functions in f_1 to powers of z and $1 - z$, times a remainder that is finite for all values of z and does not contribute sub-leading poles. This allows the dominant scaling behavior in the soft limit to be extracted. The results are given in Tab. II. Here we identify only the leading singular structure in terms of combined explicit and implicit poles.

V. OUTLOOK

In this work we re-examined the tree-level and one-loop splitting functions used to capture the infrared singular behavior of QCD scattering amplitudes in next-to-next-to-leading order QCD calculations and next-to-next-to-leading logarithmic resummation. We made use of the fact that variants of scalar QCD are minimal extensions of the semi-classical approximation, and avoided any kinematical approximations. We demonstrated that all QCD splitting functions can be obtained from dipole radiator functions computed in scalar QCD, combined with spin-dependent remainders that exist only in splitting configurations and have (sub-)sub-leading singularities in the kinematical limits. Using the background field method to construct a dipole approximation to scalar multipole radiators, we have achieved the same decomposition at one loop order.

The significance of this result is twofold. On the one hand, we are able to show that neither the soft nor the collinear kinematical limit is needed in order to derive universally applicable subtraction terms for higher-order calculations.

This is ultimately due to the fact that a classical limit of the theory must exist. On the other hand, we anticipate that the results presented here will be used to devise a subtraction or resummation scheme which does not suffer from overlaps between soft and collinear sectors, as well as overlaps between single- and double-unresolved limits. Such a scheme is urgently needed for example to construct a fully differential parton shower at next-to-next-to leading logarithmic precision. For fixed-order calculations, the reorganization and classification of infrared singularities should aid the construction of a generic subtraction scheme at NNLO precision that will have an improved convergence compared to existing methods based on leading power approximations in the soft regions.

ACKNOWLEDGMENTS

We thank Robert Szafron for discussions on sub-leading power contributions to the triple-collinear splitting functions and Bogdan Dobrescu for discussions on the Gordon identity. This manuscript has been authored by Fermi Forward Discovery Group, LLC under Contract No. 89243024CSC000002 with the U.S. Department of Energy, Office of Science, Office of High Energy Physics. The work of J.M.C., S.H. and M.K. was supported by the U.S. Department of Energy, Office of Science, Office of Advanced Scientific Computing Research, Scientific Discovery through Advanced Computing (SciDAC-5) program, grant “NeuCol”. D.R. is supported by the European Union under the HORIZON program in Marie Skłodowska-Curie project No. 101153541. D.R. was further supported by the STFC under grant agreement ST/P006744/1 and by Durham Universities Physics Department Developing Talents Award during the initial stages of this work.

Appendix A: Tree-level recursion

In this appendix, we show how the Berends-Giele recursion can be reformulated in terms of expressions for a scalar theory, and a spin-dependent remainder. Note that this does not directly translate into a separation of scalar and remainder components at the amplitude squared level.

1. The quark current at tree level

We begin the general discussion by deriving the structure of the quark-gluon vertex in terms of scalar and magnetic interactions. A similar approach was presented in [99]. Here we focus in particular on a suitable formulation in terms of building blocks for higher-order scattering matrix elements.

We use the color-dressed [68] Berends-Giele recursion [65–67] to describe an off-shell (anti-)quark of momentum p_α by a current which is obtained from the propagator times vertex for the interaction of a fermion of momentum p_β with a gluon of momentum p_γ . We sum over all partitions $\{\beta, \gamma\}$ of the set of indices, α , into two disjoint subsets.⁴ The set of all possible partitions is denoted by $P(\alpha, 2)$.

$$\begin{aligned} \Psi_i(p_\alpha, \pm m) &= i \frac{\not{p}_\alpha \pm m}{p_\alpha^2 - m^2} \sum_{\substack{\{\beta, \gamma\} \in \\ P(\alpha, 2)}} (-ig_s T_{ij}^a \gamma^\mu) J_\mu^a(p_\gamma) \Psi_j(p_\beta, \pm m) \\ &= \frac{g_s T_{ij}^a}{p_\alpha^2 - m^2} \sum_{\substack{\{\beta, \gamma\} \in \\ P(\alpha, 2)}} \left[(p_\alpha + p_\beta)^\mu J_\mu^a(p_\gamma) + i\sigma^{\mu\nu} J_\mu^a(p_\gamma) p_{\gamma, \nu} - \gamma^\mu J_\mu^a(p_\gamma) (\not{p}_\beta \mp m) \right] \Psi_j(p_\beta, \pm m). \end{aligned} \quad (\text{A1})$$

Here, Ψ is the (anti-)quark current, and J_μ is a gluon current. These currents can be either on-shell or off-shell. The first term in the square bracket on the right-hand side describes the interaction of the gluon field with the scalar current while the second term represents the magnetic interaction. The third term plays a special role. If $\Psi_j(p, \pm m)$ is an external wave function, we can use the equation of motion to show that it vanishes, i.e. $(\not{p} \mp m)\Psi_j(p, \pm m) = 0$. If $\Psi_j(p, \pm m)$ is itself an off-shell current, it is obtained as a sum of terms of the form of Eq. (A1). We can simplify the combined expression as follows

$$- \sum_{\substack{\{\beta, \gamma\} \in \\ P(\alpha, 2)}} g_s T_{ij}^a \gamma^\mu J_\mu^a(p_\gamma) (\not{p}_\beta \mp m) \Psi_j(p_\beta, \pm m) = - g_s^2 T_{ik}^a T_{kj}^b \sum_{\substack{\{\beta, \gamma\} \in \\ P(\alpha, 2)}} \sum_{\substack{\{\delta, \epsilon\} \in \\ P(\gamma, 2)}} \gamma^\mu \gamma^\nu J_\mu^a(p_\delta) J_\nu^b(p_\epsilon) \Psi_j(p_\beta, \pm m). \quad (\text{A2})$$

⁴ For details on the notation, see Ref. [68].

The factor $\gamma^\mu \gamma^\nu$ on the right-hand side of this equation can be decomposed into two types of four-point vertices, by using the relation $\gamma^\mu \gamma^\nu = g^{\mu\nu} - i\sigma^{\mu\nu}$. The first term gives the seagull vertex of the scalar theory for which Eq. (2) describes the single-emission current. It is needed in order for this theory to satisfy the Ward identities. The second term vanishes in the complete sum over partitions due to its antisymmetry. Using this methodology, we can separate the recursive formula into a scalar piece and a spin-dependent remainder.

$$\begin{aligned} \Psi_i(p_\alpha) = & \frac{ig^{\mu\nu}}{p_\alpha^2 - m^2} \sum_{\substack{\{\beta, \gamma\} \in \\ P(\alpha, 2)}} \left[-ig_s T_{ij}^a (p_\beta + p_\alpha)_\nu J_\mu^a(p_\gamma) + \sum_{\substack{\{\delta, \epsilon\} \in \\ OP(\gamma, 2)}} ig_s^2 \{T^a, T^b\}_{ij} J_\mu^a(p_\delta) J_\nu^b(p_\epsilon) \right] \Psi_j(p_\beta) \\ & + \frac{\sigma^{\mu\nu}}{p_\alpha^2 - m^2} \sum_{\substack{\{\beta, \gamma\} \in \\ P(\alpha, 2)}} (-ig_s T_{ij}^a) (p_\beta - p_\alpha)_\nu J_\mu^a(p_\gamma) \Psi_j(p_\beta) . \end{aligned} \quad (\text{A3})$$

We have made use of the Bose symmetry in the gluon fields to rewrite the sum over unordered gluon currents in the square brackets into a sum over ordered partitions of the set γ into two disjoint subsets. The complete set of such partitions is denoted by $OP(\gamma, 2)$. In an abelian theory, this rearrangement would induce a simple symmetry factor in the seagull vertex, consistent with the Feynman rules of scalar QED. Note that there is no seagull vertex for the magnetic interaction, which is a consequence of the antisymmetry of $\sigma^{\mu\nu}$.

2. The gluon current at tree level

Next we analyze the gluon current in the color-dressed Berends-Giele approach. It can be written as

$$J_\mu^a(p_\alpha) = \bar{J}_\mu^a(p_\alpha) + \tilde{J}_\mu^a(p_\alpha) . \quad (\text{A4})$$

where the gluon-induced contribution, \tilde{J}_μ , arises from triple and quartic gluon interactions and is given by

$$\begin{aligned} \tilde{J}_\mu^a(p_\alpha) = & i \frac{d_{\mu\nu}(p_\alpha)}{p_\alpha^2} \sum_{\substack{\{\beta, \gamma\} \in \\ OP(\alpha, 2)}} (-g_s f^{abc}) \left[g^{\rho\sigma} (p_\beta - p_\gamma)^\nu + g^{\sigma\nu} (2p_\gamma + p_\beta)^\rho - g^{\nu\rho} (2p_\beta + p_\gamma)^\sigma \right] J_\rho^b(p_\beta) J_\sigma^c(p_\gamma) \\ & + i \frac{d_{\mu\nu}(p_\alpha)}{p_\alpha^2} \sum_{\substack{\{\beta, \gamma\} \in \\ OP(\alpha, 2)}} \sum_{\substack{\{\delta, \epsilon\} \in \\ OP(\gamma, 2)}} ig_s^2 \left[\begin{aligned} & f^{abe} f^{ecd} (g^{\nu\tau} g^{\rho\sigma} - g^{\nu\sigma} g^{\tau\rho}) \\ & + f^{ace} f^{edb} (g^{\nu\rho} g^{\sigma\tau} - g^{\nu\tau} g^{\rho\sigma}) \\ & + f^{ade} f^{ebc} (g^{\nu\sigma} g^{\tau\rho} - g^{\nu\rho} g^{\sigma\tau}) \end{aligned} \right] J_\rho^b(p_\beta) J_\sigma^c(p_\delta) J_\tau^d(p_\epsilon) . \end{aligned} \quad (\text{A5})$$

By summing over all partitions and relabeling gluon momenta, we can reduce this expression to the simple form

$$\begin{aligned} \tilde{J}_\mu^a(p_\alpha) = & i \frac{d_{\mu\nu}(p_\alpha)}{p_\alpha^2} \sum_{\substack{\{\beta, \gamma\} \in \\ P(\alpha, 2)}} (-g_s f^{acb}) \left[g^{\nu\rho} (2p_\beta + p_\gamma)^\sigma - \frac{1}{2} g^{\rho\sigma} (p_\beta - p_\gamma)^\nu \right] J_\rho^b(p_\beta) J_\sigma^c(p_\gamma) \\ & + i \frac{d_{\mu\nu}(p_\alpha)}{p_\alpha^2} \sum_{\substack{\{\beta, \gamma\} \in \\ P(\alpha, 2)}} \sum_{\substack{\{\delta, \epsilon\} \in \\ P(\gamma, 2)}} ig_s^2 f^{ace} f^{edb} g^{\nu\rho} g^{\sigma\tau} J_\rho^b(p_\beta) J_\sigma^c(p_\delta) J_\tau^d(p_\epsilon) \\ = & \frac{ig^{\sigma\tau}}{p_\alpha^2} \sum_{\substack{\{\beta, \gamma\} \in \\ P(\alpha, 2)}} \left[-ig_s F_{ab}^c (p_\beta + p_\alpha)_\tau J_\sigma^c(p_\gamma) + \sum_{\substack{\{\delta, \epsilon\} \in \\ OP(\gamma, 2)}} ig_s^2 \{F^c, F^d\}_{ab} J_\sigma^c(p_\delta) J_\tau^d(p_\epsilon) \right] (-d_\mu{}^\rho(p_\alpha)) J_\rho^b(p_\beta) \\ & - i \frac{d_{\mu\nu}(p_\alpha)}{p_\alpha^2} \sum_{\substack{\{\beta, \gamma\} \in \\ OP(\alpha, 2)}} g_s f^{abc} (p_\beta - p_\gamma)^\nu g^{\rho\sigma} J_\rho^b(p_\beta) J_\sigma^c(p_\gamma) . \end{aligned} \quad (\text{A6})$$

We have defined $F_{ab}^c = if^{acb}$ to make the radiation pattern explicit. The quark-induced contribution to the gluon current, \bar{J}_μ , is given by

$$\bar{J}_\mu^a(p_\alpha) = i \frac{d_{\mu\nu}(p_\alpha)}{p_\alpha^2} \sum_{\substack{\{\beta, \gamma\} \in \\ P(\alpha, 2)}} \bar{\Psi}_i(p_\gamma, \pm m) (-ig_s T_{ij}^a \gamma^\nu) \Psi_j(p_\beta, \pm m). \quad (\text{A7})$$

We use the identity $\{\not{p}, \not{n}\}/(2pn) = 1$, with n an auxiliary vector, to rewrite this in the following form

$$\bar{J}_\mu^a(p_\alpha) = i \frac{d_{\mu\nu}(p_\alpha)}{p_\alpha^2} \sum_{\substack{\{\beta, \gamma\} \in \\ P(\alpha, 2)}} \bar{\Psi}_i(p_\gamma, \pm m) (-ig_s T_{ij}^a) \frac{1}{2} \left[\frac{\gamma^\nu \not{p}_\alpha \not{n} + \gamma^\nu \not{n} \not{p}_\alpha}{2p_\alpha n} + \frac{\not{p}_\alpha \not{n} \gamma^\nu + \not{n} \not{p}_\alpha \gamma^\nu}{2p_\alpha n} \right] \Psi_j(p_\beta, \pm m). \quad (\text{A8})$$

Using $\gamma^\mu \not{p} + \not{p} \gamma^\mu = 2n^\mu$, and working in an axial gauge (see the discussion in Sec. II), this expression simplifies to a purely magnetic interaction term. The complete gluon current then reads

$$\begin{aligned} J_\mu^a(p_\alpha, n) = & \frac{ig^{\sigma\tau}}{p_\alpha^2} \sum_{\substack{\{\beta, \gamma\} \in \\ P(\alpha, 2)}} \left[-ig_s F_{ab}^c (p_\beta + p_\alpha)_\tau J_\sigma^c(p_\gamma, n) \right. \\ & \left. + \sum_{\substack{\{\delta, \epsilon\} \in \\ OP(\gamma, 2)}} ig_s^2 \{F^c, F^d\}_{ab} J_\sigma^c(p_\delta, n) J_\tau^d(p_\epsilon, n) \right] (-d_\mu^\rho(p_\alpha, n)) J_\rho^b(p_\beta, n) \\ & + i \frac{d_{\mu\nu}(p_\alpha, n)}{p_\alpha^2} \sum_{\substack{\{\beta, \gamma\} \in \\ P(\alpha, 2)}} \left[-ig_s \frac{F_{bc}^a}{2} (p_\beta - p_\gamma)^\nu g^{\rho\sigma} J_\rho^b(p_\beta, n) J_\sigma^c(p_\gamma, n) \right. \\ & \left. - ig_s T_{ij}^a (p_\beta + p_\gamma)_\rho \bar{\Psi}_i(p_\gamma) \frac{\not{n} i \sigma^{\rho\nu} + i \sigma^{\nu\rho} \not{n}}{2(p_\beta + p_\gamma)n} \Psi_j(p_\beta) \right]. \quad (\text{A9}) \end{aligned}$$

The scalar parts of Eq. (A3) and (A9) are similar to the eikonal interaction Hamiltonians obtained, for example in [100, 101], but they include effects of kinematical recoil, which is essential when computing higher-point splitting functions.

Appendix B: One-loop integrals

In this section we collect the one-loop integrals required to perform the calculations in the main text. Note that we have extracted an overall factor in Eq. (90) that differs from some of the previous literature by a factor of $1/(4\pi)^2$, leading to the appearance of the same factor in the definitions below.

1. Scalar basis integrals

The standard scalar bubble and triangle integrals used in Sec. IV are given by [102]

$$\hat{I}_2(s_{12}) = 16\pi^2 \mu^{2\varepsilon} \int \frac{d^{4-2\varepsilon}k}{(2\pi)^{4-2\varepsilon}} \frac{1}{k^2(k-p_1-p_2)^2} = \frac{ic_\Gamma}{\varepsilon(1-2\varepsilon)} \left(-\frac{\mu^2}{s_{12}}\right)^\varepsilon = -\frac{i\varepsilon}{1-2\varepsilon} \left(-\frac{\mu^2}{s_{12}}\right)^\varepsilon f_2, \quad (\text{B1})$$

$$\hat{I}_3^{1m}(s_{12}) = 16\pi^2 \mu^{2\varepsilon} \int \frac{d^{4-2\varepsilon}k}{(2\pi)^{4-2\varepsilon}} \frac{1}{k^2(k-p_1)^2(k-p_1-p_2)^2} = \frac{ic_\Gamma}{\varepsilon^2} \frac{1}{s_{12}} \left(-\frac{\mu^2}{s_{12}}\right)^\varepsilon = -\frac{i}{s_{12}} \left(-\frac{\mu^2}{s_{12}}\right)^\varepsilon f_2. \quad (\text{B2})$$

The corresponding integrals needed for the computation in light-like axial gauge are given by [58]

$$\hat{J}_2(s_{12}) = 16\pi^2 \mu^{2\varepsilon} \int \frac{d^{4-2\varepsilon}k}{(2\pi)^{4-2\varepsilon}} \frac{1}{k^2(k-p_1-p_2)^2(kn)} = \frac{i}{n(p_1+p_2)} \left(-\frac{\mu^2}{s_{12}}\right)^\varepsilon f_2, \quad (\text{B3})$$

$$\hat{J}_1(s_{12}, z) = 16\pi^2 \mu^{2\varepsilon} \int \frac{d^{4-2\varepsilon}k}{(2\pi)^{4-2\varepsilon}} \frac{1}{k^2(k-p_1)^2(k-p_1-p_2)^2(kn)} = -\frac{i}{n(p_1+p_2)s_{12}} \left(-\frac{\mu^2}{s_{12}}\right)^\varepsilon f_1(z). \quad (\text{B4})$$

In addition, we need the two-mass triangle and one-mass box integrals [102]

$$\hat{I}_3^{2m}(s, t) = \frac{ic_\Gamma}{\varepsilon^2} \frac{1}{s-t} \left[\left(-\frac{\mu^2}{s} \right)^\varepsilon - \left(-\frac{\mu^2}{t} \right)^\varepsilon \right], \quad (\text{B5})$$

$$\begin{aligned} \hat{I}_4^{1m}(s, t, u) = \frac{2ic_\Gamma}{\varepsilon^2} \frac{1}{st} & \left[\left(-\frac{s+u}{st/\mu^2} \right)^\varepsilon {}_2F_1 \left(-\varepsilon, -\varepsilon; 1-\varepsilon; 1 - \frac{s}{s+u} \right) \right. \\ & + \left(-\frac{t+u}{st/\mu^2} \right)^\varepsilon {}_2F_1 \left(-\varepsilon, -\varepsilon; 1-\varepsilon; 1 - \frac{t}{t+u} \right) \\ & \left. - \left(-\frac{(s+u)(t+u)}{st(s+t+u)/\mu^2} \right)^\varepsilon {}_2F_1 \left(-\varepsilon, -\varepsilon; 1-\varepsilon; 1 - \frac{st}{(s+u)(t+u)} \right) \right]. \end{aligned} \quad (\text{B6})$$

2. Tensor integrals

The tensor one-loop integrals needed for the computation of the splitting functions in Sec. IV A are given by [58]

$$\hat{I}_{2a}^\mu(s_{12}) = 16\pi^2 \mu^{2\varepsilon} \int \frac{d^{4-2\varepsilon}k}{(2\pi)^{4-2\varepsilon}} \frac{k^\mu}{k^2(k-p_1-p_2)^2} = -\frac{i\varepsilon}{2(1-2\varepsilon)} \left(-\frac{\mu^2}{s_{12}} \right)^\varepsilon f_2(p_1+p_2)^\mu, \quad (\text{B7})$$

$$\begin{aligned} \hat{I}_{2b}^{\mu\nu}(s_{12}) &= 16\pi^2 \mu^{2\varepsilon} \int \frac{d^{4-2\varepsilon}k}{(2\pi)^{4-2\varepsilon}} \frac{k^\mu k^\nu}{k^2(k-p_1-p_2)^2} \\ &= \frac{i\varepsilon}{2(3-2\varepsilon)(1-2\varepsilon)} \left(-\frac{\mu^2}{s_{12}} \right)^\varepsilon f_2 \left(\frac{s_{12}}{2} g^{\mu\nu} - (2-\varepsilon)(p_1+p_2)^\mu(p_1+p_2)^\nu \right). \end{aligned} \quad (\text{B8})$$

and

$$\hat{I}_{3a}^\mu(s_{12}) = 16\pi^2 \mu^{2\varepsilon} \int \frac{d^{4-2\varepsilon}k}{(2\pi)^{4-2\varepsilon}} \frac{k^\mu}{k^2(k-p_1)^2(k-p_1-p_2)^2} = -\frac{i}{s_{12}} \left(-\frac{\mu^2}{s_{12}} \right)^\varepsilon f_2 \left[\frac{1-\varepsilon}{1-2\varepsilon} p_1^\mu - \frac{\varepsilon}{1-2\varepsilon} p_2^\mu \right], \quad (\text{B9})$$

$$\begin{aligned} \hat{I}_{3b}^{\mu\nu}(s_{12}) &= 16\pi^2 \mu^{2\varepsilon} \int \frac{d^{4-2\varepsilon}k}{(2\pi)^{4-2\varepsilon}} \frac{k^\mu k^\nu}{k^2(k-p_1)^2(k-p_1-p_2)^2} \\ &= -\frac{i}{s_{12}} \left(-\frac{\mu^2}{s_{12}} \right)^\varepsilon f_2 \left[s_{12} \frac{\varepsilon}{4(1-\varepsilon)(1-2\varepsilon)} g^{\mu\nu} + \frac{2-\varepsilon}{2(1-2\varepsilon)} p_1^\mu p_1^\nu \right. \\ &\quad \left. - \frac{\varepsilon}{2(1-2\varepsilon)} p_2^\mu p_2^\nu - \frac{\varepsilon(2-\varepsilon)}{2(1-\varepsilon)(1-2\varepsilon)} (p_1^\mu p_2^\nu + p_2^\mu p_1^\nu) \right], \end{aligned} \quad (\text{B10})$$

$$\begin{aligned} \hat{I}_{3c}^{\kappa\mu\nu}(s_{12}) &= 16\pi^2 \mu^{2\varepsilon} \int \frac{d^{4-2\varepsilon}k}{(2\pi)^{4-2\varepsilon}} \frac{k^\kappa k^\mu k^\nu}{k^2(k-p_1)^2(k-p_1-p_2)^2} \\ &= -\frac{i}{s_{12}} \left(-\frac{\mu^2}{s_{12}} \right)^\varepsilon f_2 \left[\frac{(2-\varepsilon)(3-\varepsilon)}{2(1-2\varepsilon)(3-2\varepsilon)} p_1^\kappa p_1^\mu p_1^\nu - \frac{(2-\varepsilon)\varepsilon}{2(1-2\varepsilon)(3-2\varepsilon)} p_2^\kappa p_2^\mu p_2^\nu \right. \\ &\quad - \frac{(3-\varepsilon)\varepsilon}{2(1-2\varepsilon)(3-2\varepsilon)} (p_1^\kappa p_2^\mu p_2^\nu + p_1^\mu p_2^\nu p_2^\kappa + p_1^\nu p_2^\kappa p_2^\mu) \\ &\quad - \frac{(2-\varepsilon)(3-\varepsilon)\varepsilon}{2(1-\varepsilon)(1-2\varepsilon)(3-2\varepsilon)} (p_2^\kappa p_1^\mu p_1^\nu + p_2^\mu p_1^\nu p_1^\kappa + p_2^\nu p_1^\kappa p_1^\mu) \\ &\quad + s_{12} \frac{(2-\varepsilon)\varepsilon}{4(1-\varepsilon)(1-2\varepsilon)(3-2\varepsilon)} (p_1^\kappa g^{\mu\nu} + p_1^\mu g^{\nu\kappa} + p_1^\nu g^{\kappa\mu}) \\ &\quad \left. + s_{12} \frac{\varepsilon}{4(1-2\varepsilon)(3-2\varepsilon)} (p_2^\kappa g^{\mu\nu} + p_2^\mu g^{\nu\kappa} + p_2^\nu g^{\kappa\mu}) \right]. \end{aligned} \quad (\text{B11})$$

The required light-cone bubble integrals read

$$\begin{aligned}\hat{J}_4^\mu(s_{12}) &= 16\pi^2\mu^{2\varepsilon} \int \frac{d^{4-2\varepsilon}k}{(2\pi)^{4-2\varepsilon}} \frac{k^\mu}{k^2(k-p_1-p_2)^2(kn)} \\ &= \frac{i}{n(p_1+p_2)} \left(-\frac{\mu^2}{s_{12}}\right)^\varepsilon f_2 \left[-\frac{\varepsilon}{1-2\varepsilon} (p_1+p_2)^\mu + \frac{s_{12}}{2n(p_1+p_2)} \frac{1}{1-2\varepsilon} n^\mu \right],\end{aligned}\tag{B12}$$

$$\begin{aligned}\hat{J}_6^{\mu\nu}(s_{12}) &= 16\pi^2\mu^{2\varepsilon} \int \frac{d^{4-2\varepsilon}k}{(2\pi)^{4-2\varepsilon}} \frac{k^\mu k^\nu}{k^2(k-p_1-p_2)^2(kn)} \\ &= \frac{i}{n(p_1+p_2)} \left(-\frac{\mu^2}{s_{12}}\right)^\varepsilon f_2 \left[s_{12} \frac{\varepsilon}{4(1-\varepsilon)(1-2\varepsilon)} g^{\mu\nu} - \frac{\varepsilon}{2(1-2\varepsilon)} (p_1+p_2)^\mu (p_1+p_2)^\nu \right. \\ &\quad \left. + \left(\frac{s_{12}}{n(p_1+p_2)}\right)^2 \frac{1}{4(1-\varepsilon)(1-2\varepsilon)} n^\mu n^\nu \right. \\ &\quad \left. - \frac{s_{12}}{n(p_1+p_2)} \frac{\varepsilon}{4(1-\varepsilon)(1-2\varepsilon)} ((p_1+p_2)^\mu n^\nu + (p_1+p_2)^\nu n^\mu) \right].\end{aligned}\tag{B13}$$

The required light-cone triangle integrals are (note that there is a typo in Eq. (3.15) of [58])

$$\begin{aligned}\hat{J}_3^\mu(s_{12}, z) &= 16\pi^2\mu^{2\varepsilon} \int \frac{d^{4-2\varepsilon}k}{(2\pi)^{4-2\varepsilon}} \frac{k^\mu}{k^2(k-p_1)^2(k-p_1-p_2)^2(kn)} \\ &= -\frac{i}{2n(p_1+p_2)s_{12}} \left(-\frac{\mu^2}{s_{12}}\right)^\varepsilon \left[f_1(z) p_1^\mu + \frac{2f_2 - zf_1(z)}{1-z} p_2^\mu - \frac{s_{12}}{2n(p_1+p_2)} \frac{2f_2 - f_1(z)}{1-z} n^\mu \right]\end{aligned}\tag{B14}$$

$$\begin{aligned}\hat{J}_5^{\mu\nu}(s_{12}, z) &= 16\pi^2\mu^{2\varepsilon} \int \frac{d^{4-2\varepsilon}k}{(2\pi)^{4-2\varepsilon}} \frac{k^\mu k^\nu}{k^2(k-p_1)^2(k-p_1-p_2)^2(kn)} \\ &= -\frac{i}{n(p_1+p_2)s_{12}} \left(-\frac{\mu^2}{s_{12}}\right)^\varepsilon \left[C_{5g} g^{\mu\nu} + C_{511} p_1^\mu p_1^\nu + C_{522} p_2^\mu p_2^\nu + C_{512} (p_1^\mu p_2^\nu + p_1^\nu p_2^\mu) \right. \\ &\quad \left. + C_{51n} (p_1^\mu n^\nu + p_1^\nu n^\mu) + C_{52n} (p_2^\mu n^\nu + p_2^\nu n^\mu) + C_{5n} n^\mu n^\nu \right]\end{aligned}\tag{B15}$$

with the coefficients

$$\begin{aligned}C_{5g} &= s_{12} \left(\frac{z}{4(1-2\varepsilon)(1-z)} f_1(z) - \frac{1}{2(1-2\varepsilon)(1-z)} f_2 \right), \\ C_{511} &= \frac{1-\varepsilon}{2(1-2\varepsilon)} f_1(z), \\ C_{522} &= \frac{(1-\varepsilon)z^2}{2(1-2\varepsilon)(1-z)^2} f_1(z) - \frac{\varepsilon + (1-2\varepsilon)z}{(1-2\varepsilon)(1-z)^2} f_2, \\ C_{512} &= -\frac{(1-\varepsilon)z}{2(1-2\varepsilon)(1-z)} f_1(z) + \frac{1-\varepsilon}{(1-2\varepsilon)(1-z)} f_2, \\ C_{51n} &= \frac{s_{12}}{2n(p_1+p_2)} \left(-\frac{\varepsilon}{2(1-2\varepsilon)(1-z)} f_1(z) + \frac{\varepsilon}{(1-2\varepsilon)(1-z)} f_2 \right), \\ C_{52n} &= \frac{s_{12}}{2n(p_1+p_2)} \left(-\frac{(1-\varepsilon)z}{2(1-2\varepsilon)(1-z)^2} f_1(z) + \frac{1-\varepsilon z}{(1-2\varepsilon)(1-z)^2} f_2 \right), \\ C_{5n} &= \left(\frac{s_{12}}{2n(p_1+p_2)} \right)^2 \left(\frac{1-\varepsilon}{2(1-2\varepsilon)(1-z)^2} f_1(z) - \frac{2-\varepsilon-z}{(1-2\varepsilon)(1-z)^2} f_2 \right).\end{aligned}\tag{B16}$$

Appendix C: Explicitly gauge dependent parts of three-particle off-shell currents

The one-to-three gluon-to-quark splitting tensor is given by Eq. (46). Its explicitly \bar{n} -dependent component reads

$$P_{g \rightarrow q\bar{q}\bar{n}}^{\mu\nu(\text{nab},\bar{n})}(p_1, p_2, p_3) = \frac{C_{AT_R}}{2} \frac{s_{123}}{s_{23}} \left\{ \frac{\tilde{p}_{1,23}^\mu \bar{n}^\nu + \tilde{p}_{1,23}^\nu \bar{n}^\mu}{(z_2 + z_3) p_{123} \bar{n}} \left[\frac{s_{123}}{s_{13}} \frac{z_3}{z_1} - \frac{s_{23}}{s_{13}} \frac{z_2}{1 - z_1} - 1 \right] \right. \\ \left. - \frac{\tilde{p}_{2,3}^\mu \bar{n}^\nu + \tilde{p}_{2,3}^\nu \bar{n}^\mu}{(z_2 + z_3) p_{123} \bar{n}} \left[\frac{2s_{123}}{s_{23}} \frac{z_3}{z_1} + \frac{2s_{12}}{s_{23}} \frac{1 - z_1}{z_1} + \frac{s_{23}}{s_{12}} \right] - \frac{s_{123}}{z_1(1 - z_1)} \frac{\bar{n}^\mu \bar{n}^\nu}{(p_{123} \bar{n})^2} + (2 \leftrightarrow 3) \right\}. \quad (\text{C1})$$

The one-to-three all-gluon splitting tensor is given by Eq. (47) Its explicitly \bar{n} -dependent component is given by

$$P_{g \rightarrow ggg}^{\mu\nu(\bar{n})}(p_1, p_2, p_3) = C_A^2 \left\{ - \frac{\tilde{p}_{1,2}^\mu \bar{n}^\nu + \tilde{p}_{1,2}^\nu \bar{n}^\mu}{p_{123} \bar{n}} \frac{1 - \varepsilon}{2z_3} \frac{s_{123}}{s_{12}^2} t_{12,3} \right. \\ + \frac{\tilde{p}_{1,23}^\mu \bar{n}^\nu + \tilde{p}_{1,23}^\nu \bar{n}^\mu}{p_{123} \bar{n}} \left[\frac{s_{123}s_{12}}{s_{23}s_{13}} \left(\frac{1 - 4z_1(1 - z_1)}{2(1 - z_1)(1 - z_2)} + \frac{(1 - z_1)(1 - 2z_1)}{2z_1 z_2} - \frac{z_3(2 - 3z_1)}{z_1(1 - z_1)} + \frac{1 - 2z_1}{2(1 - z_1)} \right) \right. \\ + \frac{s_{123}}{s_{23}z_1} \left(\frac{1 - 4z_1(1 - z_1)}{2(1 - z_1)(1 - z_2)} + \frac{z_3(1 - 2z_1)}{z_2} + \frac{z_1(2 - 3z_1)}{2(1 - z_1)} \right) - \frac{s_{123}s_{23}}{s_{13}s_{12}} \left(\frac{(1 - z_3 + z_2 z_3)(1 - 2z_3)}{2z_2(1 - z_2)(1 - z_3)} - \frac{2z_1}{1 - z_2} \right) \\ + \left. \frac{s_{123}}{s_{13}} \left(\frac{1 - z_2(1 - 2z_2)}{2z_2(1 - z_2)(1 - z_3)} + \frac{2 - 5z_2 + 6z_2^2}{2z_1 z_2} + \frac{z_2(3 - 2z_2)}{2(1 - z_1)(1 - z_2)} - \frac{3 - 5z_2 + 7z_2^2}{z_2(1 - z_2)} - \frac{1 - 2z_2}{z_3} \right) \right] \\ - \frac{1}{z_1(1 - z_1)} \frac{1}{z_3} \frac{\bar{n}^\mu \bar{n}^\nu}{(p_{123} \bar{n})^2} \left[\frac{s_{13}^3}{4s_{12}s_{23}} \frac{z_2 + 2z_1 z_3}{1 - z_3} + s_{23} \left(9(1 - z_2) + \frac{1 + 6z_2 z_3}{1 - z_2} - \frac{z_2^2(1 + 8z_2) - 18z_2 + 11}{2(1 - z_2)(1 - z_3)} \right) \right. \\ + \left. \frac{s_{12}s_{13}}{4s_{23}} \left(8z_2 + \frac{z_3(1 + z_1)}{(1 - z_2)(1 - z_3)} \right) + \frac{s_{13}^2}{2s_{23}} \left(\frac{1 - z_2}{1 - z_3} - 1 + 4z_2 \right) + \frac{s_{12}^2}{s_{23}} (1 - z_1) \right] \left. \right\} + (5 \text{ permutations}). \quad (\text{C2})$$

-
- [1] R. K. Ellis *et al.*, (2019), arXiv:1910.11775 [hep-ex].
 - [2] J. N. Butler *et al.*, (2023), 10.2172/1922503.
 - [3] F. Gross *et al.*, Eur. Phys. J. C **83**, 1125 (2023), arXiv:2212.11107 [hep-ph].
 - [4] G. Heinrich, Phys. Rept. **922**, 1 (2021), arXiv:2009.00516 [hep-ph].
 - [5] F. Febres Cordero, A. von Manteuffel, and T. Neumann, Comput. Softw. Big Sci. **6**, 14 (2022), arXiv:2204.04200 [hep-ph].
 - [6] J. M. Campbell *et al.*, in *2022 Snowmass Summer Study* (2022).
 - [7] A. Huss, J. Huston, S. Jones, M. Pellen, and R. Röntsch, (2025), arXiv:2504.06689 [hep-ph].
 - [8] F. Bloch and A. Nordsieck, Phys. Rev. **52**, 54 (1937).
 - [9] D. R. Yennie, S. C. Frautschi, and H. Suura, Annals Phys. **13**, 379 (1961).
 - [10] T. Kinoshita, J. Math. Phys. **3**, 650 (1962).
 - [11] T. D. Lee and M. Nauenberg, Phys. Rev. **133**, B1549 (1964).
 - [12] S. Frixione, Z. Kunszt, and A. Signer, Nucl. Phys. B **467**, 399 (1996), arXiv:hep-ph/9512328.
 - [13] S. Catani and M. H. Seymour, Nucl. Phys. B **485**, 291 (1997), [Erratum: Nucl.Phys.B 510, 503–504 (1998)], hep-ph/9605323.
 - [14] S. Catani, S. Dittmaier, M. H. Seymour, and Z. Trocsanyi, Nucl. Phys. B **627**, 189 (2002), hep-ph/0201036.
 - [15] Y. Nambu, Phys. Lett. B **26**, 626 (1968).
 - [16] D. G. Boulware and L. S. Brown, Phys. Rev. **172**, 1628 (1968).
 - [17] M. Gell-Mann and M. L. Goldberger, Phys. Rev. **96**, 1433 (1954).
 - [18] L. S. Brown and R. L. Goble, Phys. Rev. **173**, 1505 (1968).
 - [19] S. Catani, Phys. Lett. B **427**, 161 (1998), arXiv:hep-ph/9802439.
 - [20] G. F. Sterman and M. E. Tejeda-Yeomans, Phys. Lett. B **552**, 48 (2003), arXiv:hep-ph/0210130.
 - [21] S. Catani and M. Grazzini, Nucl. Phys. B **570**, 287 (2000), arXiv:hep-ph/9908523.
 - [22] S. Catani and M. Grazzini, Nucl. Phys. B **591**, 435 (2000), arXiv:hep-ph/0007142.
 - [23] J. Frenkel and J. C. Taylor, Nucl. Phys. B **109**, 439 (1976), [Erratum: Nucl.Phys.B 117, 546–546 (1976), Erratum: Nucl.Phys.B 155, 544 (1979)].
 - [24] Y. L. Dokshitzer, D. Diakonov, and S. I. Troian, Phys. Rept. **58**, 269 (1980).
 - [25] D. Amati, R. Petronzio, and G. Veneziano, Nucl. Phys. B **140**, 54 (1978).
 - [26] D. Amati, R. Petronzio, and G. Veneziano, Nucl. Phys. B **146**, 29 (1978).
 - [27] R. K. Ellis, H. Georgi, M. Machacek, H. D. Politzer, and G. G. Ross, Phys. Lett. B **78**, 281 (1978).
 - [28] R. K. Ellis, H. Georgi, M. Machacek, H. D. Politzer, and G. G. Ross, Nucl. Phys. B **152**, 285 (1979).
 - [29] J. Kalinowski, K. Konishi, and T. R. Taylor, Nucl. Phys. B **181**, 221 (1981).

- [30] J. Kalinowski, K. Konishi, P. N. Scharbach, and T. R. Taylor, Nucl. Phys. B **181**, 253 (1981).
- [31] B. S. DeWitt, Phys. Rev. **162**, 1195 (1967).
- [32] J. Honerkamp, Nucl. Phys. B **48**, 269 (1972).
- [33] H. Kluberg-Stern and J. B. Zuber, Phys. Rev. D **12**, 482 (1975).
- [34] L. F. Abbott, Nucl. Phys. B **185**, 189 (1981).
- [35] L. F. Abbott, Acta Phys. Polon. B **13**, 33 (1982).
- [36] L. F. Abbott, M. T. Grisaru, and R. K. Schaefer, Nucl. Phys. B **229**, 372 (1983).
- [37] K. A. Meissner, Acta Phys. Polon. B **17**, 409 (1986).
- [38] A. H. Mueller, Phys. Lett. **B104**, 161 (1981).
- [39] B. I. Ermolaev and V. S. Fadin, JETP Lett. **33**, 269 (1981).
- [40] Y. L. Dokshitzer, V. S. Fadin, and V. A. Khoze, Phys. Lett. B **115**, 242 (1982).
- [41] Y. L. Dokshitzer, V. S. Fadin, and V. A. Khoze, Z. Phys. **C15**, 325 (1982).
- [42] A. Bassetto, M. Ciafaloni, G. Marchesini, and A. H. Mueller, Nucl. Phys. **B207**, 189 (1982).
- [43] A. Bassetto, M. Ciafaloni, and G. Marchesini, Phys. Rept. **100**, 201 (1983).
- [44] J. D. Jackson, *Classical Electrodynamics* (Wiley, 1998).
- [45] M. E. Peskin and D. V. Schroeder, *An Introduction to quantum field theory* (Addison-Wesley, Reading, USA, 1995).
- [46] W. Gordon, Zeitschrift für Physik **140**, 630 (1928).
- [47] M. Stone, Int. J. Mod. Phys. B **30**, 1550249 (2015), arXiv:1507.01807 [physics.optics].
- [48] D. T. Son and N. Yamamoto, Phys. Rev. D **87**, 085016 (2013), arXiv:1210.8158 [hep-th].
- [49] J.-Y. Chen, D. T. Son, M. A. Stephanov, H.-U. Yee, and Y. Yin, Phys. Rev. Lett. **113**, 182302 (2014), arXiv:1404.5963 [hep-th].
- [50] R. L. Arnowitt and S. I. Fickler, Phys. Rev. **127**, 1821 (1962).
- [51] W. Konetschny and W. Kummer, Nucl. Phys. B **100**, 106 (1975).
- [52] W. Konetschny and W. Kummer, Nucl. Phys. B **108**, 397 (1976).
- [53] J. Frenkel, Phys. Rev. D **13**, 2325 (1976).
- [54] W. Konetschny, Phys. Lett. B **90**, 263 (1980), [Erratum: Phys.Lett.B 115, 503 (1982)].
- [55] B. Humpert and W. L. van Neerven, Phys. Lett. B **101**, 101 (1981).
- [56] R. D. Field, *Applications of Perturbative QCD*, Vol. 77 (Front.Phys., 1989).
- [57] L. J. Dixon, in *Theoretical Advanced Study Institute in Elementary Particle Physics (TASI 95): QCD and Beyond* (1996) pp. 539–584, arXiv:hep-ph/9601359.
- [58] D. A. Kosower and P. Uwer, Nucl. Phys. B **563**, 477 (1999), arXiv:hep-ph/9903515.
- [59] Z. Bern, L. J. Dixon, and D. A. Kosower, JHEP **08**, 012 (2004), arXiv:hep-ph/0404293.
- [60] Z. Bern, V. Del Duca, and C. R. Schmidt, Phys. Lett. B **445**, 168 (1998), arXiv:hep-ph/9810409.
- [61] Z. Bern, V. Del Duca, W. B. Kilgore, and C. R. Schmidt, Phys. Rev. D **60**, 116001 (1999), arXiv:hep-ph/9903516.
- [62] A. Denner, G. Weiglein, and S. Dittmaier, Phys. Lett. B **333**, 420 (1994), arXiv:hep-ph/9406204.
- [63] S. Hashimoto, J. Kodaira, Y. Yasui, and K. Sasaki, Phys. Rev. D **50**, 7066 (1994), arXiv:hep-ph/9406271.
- [64] A. Pilaftsis, Nucl. Phys. B **487**, 467 (1997), arXiv:hep-ph/9607451.
- [65] F. A. Berends and W. T. Giele, Nucl. Phys. B **306**, 759 (1988).
- [66] F. A. Berends, W. T. Giele, and H. Kuijf, Nucl. Phys. B **321**, 39 (1989).
- [67] F. A. Berends, H. Kuijf, B. Tausk, and W. T. Giele, Nucl. Phys. B **357**, 32 (1991).
- [68] C. Duhr, S. Hoeche, and F. Maltoni, JHEP **08**, 062 (2006), arXiv:hep-ph/0607057.
- [69] V. V. Sudakov, Sov. Phys. JETP **3**, 65 (1956).
- [70] Z. Bern and D. A. Kosower, Nucl. Phys. B **379**, 451 (1992).
- [71] Z. Bern, A. De Freitas, L. J. Dixon, and H. L. Wong, Phys. Rev. D **66**, 085002 (2002), arXiv:hep-ph/0202271.
- [72] G. Somogyi, Z. Trocsanyi, and V. Del Duca, JHEP **06**, 024 (2005), arXiv:hep-ph/0502226.
- [73] J. M. Campbell and E. W. N. Glover, Nucl. Phys. B **527**, 264 (1998), arXiv:hep-ph/9710255.
- [74] G. Marchesini and B. R. Webber, Nucl. Phys. **B310**, 461 (1988).
- [75] G. Marchesini and B. R. Webber, Nucl. Phys. B **330**, 261 (1990).
- [76] M. Czakon, Nucl. Phys. B **849**, 250 (2011), arXiv:1101.0642 [hep-ph].
- [77] T. Kugo and I. Ojima, Prog. Theor. Phys. Suppl. **66**, 1 (1979).
- [78] T. Gottschalk and D. W. Sivers, Phys. Rev. D **21**, 102 (1980).
- [79] Z. Kunszt and E. Pietarinen, Nucl. Phys. B **164**, 45 (1980).
- [80] R. K. Ellis and J. C. Sexton, Nucl. Phys. B **269**, 445 (1986).
- [81] G. Curci, W. Furmanski, and R. Petronzio, Nucl. Phys. **B175**, 27 (1980).
- [82] W. Furmanski and R. Petronzio, Phys. Lett. B **97**, 437 (1980).
- [83] G. Heinrich and Z. Kunszt, Nucl. Phys. B **519**, 405 (1998), arXiv:hep-ph/9708334.
- [84] A. Bassetto, G. Heinrich, Z. Kunszt, and W. Vogelsang, Phys. Rev. D **58**, 094020 (1998), arXiv:hep-ph/9805283.
- [85] Z. Bern and G. Chalmers, Nucl. Phys. B **447**, 465 (1995), arXiv:hep-ph/9503236.
- [86] M. Tentyukov and J. A. M. Vermaseren, Comput. Phys. Commun. **181**, 1419 (2010), arXiv:hep-ph/0702279.
- [87] J. Kuipers, T. Ueda, J. A. M. Vermaseren, and J. Vollinga, Comput. Phys. Commun. **184**, 1453 (2013), arXiv:1203.6543 [cs.SC].
- [88] B. Ruijl, T. Ueda, and J. Vermaseren, (2017), arXiv:1707.06453 [hep-ph].
- [89] C. A. Cole and S. Wolfram, (1981), print-81-0588 (Caltech).
- [90] G. Passarino and M. J. G. Veltman, Nucl. Phys. B **160**, 151 (1979).

- [91] T. Hahn and M. Perez-Victoria, *Comput. Phys. Commun.* **118**, 153 (1999), arXiv:hep-ph/9807565.
- [92] T. Hahn, *Comput. Phys. Commun.* **140**, 418 (2001), arXiv:hep-ph/0012260.
- [93] T. Hahn, *Nucl. Phys. B Proc. Suppl.* **89**, 231 (2000), arXiv:hep-ph/0005029.
- [94] A. Denner and S. Dittmaier, *Nucl. Phys. B* **734**, 62 (2006), arXiv:hep-ph/0509141.
- [95] N. D. Christensen and C. Duhr, *Comput. Phys. Commun.* **180**, 1614 (2009), arXiv:0806.4194 [hep-ph].
- [96] A. Alloul, N. D. Christensen, C. Degrande, C. Duhr, and B. Fuks, *Comput. Phys. Commun.* **185**, 2250 (2014), arXiv:1310.1921 [hep-ph].
- [97] H. H. Patel, *Comput. Phys. Commun.* **197**, 276 (2015), arXiv:1503.01469 [hep-ph].
- [98] H. H. Patel, *Comput. Phys. Commun.* **218**, 66 (2017), arXiv:1612.00009 [hep-ph].
- [99] Z. Bern and A. G. Morgan, *Phys. Rev. D* **49**, 6155 (1994), arXiv:hep-ph/9312218.
- [100] P. P. Kulish and L. D. Faddeev, *Theor. Math. Phys.* **4**, 745 (1970).
- [101] S. Catani, M. Ciafaloni, and G. Marchesini, *Nucl. Phys. B* **264**, 588 (1986).
- [102] Z. Bern, L. J. Dixon, and D. A. Kosower, *Nucl. Phys. B* **412**, 751 (1994), arXiv:hep-ph/9306240.